# *Scalable VR & AR Technologies for Surgical Planning in Clinical Medicine*

DAVID SIBRINA

# Durham University

**Department of Computer Science**
United Kingdom


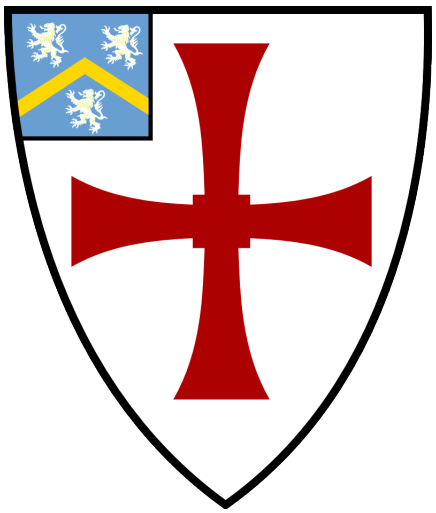

# Scalable VR & AR Technologies for Surgical Planning in Clinical Medicine

**by**


**David Sibrina BA(Hons) MSc**

Supervisor: Dr George Alex Koulieris


**A thesis presented for the degree of**
***Doctor of Philosophy***

March 2024

# Declaration of Authorship

The research presented in this thesis was conducted in the Department of Computer Science at Durham University, United Kingdom. I affirm that this thesis has not been submitted for any other degree or qualification at any other institution. Except where explicitly referenced in the text, this work is entirely my own.

DURHAM UNIVERSITY

# *Abstract*

**Department of Computer Science**

by David Sibrina

The surgical planning landscape is undergoing a significant transformation due to technological advancements and the increasing complexity of surgical interventions. The integration of scalable Virtual Reality (VR) systems into surgical planning has emerged as a key innovation. Traditionally, surgical planning depends on imaging techniques like X-rays, CT scans, and MRI, offering a limited perspective due to their two-dimensional nature. Surgeons often have to mentally reconstruct a three-dimensional understanding from these two-dimensional images, a process that can lead to errors. Further, these methods struggle to accurately represent the spatial relationship between critical structures and variations in patient anatomy, and do not allow for pre-surgical simulations. VR technology offers an immersive, interactive 3D environment that closely mimics the surgical field, enabling surgeons to visualise and interact with patient-specific anatomical models derived from actual patient imaging data. This enhances understanding of complex anatomical relationships and facilitates precise surgical planning. VR's potential to revolutionise surgical planning and execution is further supported by the increase in data collected before a surgical procedure.

Previous research demonstrated the positive contribution VR can offer in surgical planning in various medical fields, such as chest wall resections, oral and maxillofacial surgery, robotic-assisted partial nephrectomy, tracheoplasty, and cranial aneurysm clipping. Although these implementations are functional and contributed great knowledge to the field, adoption of these VR surgical planning tools has struggled with scalability and validation in real clinical environments. Oftentimes these systems are built upon ad hoc platforms and are not a part of a medical data acquisition and processing pipeline and as such cannot be adapted to different types of operations and, therefore, cannot be scaled and reused into other disciplines. Most of previous research also lacks clinical deployment on a day-to-day basis and validation with real-patient cases, mostly due to high friction to change clinical data acquisition protocols and regulatory affairs. Making matters worse, current VR solutions, both research and commercial, have non-standardised user interaction interfaces and paradigms between different operation types to navigate medical visualisations, preventing wider adoption by heavily time-constrained

clinical experts. Finally, there is a need to establish a -secure- system for the distribution of data required to generate 3D-VR-ready reconstruction of patient models, akin to the functionality offered by Picture Archiving and Communication Systems (PACS) for the distribution of standard medical imaging.

In this thesis, in an attempt to improve upon the aforementioned issues, we first introduce IKEM VRLab. The system represents a modular and extensible VR platform designed from the bottom-up to integrate in a medical data pipeline for clinical deployment. Developed with a focus on scalability and adaptability, IKEM VRLab facilitates immersive, interactive examinations of patient-specific anatomical data in 3D. IKEM VRLab supports the implementation of specialised toolkits for a variety of surgical procedures, enabling VR technologies to pervade in various clinical settings. We extensively validated our system with a novel method to examine the volumetric accuracy of CT-derived VR-optimised 3D models. The results indicated that there was no statistically significant difference between the volume estimated using IKEM VRLab and the actual organ volume, which is crucial for pre-operative planning.

Building upon the capabilities of IKEM VRLab, we then introduce OrthopedVR as the first specialised application toolkit for the planning and visualisation of corrective surgeries for lower limb abnormalities, such as rotational deformities causing patellar mal-tracking. This application allows orthopaedic surgeons to simulate derotational osteotomies in a 3D environment, offering a more intuitive understanding of patient anatomy and enhancing surgical precision. The evaluation of OrthopedVR by experienced surgeons highlights its superiority over traditional 2D imaging techniques, indicating its potential to significantly improve pre-operative planning, surgical outcomes, and clinical training.

We then further expand the scope of IKEM VRLab, exploring its application in liver resection planning, a critical aspect of treating primary and secondary liver cancers as well as echinococcal cysts. The VRLab toolkit for liver resections enables detailed visualisation and interaction with 3D reconstructions of the liver, facilitating accurate and personalised surgical planning. Through immersive VR, surgeons demonstrably achieved a deeper comprehension of complex anatomical structures, improving decision-making and potentially reducing post-operative complications. Evaluation of the toolkit involving experienced liver surgeons confirmed the system's effectiveness in enhancing the accuracy and efficacy of liver surgeries compared to conventional medical visualisation standards.

We finally shift our attention to lung surgeries. We first extend IKEM VRLab to support Augmented Reality (AR) to assist with planning port placements for

Robotic-Assisted Thoracic Surgery (RATS) during lung segmentectomies. This AR Lung toolkit aims to minimise the invasive impact of RATS by enhancing the visualisation and planning of trocars and instrument placements. We then focus on lung transplant, attempting organ transplant size matching. IKEM VRLab's Fitting Room offers an innovative approach to donor-recipient child-adult size-matching, providing surgeons with an immersive platform to assess and optimise lung transplant compatibility. The lung toolkit demonstrates VR's potential to improve the precision of organ matching and lung surgeries, contributing to better post-operative outcomes and patient survival rates.

The integration of scalable VR and AR systems in surgical planning, as achieved by IKEM VRLab, marks a significant advancement in the field. This thesis demonstrates that VR technologies, by providing an immersive and interactive 3D environment, enhance the understanding of complex anatomical structures and improve the precision of surgical interventions across various medical fields. The modular and adaptable nature of IKEM VRLab allows it to integrate seamlessly into medical data pipelines, supporting a range of specialized surgical procedures. Evaluations of specific toolkits for orthopaedic, liver, and lung surgeries validate the system's effectiveness in clinical settings, indicating its potential to improve pre-operative planning, surgical outcomes, and clinical training. This work also underscores the importance of standardizing VR interfaces and ensuring secure data distribution to foster wider adoption and scalability in clinical environments.

# Ethics Statement

This research was conducted following the ethical guidelines provided by Durham University's Department of Computer Science. Ethical approval for this study was obtained from the department in accordance with their research standards (reference: COMP-2022-09-23T17_08_47-lfld87).

For the purpose of evaluation in Chapter. 4., the patient data were sourced from the Research Team at NHS Foundation Trust of County Durham and Darlington. Based on the NHS Health Research Authority Decision Tool, it was concluded that an NHS Research Ethics Committee review was not necessary at the time of this study due to its non-invasive and retrospective nature. All patient data used in this research was anonymized, ensuring compliance with the General Data Protection Regulation (GDPR).

In the projects described in Chapters 5. and 6., it is important to clarify that the systems were used as supplementary visualisation tools in a clinical setting, rather than certified medical devices. Consent for the use of patient data was secured by the Institute for Clinical and Experimental Medicine (IKEM) and University Hospital Motol, both of which collaborated actively on these projects. The reconstructions of these patients' data stayed on a local storage at these institutions. For the study discussed in Chapter 5., the patient data were anonymized during export, with randomized identifiers assigned to ensure privacy. VRLab was used to enhance the visualization of surgical data obtained from certified imaging techniques such as CT, MRI, and Ultrasound. As the visualization relied on existing patient data, there was no additional radiation exposure involved. Moreover, none of the adaptations of IKEM VRLab—whether for liver resection planning, lung transplant size matching, or lung segmentectomies—provided surgeons with advice or recommendations. The tool did not dictate any new procedures beyond those that would have occurred under standard clinical practice. The purpose of deploying VRLab in these clinical cases was to test its utility and effectiveness as a visualization aid in a real-world clinical environment. VRLab served as an additional layer of visualisation, allowing clinicians to review and refine their surgical plans. It is a supplementary tool, and all decisions regarding patient care and surgical interventions were made by the surgeons based on certified medical data and established clinical protocols.

# *Acknowledgements*

I am deeply grateful to my supervisor, Dr. George Alex Koulieris, for his guidance, invaluable insights, and continuous support throughout this research journey. His expertise, patience, and encouragement have significantly shaped my work and fostered an environment that encouraged intellectual growth.

I would like to express my appreciation to Petr Raska for his expertise and substantial support during my PhD studies. Furthermore, I would like to thank Prof. Jiri Fronek, Prof. Robert Lischke, Dr. Sarath Bethapudi, and Dr. Jan Kolarik for sharing their knowledge in their respective medical fields and for collaborating on projects I thoroughly enjoyed.

Heartfelt appreciation goes to my parents, Martin and Marie Sibrina, for their boundless love, encouragement, and unwavering faith in my ambitions. Their sacrifices, constant motivation, and enduring support have been the solid foundation of this academic pursuit.

To my beloved wife, Kiera, your unwavering belief in me and your understanding during the long hours of research and writing have been my sanctuary. Your encouragement, patience, and constant presence have provided the necessary emotional support even during my most challenging times.

I am also deeply grateful to my sister, Paja, who is always there for me.

In conclusion, this thesis is a testament to the collective efforts of many individuals, and I am deeply thankful to each and every one of them for participating in this demanding journey, both professionally and personally.

**With deep respect and gratitude,**

David Sibrina

*Dedicated to my encouraging grandfather.*

# Contents

# List of Figures

# List of Tables

# Abbreviations

**3D** - 3-Dimensional
**VR** - Virtual Reality
**AR** - Augmented Reality
**UI** - User Interface
**CT** - Computed Tomography
**MRI** - Magnetic Resonance Imaging
**PACS** - Picture Archiving and Communication System
**RATS** - Robotic-assisted Thorascopic Surgery
**VATS** - Video-assisted Thoracoscopic Surgery
**PFJ** - Patellofemoral Joint
**FV** - Femoral Version
**KJRA** - Knee Joint Rotation Angle
**TLC** - Total Lung Capacity
**pTLC** - Predicted Total Lung Capacity
**TLV** - Total Lung Volume
**pTLV** - Predicted Total Lung Volume
**RUL** - Right Upper Lobe
**RML** - Right Middle Lobe
**RLL** - Right Lower Lobe
**LUL** - Left Upper Lobe
**LLL** - Left Lower Lobe
**GT** - Ground Truth
**SUS** - System Usability Scale
**IPQ** - Igroup Presence Questionnaire
**IPQ-XRMSE** - Igroup Presence Questionnaire For XR Medical System Evaluation

# Publication Record

## Journal Publications

1. **D. Sibrina**, S. Bethapudi & G.A. Koulieris. OrthopedVR: clinical assessment and pre-operative planning of paediatric patients with lower limb rotational abnormalities in virtual reality. Vis Comput 39, 3621–3633 (2023). https://doi.org/10.1007/s00371-023-02949-0. **CGI 2023's - Best Visual Computer Paper Award**. **(Contributing to Chapters 3 & 4)**

2. **D. Sibrina**, J. Fronek, M. Kocik, J. Chlupac, P. Raska, J. Rydlo, T. Adla, D. Cupalova, L. Sukupova, G.A. Koulieris. IKEM VRLab: VR System for Surgical Planning of Liver Resections. Submitted to be published in Springer Virtual Reality. **(Contributing to Chapters 3 & 5)**

3. J. Kolařík, J. Tavandžis, R. Novysedlák, J. Vachtenheim, **Sibřina D**, Švorcová M, Pozniak J, Šimonek J, J. Schützner, R. Lischke. Robotic pulmonary segmentectomy, initial experience in the Czech Republic. Rozhl Chir. 2023 Summer;102(5):199-203. English. doi: 10.33699/PIS.2023.102.5.199-203. PMID: 37527946. **(Contributing to Chapter 6)**

## Conference Publications

4. **D. Sibrina**, S. Bethapudi and G. A. Koulieris, A Virtual Reality System for the Assessment of Patients with Lower Limb Rotational Abnormalities, 2023 IEEE Conference on Virtual Reality and 3D User Interfaces (IEEE VR) Abstracts and Workshops (VRW), Shanghai, China, 2023, pp. 783-784, doi: 10.1109/VRW58643.2023.00234. **(Contributing to Chapters 3 & 4)**

5. **D. Sibrina**, R. Novysedlak, J. Kolarik, J. Vachtenheim, R. Lischke, G.A. Koulieris.Fitting Room: Lung Transplantation Donor-Recipient Size-matching in Virtual Reality. In Special Interest Group on Computer Graphics and Interactive Techniques Conference Posters (SIGGRAPH Posters '24), Denver, CO, USA. ACM, New York, NY, USA 2 Pages. doi: 10.1145/3641234.3671048. **(Contributing to Chapter 6)**

## Book Publications

6. **D. Sibřina** (2022). Virtual reality in medicine. In M. Táborský et al. (Eds.), Digital Medicine 2022 (pp. 153-163). [ISBN 978-80-908638-8-0]. **(Contributing to Chapters 2 & 5 )**

# Public Speaking & Awards

## Public Speaking

- October 2023, **Rising Stars 2023**, *IKEM VRLab Liver Fitting Room: Liver Donor-Recipient Size-matching in Virtual Reality*, Speaker, Prague (Czech Rep.)
- October 2023, **Forbes: Better Czech**, *Innovation in Medicine*, Innovation Panel Speaker, Carlsbad (Czech Rep.)
- September 2023, **Shift Medical 2023**, *Virtual Reality in Surgical Planning at Transplantation Center, and VR Patient Specific Model Validation*, Speaker, Heidelberg (Germany)
- September 2023, **Computer Graphics International 2023**, *OrthopedVR: clinical assessment and pre-operative planning of paediatric patients with lower limb rotational abnormalities in virtual reality.* , Speaker, Shanghai (China)
- March 2023, **IEEEVR 2023**, *A Virtual Reality System for the Assessment of Patients with Lower Limb Rotational Abnormalities*, Poster Session, Shanghai (China)
- September 2022, **Rising Stars 2022**, *Message from practice: Liver Resection Planning in Paediatric Patients in Virtual Reality*, Main Panel Speaker, Prague (Czech Rep.)
- June 2022, **Conference of Czech Society for Medical Technology**, *Planning liver transplants and resections in virtual reality*, Main Panel Speaker, Pardubice (Czech Rep.)

- April 2022, **Czech Digital Medicine Summit**, *Virtual Reality in Liver Resection and Liver Split Planning*, Technical Panel Speaker, Prague (Czech Rep.)
- October 2020, **Rising Stars 2020**, *Potential of Virtual Reality in Surgical Planning*, Main Panel Speaker, Prague (Czech Rep.)

## Awards

- January 2024, **Forbes: Top 5 MedTech Applications**, *IKEM VRLab* **(Associated with Chapters 3 & 5)**
- September 2023, **CGI 2023: Best Visual Computer Paper Award**, *OrthopedVR: clinical assessment and pre-operative planning of paediatric patients with lower limb rotational abnormalities in virtual reality.* **(Associated with Chapter 4)**
- January 2023, **Forbes Top 30 Under 30**, *Selected for the impact of my work and research in the field of surgical planning in VR/AR.*

Chapter 1

# Introduction

## 1.1 Context

The landscape of surgical planning is experiencing a significant shift driven both by technological advancements and the growing complexity of surgical procedures. As the medical community strives to enhance patient outcomes and operational efficiencies, the integration of scalable VR systems into surgical planning emerges as a critical innovation. Conventionally, surgical planning has relied heavily on two-dimensional imaging techniques, such as X-rays, Computational Tomography (CT) scans, and Magnetic Resonance Imaging (MRI), that generate 2D projections of 3D structures. While invaluable, these methods often provide a limited perspective since they are mostly consumed by medical specialists in the two-dimensional (2D) domain on 2D screens, lacking the depth and spatial awareness crucial for navigating complex anatomical structures [5]. Surgeons are required to mentally reconstruct three-dimensional perceptions from these images, leading to potential errors [6]. Additionally, these methods are limited in accurately representing spatial relationships between critical structures and variations in patient anatomy, and lack pre-surgical simulation capabilities [7].

The general assumption across the field of surgical planning is that three-dimensional visualisation of three-dimensional data provided by CT/MRI offer considerable benefits to better understanding a patient's anatomy. 3D reconstruction and representation of data is considered to be preferable in the examination of 3D structures [8, 9, 10, 11]. 3D methods of studying complex 3D structures have become a clinical standard, including 3D-PDF and 3D printing, reconstructed from 2D scans. However, both 3D-PDF and 3D printing suffer from significant shortcomings. In the case of 3D-PDF, data are presented in 3D environments but on 2D screens, limiting the accuracy of surgical planning [12, 13]. 3D printing offers a haptic ele-

ment and better spatial representation of the anatomy, although 3D printing can take up to several hours of processing, and the plastic filaments still do not offer full transparency through the surface of the tissue. That means 3D printing does not allow surgeons to observe the internal structures of the organs and the position of the outer structure of the organ itself [14, 15].

Virtual Reality technologies offer a paradigm shift by providing an immersive, interactive 3D environment that closely mimics the surgical field. VR systems enable surgeons to visualise and interact with patient-specific anatomical models derived from actual patient imaging data. As VR hardware is becoming more affordable, VR allows the transformation of 3D images into a stereoscopic patient model based on CT and MRI imaging that creates a complex representation using a cost-effective method [16]. VR planning of surgery with computer-generated data can further simulate the real procedure's mechanics closely. Surgeons previously indicated that VR surgical planning had provided them with a deeper understanding of the pathological and anatomical spatial relationship that resulted in strengthening surgical confidence [17, 18].

This leap in visualization capabilities offers a more intuitive understanding of complex anatomical relationships, facilitates precise surgical planning, and allows for virtual rehearsals of the procedure, potentially reducing intra-operative risks and improving surgical outcomes. There is a consensus across the bio-engineering field that VR examinations of patients' radiological data will become a standard in the next ten years in all developed countries [19, 20]. For example, Tomlison et al. (2019) assume that the future of surgical planning for neuro-surgeries is in VR rather than using conventional methods [21]. Moreover, the amount of data collected before a surgical procedure has significantly increased in recent years due to the better imaging systems available and improved accessibility to them. This correlates with added benefits for medical judgement, clinical training and operation planning.

While previous research has demonstrated VR's positive impact on surgical planning in various medical fields, such as chest wall resections, cranial aneurysm clipping, invasive coronary artery bypass for Kawasaki disease or in preoperative planning in temporal bones [22, 23, 24], employing VR in real clinical environments remains challenging. Existing VR surgical planning tools often lack integration into medical data acquisition and processing pipelines, hindering versatility across different types of operations and limiting scalability. The concept of scalability is crucial for the widespread adoption of VR in surgical planning. Scalable VR systems can be tailored to meet the diverse needs of healthcare facilities, from community hospitals to large academic medical centres, ensuring that advanced

surgical planning tools are accessible to a broader range of practitioners and patients.

Moreover, the lack of standardized user interfaces and paradigms among VR solutions complicates adoption by the heavily time-constrained clinical experts. Additionally, there is a pressing need for a secure system for distributing data required for generating 3D VR-ready patient models, similar to the functionality offered by the ubiquitous Picture Archiving and Communication Systems (PACS) for medical imaging distribution.

In this dissertation, aiming to address the aforementioned challenges, we introduce IKEM VRLab (IKEM, Institute of Clinical and Experimental Medicine, Czech Republic). This system serves as a modular and expandable VR platform designed to seamlessly integrate into medical data pipelines for clinical use. Engineered with a focus on scalability and flexibility, IKEM VRLab enables immersive, interactive exploration of patient-specific anatomical data in three dimensions. Moreover, it facilitates the incorporation of specialized toolkits tailored for diverse surgical procedures, fostering the integration of VR technologies across various clinical environments.

The involvement of the IKEM in this thesis was pivotal, primarily through their provision of feedback, testing, resources, and imaging technology. IKEM's contributions significantly shaped the development and validation of the Extended Reality (XR) systems for surgical planning. The surgeons at IKEM played a critical role in testing the VR solutions, providing practical feedback that was instrumental in refining these systems to meet the real-world needs of clinical environments. This collaborative effort ensured that the solutions were both practical and effective in surgical planning. Additionally, IKEM provided essential resources and access to advanced imaging technology, which were crucial for the accurate reconstruction of patient-specific anatomical models.

This chapter outlines the motivation behind this research, details the innovative contributions of the developed VR framework to the fields of surgical planning in clinical medicine and provides the structure of this thesis.

## 1.2 Problem Statement

This section provides insight into the current issues of the standard of clinical examination in the fields of lower limb osteotomy, oncologic liver resection, and lung surgeries and transplantation which we deemed potential candidates to apply

VR pre-operative planning. It also resummarises & delves deeper into the reasons behind VR not been widely adopted in those clinical settings yet, for example, the lack of quantitative validation of previously proposed VR systems.

**Osteotomy for the Lower Limbs.** Rotational abnormalities in the lower limbs causing patellar mal-tracking negatively affect patients' lives, particularly young patients (10–17 years old). Recent studies suggest that rotational abnormalities can increase degenerative effects on the joints of the lower limbs. In osteotomy planning for the lower limbs, the challenge is to achieve optimal alignment and weight distribution post-surgery, which requires a precise understanding of the three-dimensional geometry of the bones and the mechanical axis of the limb [25, 26]. Traditional imaging techniques such as bi-planar radiography or CT imaging, while useful, often are not being presented in a three-dimensional domain and immersive environments, leading to less effective comprehension of the patient's skeletal anatomy of the lower limbs [27, 28, 29]. Misinterpretation or insufficient analysis can lead to suboptimal surgical outcomes, such as incorrect bone alignment or inadequate correction of deformities, potentially resulting in persistent pain or mobility issues for the patient.

**Liver Resection.** In the domain of oncologic liver resection, the primary challenge lies in the surgeon's ability to accurately delineate the boundaries between tumor tissue, vascular structures, bile ducts, and healthy liver parenchyma. The intricate anatomy of the liver, often altered by the presence of tumors, complicates the interpretation of traditional imaging modalities such as CT and MRI. The complexity of pathological liver anatomy can lead to difficulties in surgical planning, with a high risk of either insufficient resection of tumor tissue or unnecessary sacrifice of healthy liver tissue, which can significantly affect patient outcomes [30, 31].

**Porting Robotic Arms during Robotic Lung Segmentectomy.** The implementation of robotic systems, such as the da Vinci Xi, for conducting pulmonary segmentectomies presents a series of challenges, among which optimizing the port placement process is key - currently mostly based on 2D CT/MRI medical data [32]. This operation involves the precise placement of trocars and manipulators in the patient's chest wall, a critical step to ensure an effective and safe surgical approach to the target area [33]. Accurate port placement is essential for minimizing tissue trauma, optimizing the robotic visual field, and ensuring adequate manipulative capacity for the instruments, significantly influencing the overall success of the surgery. Challenges associated with port placement arise from a combination of anatomical, ergonomic, and technical factors. Anatomical variability among patients requires a customized approach to planning port locations, often complicating the standardization of surgical protocols. Ergonomic aspects concern the optimization

of port layout to prevent collision of the robotic arms while maintaining an optimal ergonomic working environment for the surgical team [34]. Technical challenges include limitations in the spatial range and mobility of the robotic instruments within the chest, necessitating careful planning of instrument trajectories to ensure precise manipulation and minimize the risk of iatrogenic damage. This issue is particularly relevant in the context of pulmonary segmentectomies, where precise dissection and resection of specific lung segments with limited damage to surrounding structures are required. Another significant aspect is the need to anticipate the potential impact of port placement on future surgical interventions. Incorrectly placed ports can complicate or even prevent access for future operations, emphasizing the need for strategic planning and foresight [35].

**Lung Transplantation Donor-Recipient Size-matching.** Size matching between the donor lung and the recipient's thoracic cavity is a critical factor in the success of lung transplantation and a longer survival rate. Traditional evaluation methods, such as predicted total lung capacity by using generalised computational models or 3D volume calculation from CT, can make it challenging to accurately assess the size and shape of the donor's lung in relation to the recipient's thoracic space, potentially leading to complications such as poor fit or impaired lung function post-transplant [36, 37, 38]. The precision required in evaluating the volumetric and spatial compatibility necessitates a more personalised approach including volume distribution and shape of individual lung lobes on the donor as well as the volume of the thoracic cavity or the recipient [39].

**Limited VR adoption.** As mentioned previously, present VR surgical planning tools, encompassing both scholarly and commercial approaches, face substantial hurdles in their integration into clinical settings. These challenges include difficulty incorporating such technologies into existing clinical workflows (including but not limited to medical imaging processing pipelines), limited scalability due to elevated costs, and the necessity for specialized training. Additionally, medical professionals, often not well-versed in VR technology, find the complex, non-standardised UIs unituitive, which steepens the learning curve and impedes effective use. The limited adoption of these systems can also be attributed to their lack of portability, requiring wired connections to high-powered computing stations or reliance on cloud rendering services that require high-speed, low-latency internet connections. Finally, there is also a lack of validation of VR surgical planning methods. Previous studies on VR applications for surgical planning have predominantly relied on standardized qualitative feedback questionnaires and users' testimonials, showing a gap in quantitative clinical data [18, 40, 15]. This highlights a critical need for thorough quantitative evaluations of VR's effectiveness in ensuring accurate

surgical decision-making.

## 1.3 Thesis Contributions & Structure

Following this short Introductory Chapter, Chapter 2 summarises the relevant literature. Chapters 3, 4, 5 & 6 present the main contributions of this work (see below for a summary of each contribution). Chapter 7 concludes the thesis and provides insights into possible future work. Specifically:

**IKEM VRLab: Development of a Virtual Reality System for Clinical Use (Chapter 3)**

We introduce a pioneering virtual reality system, IKEM VRLab, designed specifically for scalable clinical deployment, aiming to improve collaborative efforts across medical disciplines both locally (within a hospital) and nationally/internationally. This system stands out by creating a unified platform for patient data distribution, integrating a VR platform with collaborative networking capabilities, and incorporating advanced segmentation and optimization tools for the detailed visualization of complex patient data on stand-alone VR devices. Its design ensures broad applicability across various medical fields by allowing for the integration of diverse surgical toolkits. This adaptability facilitates a wide range of surgical procedures, bridging the gap between different specialities. The workflow of distributing patient 3D reconstructions includes optimisation processes ensuring effective rendering on stand-alone VR devices.

To evaluate the correctness of our system, we developed a novel method to validate the volumetric accuracy of CT-derived models in a virtual reality setting, ensuring the fidelity of our conversion algorithms against the ground truth. The results of the volume validation study show that there is no statistically significant difference between the ground truth volume and volume obtained from a volumetric calculation in the IKEM VRLab. We also collected data demonstrating time efficiency when instantiating new virtual rooms and reconstruction of patients data in the VR environment.

**OrthopedVR for Visualizing Surgical Outcomes (pre-surgery) (Chapter 4)**

We present a VR system (OrthopedVR) which is a specialized VR application toolkit extending IKEM VRLab, that allows orthopaedic surgeons to examine patients' specific anatomy of the lower limbs in an immersive three-dimensional environment and to simulate the effect of potential surgical interventions such as

corrective osteotomies in VR. In OrthopedVR, surgeons can examine & manipulate 3D reconstructions of CT scans of patients suffering from rotational abnormalities and patellar mal-tracking in an immersive, multi-user, collaborative environment. To facilitate this, we designed an application-specific, hybrid 3DUI combining contextual and static UI designs. The 3DUI controls the surgical planning simulation by providing incision positioning, post-incision leg re-alignment, and post-operative angles calculation & visualisation.

OrthopedVR stands as the first of its kind in the growing demand for advanced VR visualization tools in the orthopaedic field, leveraging the affordability of standalone VR hardware to bring 3D models of patients suffering from lower limb rotational abnormalities. This innovation increases surgeons' confidence by enabling a deeper understanding of pathological rotational profiles of the lower limbs and spatial relationships. The application fosters collaboration and remote consultation building upon the functionality of IKEM VRLab. We performed a quantitative and qualitative evaluation for corrective osteotomy planning of the lower limbs in VR; four expert orthopaedic surgeons from the National Healthcare Service (NHS) endorsed our methodology. Through this assessment it emerged that OrthopedVR enhances comprehension of lower limb alignment and rotational profiles more effectively than standalone 2D CT DICOM viewers. Furthermore, OrthopedVR was shown to augment pre-operative planning, refine surgical accuracy, and enhance patient post-surgery outcomes. The findings of our study suggest that our system holds the potential to pioneer the simulation of corrective surgeries for lower limbs and points towards future enhancements that could facilitate the integration of VR-based surgical planning into orthopaedic clinical practice.

**IKEM VRLab in Liver Resection Planning (Chapter 5)**

In the fifth chapter, we introduce the deployment of IKEM VRLab into oncologic liver resection planning with 300 patient cases either indicated or contraindicated for procedures to this date by our system. This application-specific toolkit of IKEM VRLab significantly aids surgeons in decision-making for liver surgery planning, offering a more intuitive understanding of patient anatomy and facilitating the selection of the most appropriate surgical approaches.

In our work, we developed a CT and MRI acquisition protocol aimed at enabling the highly detailed reconstruction of patient-specific liver anatomy, seamlessly integrating this with a newly developed toolkit within the IKEM VRLab system. This toolkit enhances liver resection procedures by providing real-time volumetric estimates, clipping, and measuring tools tailored for anatomical and non-anatomical resections. We conducted a thorough quantitative evaluation of the study's meth-

odology with six experienced abdominal and hepatic-biliary surgeons across 60 instances of examining real patient cases. The evaluation also included a qualitative component. This involved a modified version of the Igroup Presence Questionnaire (IPQ), which we call IPQ-XRMSE, designed to capture the nuances of how medical professionals interact with XR applications in a clinical context. This approach ensures that our findings are applicable to practical and real-world surgical scenarios.

The evaluation of our toolkit demonstrated that the use of VRLab significantly improves surgeons' understanding of complex anatomical structures of the liver, potentially reducing complications in high-risk liver resections. VRLab offers superior depth perception and accuracy compared to conventional 3D technologies. Its utility extends to increasing user confidence, facilitating decision-making, and providing transparent data presentation. The results of the liver resection accuracy study present signification improvements with the use of VRLab when indicating patients for specific procedures compared to current standard clinical visualisation. The deployment of this system also shows an increased time efficiency during surgical planning. The use of real patient cases in the trials further validates these findings, suggesting potential applications in other surgical contexts.

**Extending IKEM VR Lab for Robotic Lung Segmentectomies and Donor-Recipient Size-matching in Lung Transplants (Chapter 6)**

The sixth chapter expands the application of IKEM VR Lab to include its use in robotic lung segmentectomies and virtual reality-assisted donor-recipient size matching for lung transplants.

First, we introduce our initial experience of using an AR modification of IKEM VRLab during two robotic lung segmentectomies. The system provided surgeons and supporting staff with a superimposed visualisation of patients anatomy on their body. This enhanced and corrected surgeons' initial marks on the patient's body for port insertion into the patient's thorax. We collected feedback from the surgeons and the supporting staff that indicated higher awareness of the extent of the surgery and improved readiness for potential events that can happen in the operating room.

We then extend IKEM VRLab to support enhanced size-matching of lung donors and potential recipients in lung transplants. This approach provides surgeons with interactive, three-dimensional, immersive size-matching in a case when dealing with adult and paediatric donors and recipients. This application showcases its potential to improve the correct pairing of donors and recipients, leading to a lower number of complications and fewer needs for graft alteration. This chapter underscores

the versatility and impact of VR technology in pushing the boundaries of surgical precision and patient care in highly specialized medical fields in comparison to current standard gold clinic methods.

---

**Note on significance:** The work presented in this thesis is currently under consideration for a Research Excellence Framework (REF) 2029 Impact Case Study. A REF impact case study is a report prepared by academic institutions in the UK as part of the REF assessment process, which assesses the quality of research conducted in UK HE institutions. Impact case studies are a crucial component of this assessment, as they **demonstrate the real-world impact and significance of the research conducted by staff & students**.

Chapter 2

# Related Work

## 2.1 3D Visualisation in Surgical Planning

The use of 3D visualisation software in surgery gained attention in recent years as it can provide valuable support in preoperative planning, surgical navigation, and decision-making during surgery. There is consensus recommendations for the application of 3D visualization technology in the accurate diagnosis and treatment of complicated tumours, forming standardized protocols for its use [41].

The integration of 3D visualization technology specifically in surgical planning has significantly advanced medical practice. It provides improved insights into patient anatomy, precise surgical strategies, and better patient outcomes. Research has shown how 3D models and augmented reality enhance patient education, help surgical teams understand complex anatomical structures, and refine surgical plans [42, 43, 5].

In medical specialties like neurosurgery, thoracic surgery, and maxillofacial surgery, 3D models have proven superior to traditional imaging methods for surgical planning. They are particularly useful in determining surgical approaches, resectability, and guiding complex procedures [44, 45, 46]. The application of 3D visualization in surgical planning can play a crucial role in a range of procedures, from cranial to abdominal surgeries, enabling precise localization of anatomical structures [47, 48, 49].

For example, Oshiro & Ohkohchi highlighted the increasing prevalence of three-dimensional preoperative simulation for liver surgery, corroborating the growing acceptance and integration of 3D visualization in surgical practice [50]. Another study focussed on using 3D visualisation in predicting the degree of ischemia in liver segments, providing valuable insights for surgical planning in split liver trans-

plantation [51].

However, the use of 3D visualization tools for surgery on standard 2D monitors is constrained by several limitations. These include the loss of depth perception which directly affects the assessment of spatial relationships between organ structures; the limited spatial interaction with 3D models on a 2D display which impacts the understanding of anatomy; and the absence of haptic feedback in a 3D environment, possibly leading to misinterpreting anatomical structures with a negative effect on surgical planning and outcomes [52, 53, 54, 55, 56, 57].

The utilization of 3D printing has offered valuable insights into patient-specific anatomy, enabling better visualization and comprehension by surgical teams, ultimately resulting in improved surgical outcomes, especially in the fields of pancreatic surgery, tibial plateau fractures, and marsupialization of odontogenic keratocyst [58, 59, 6]. 3D printing has demonstrable potential for preoperative planning in living donor liver transplantation, particularly in identifying vascular and biliary tract anatomy to improve surgical planning and reduce complications [52]. However, while this solution is innovative, it has not proven to be as beneficial as initially hypothesised due to its high cost and time-consuming nature of 3D printing, especially of high-fidelity organ models[60, 61].

The number of published papers in the field of virtual reality in anatomy education and surgical planning has been increasing in recent years. By providing a virtual environment, VR enables the evaluation of different anatomical regions of the body, facilitating the development of an accurate preoperative plan and the visualization of the entire operative process [62]. For example, in a case report by Kim et al. 2020 [63], surgeons conducted preoperative planning in VR for total maxillectomy and orbital floor reconstruction and they particularly remarked the strengths of this technology. The use of VR in orthopaedic surgery training has also demonstrated a measurable improvement of surgical skills and knowledge acquisition among orthopaedic surgeons and a flattening of the initial learning curve [64, 65]. Orthopedic surgery has also benefited from XR technologies, with studies indicating that XR-assisted intraoperative navigation can enhance the accuracy of implant placement, reduce postoperative complications, shorten surgical duration, and minimize radiation exposure for both patients and surgeons [66]. In spine medicine, XR technologies have been used for surgical planning, consultation, education, and rehabilitation. Studies show that XR can enhance spatial awareness, improve surgical accuracy, and facilitate communication among surgical teams in spine surgeries [67].

XR technologies also have promising roles in cardiothoracic surgery, particularly

in televirtuality, surgical planning, simulation, and perioperative management [68]. VR surgical planning has also shown its potential in clip pre-selection in aneurysms [22], where VR provided neurosurgeons with improved spatial understanding of vascular anatomy leading to outstanding aneurysm closure rates. Invasive coronary artery bypass for Kawasaki disease [69] has also been demonstrated, where the interactive reconstruction of CT images helped plan the insertion of thoracoscopic ports and determine the ideal location for anterior mini-thoracotomy. Schott et al. (2021) created a VR and AR platform for multi-user liver anatomy education [70]. The evaluation was conducted through a user study involving medical students. The study evaluated the platform's usability and effectiveness based on participant feedback. The findings revealed that the students received the VR/AR environment positively. However, the study also points out the need to further refine the user interface design and interactive features to improve the educational platform's comprehensiveness and effectiveness.

While the benefits of XR technologies in surgical settings are evident, challenges related to safety, security, and privacy have been identified. Addressing these issues is crucial to ensure the successful implementation of XR in healthcare [71]. Additionally, the effectiveness of XR technologies may vary across different surgical contexts, emphasizing the need for careful consideration when applying these technologies in diverse surgical domains [72].

## 2.2 Rotational Deformities in Femur/Tibia

Several factors ensure a normally working patellofemoral joint (PFJ) (Figure. 2.2): soft connective tissues around the knee, the correct geometry of osseous structures and properly aligned components in the lower limb. The rotational alignment of the femur and tibia determine the correct patellofemoral tracking and properly working knee joint. Orthopaedic doctors are especially interested in the femoral version (FV), tibial rotation and knee joint rotation angle (KJRA) [73] (Figure. 2.3). Significant femoral anteversion leads to an internally rotated gait unless a simultaneous external tibial torsion rotates the leg outward maintaining a normal foot progression angle during gait. Increased femoral anteversion and tibial torsion produce patellofemoral instability. The patellar mal-tracking manifests itself in occasional or permanent instability & chronic pain in the knee region. The anatomic relationship between the resultant force from the quadriceps and the line of pull of the patellar tendon is called the Q-angle and is normally 10-15°. The first deformity that affects the patella tracking is valgus (knock knee syndrome) or varus (bow leg syndrome) of the tibia (Figure. 2.1). Commonly in paediatric patients, the tibia

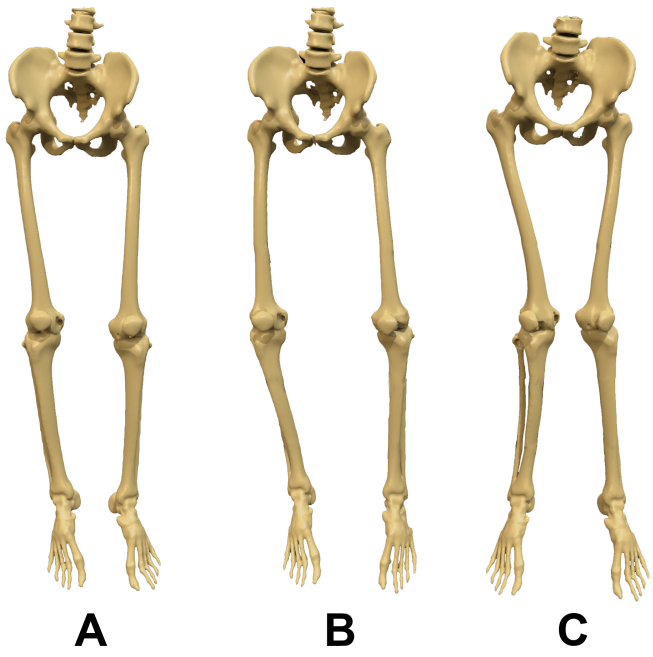


**Figure 2.1:** Difference between a *healthy* anatomy of the lower limbs (A), pathological anatomy affected by *varus deformity* (B), and pathological anatomy affected by *valgus deformity* (C).

is in the valgus. The varus-valgus deformities in the tibia are the most common. Secondary deformities are also, in some cases, found in the rotated distal femur [74, 75].

**Clinical diagnostics & surgical treatment.** The patient history, physical examination and gait observations can indicate signs of patellar mal-tracking, in-toeing or out-toeing gait. Sometimes, malalignments of the hips and knees go unnoticed, perpetuating pain and discomfort, due to the two adverse rotations of the femur and tibia that would otherwise maintain the patient's feet in a parallel position when walking. Images taken from the front of the leg, the back, or the side during single or bi-planar X-ray examinations do not reveal the rotational abnormalities [29, 76]. Moreover, the assessment accuracy solely by CT/radiography is questionable [27, 28]. Previous studies showed that 3D reconstruction of bi-planar radiographs or CT vs standard 2D visualisation of radiological data on PACS systems, did not exhibit significant differences during the lower limb length and alignment angle measurements. Significant differences were found only for pelvic obliquity and rotation. Even though 3D reconstructions of radiological data are interchangeable with clinically standard 2D viewing methods, they presented a

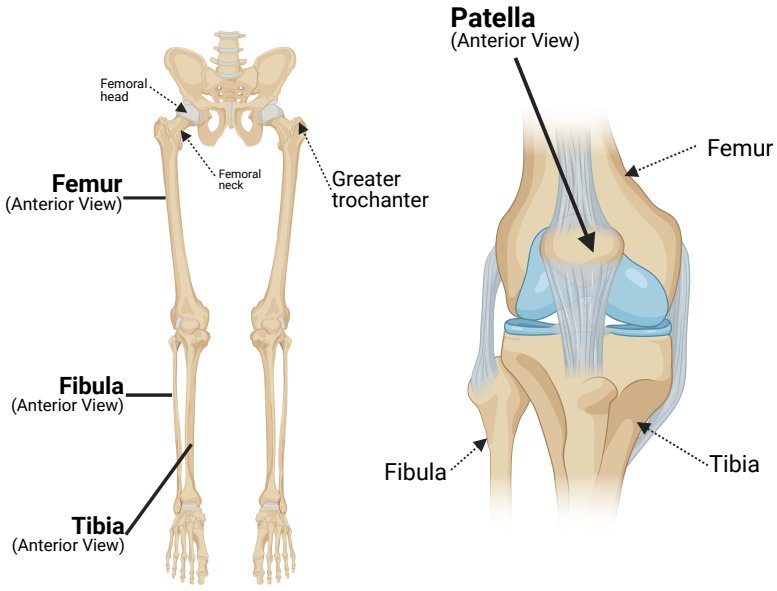


**Figure 2.2:** Lower limb anatomy (left), including the patello-femoral knee joint (right). Created with BioRender.com.

superior inter-reader agreement [77, 78].

The Modified Perth Protocol, employing 2 mm thick select axial CT scan acquisition through femoral necks, knees and ankle joints, is often used to diagnose rotational abnormalities [79, 80]. Conventionally, radiologists determine the lower limb rotational profile by measuring various CT angles directly on 2D CT slices (Figure. 2.3). The femoral neck-horizontal axis angle determines the femoral neck anteversion/retroversion angle. The distal femoral condyle-horizontal axis angles are then measured and the degree of femoral rotation is determined as a relative angle between proximal femoral neck-horizontal axis and distal femoral condyle-horizontal axis angles, expressed as femoral internal or external rotational angles. The tibial torsion angles are calculated as a relative angle between the proximal tibial condyles-horizontal axis at the level of the knees and bimalleolar-horizontal axis angles at the level of the ankles; the tibial torsion is described either as positive external rotational or negative internal rotation [81].

Patella tracking can be treated surgically [82, 83, 84, 85] when the tibia is in valgus or varus deformity, by guided growth using plates. However, if the correction of the varus/valgus deformity does not improve the Q-angle, the external rotation of the distal segment of the femur must be considered. If mal-tracking persists, a displacement osteotomy of the patella insertion on the tibia may be required.

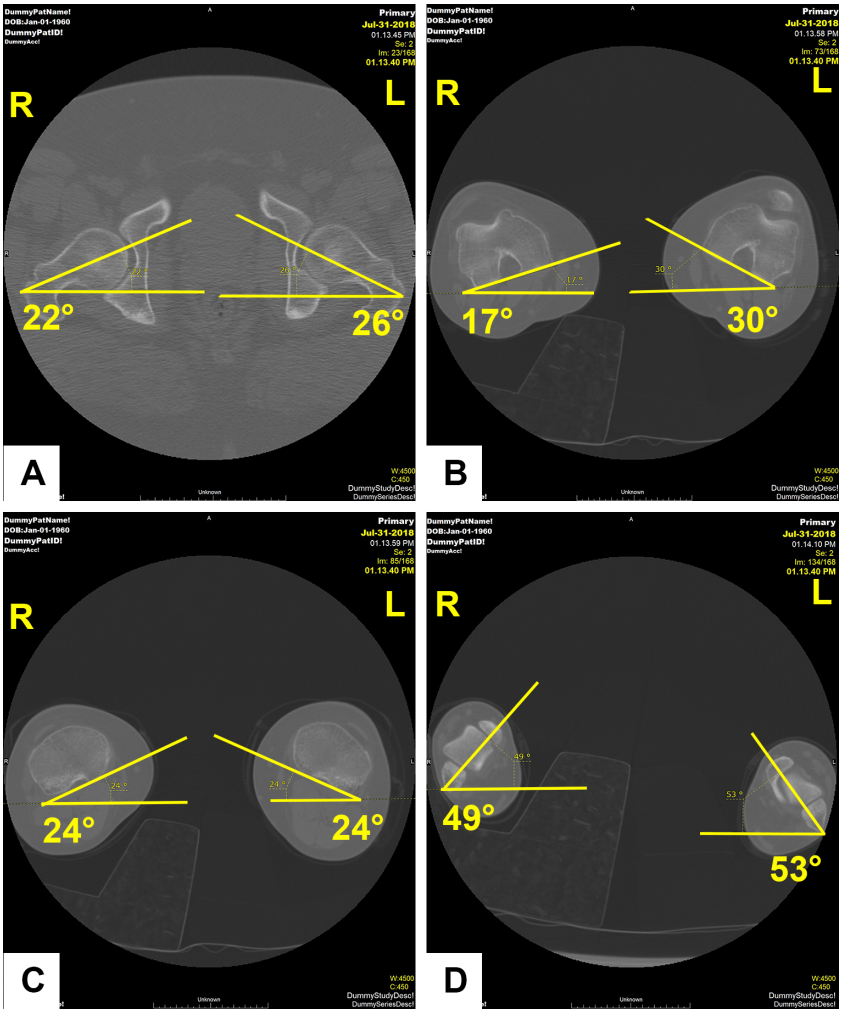


**Figure 2.3:** The femoral neck-horizontal axis angle (A); distal femoral condyle-horizontal axis angles (B); Proximal tibial condyles-horizontal axis at the level of the knees (C); Bimalleolar-horizontal axis angles at the level of the ankles (D).

## 2.3 Liver Pathologies & Resection

Primary and secondary (metastatic) liver cancer is the sixth most common malignancy and the third leading cause of cancer-related deaths worldwide [86], hence its epidemiology is of major interest in Europe and North America. The European Commission's estimates of new cancer cases in the EU in 2022 increased by 2.3% in comparison to 2020 totaling 2.75 million cases. Cancer deaths went up by 2.4% since 2020. The incidence in 2022 across the EU27 is 12.8 and the mortality is 11.1 people per 100,000 [87]. In the United States, the CDC reports incidence of liver and intrahepatic bile duct cancer between the years 2016 and 2020 of 8.6 and mortality of 6.6 people per 100,000 [88].

Specifically primary liver cancer, including hepatocellular carcinoma (HCC) and intrahepatic cholangiocarcinoma (ICC), has been particularly common in Europe, North America, and Oceania [89]. HCC, the more common type, develops from the liver's hepatocytes, whereas ICC originates within the bile ducts inside the liver [90, 91]. Risk factors contributing to the development of primary liver cancer encompass chronic hepatitis infections, hepatitis C virus, alcohol abuse or non-alcoholic fatty liver disease [92, 93]. Secondary liver cancer, also known as metastatic liver cancer, occurs when cancer cells from other parts of the body spread to the liver. In Europe and the United States, secondary cancer is more common than primary liver cancer [94] and the one-year survival rate is lower in the case of secondary liver cancer [95]. The most widespread cause of secondary liver cancer is colorectal cancer [96]. The incidence of secondary liver cancer is associated with specific etiologies with lower levels of economic development being linked to higher incidence rates [97].

The International Hepato-Pancreato-Biliary Association (IHPBA) classifies liver resections into four types: *minor* resections for smaller, peripheral tumours; *major* resections for larger, centrally-located tumours; *anatomical* resections for specific liver segments; and *extended* resections for advanced liver disease, possibly requiring liver transplantation [98, 99] (Figure. 2.4). In terms of procedures performed, IHPBA classifies them into large lesion removal including open resection of the right or left lobe of the liver, hepatic vascular resection for tumours near vital liver connections, and targeted segment resections for peripheral tumours [100, 101, 102]. Treatments also extend to liver adenomas and echinococcal cysts, with a focus on preserving liver functionality [103, 104]. In children, hepatoblastoma treatment may involve liver resection combined with chemotherapy and radiotherapy [105, 106, 107]. In terms of surgical outcomes, major liver resection is associated with increased morbidity and mortality, while minor liver resection has similar peri-operative results with a staged approach of removing liver segments [108]. Liver resection is a critical aspect of liver cancer treatment, and understanding the various types of liver resections and their implications is essential for optimizing patient outcomes [30, 31].

## 2.4 Robotic-assisted Thoracoscopic Surgery (RATS)

Robotic-assisted thoracoscopic surgery (RATS) represents an evolution in thoracic surgery, offering an array of advantages over conventional open approaches and video-assisted thoracoscopic surgery (VATS) [109]. Its adoption has increased for a range of procedures, from lobectomies and segmentectomies to complex surgeries such as resections of mediastinal cysts and tumours [110, 111].

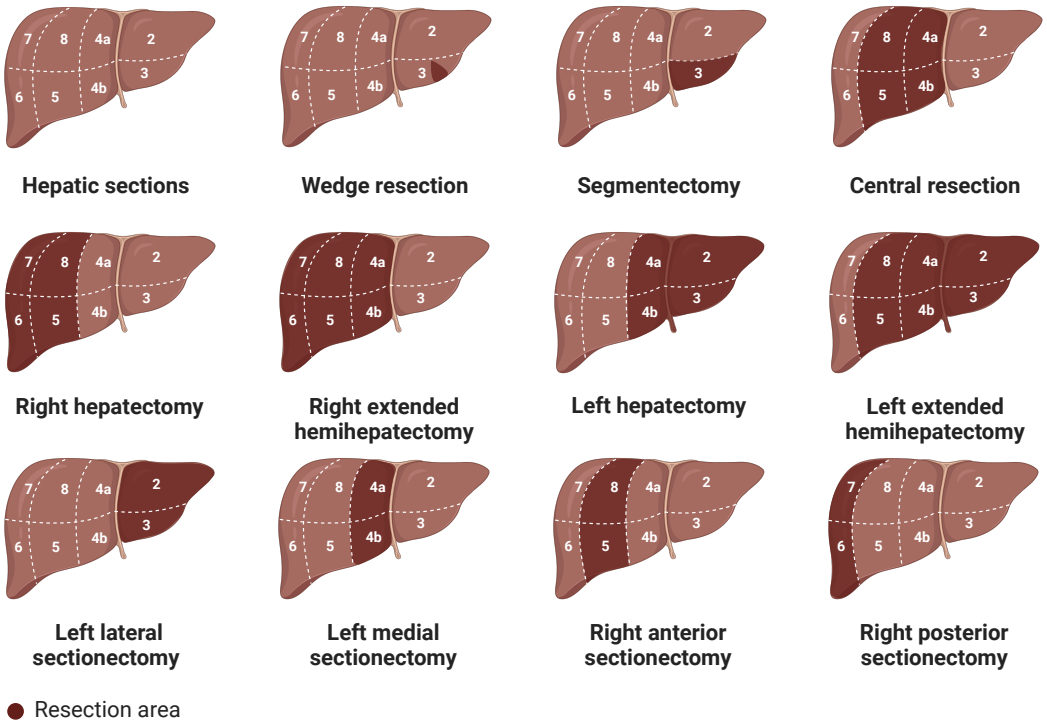


**Figure 2.4:** A visual representation of the major liver resection types. Numbers in the hepatic areas indicate a number of individual liver segments. The left lobe of the liver includes segments 2, 3, 4a, 4b. The right lobe is made out of segments 5, 6, 7, 8. Segment 1 is the caudate lobe located posteriorly (not displayed in the render). Created with BioRender.com

RATS provides surgeons with improved three-dimensional visualization, enhanced precision, and reduced tremor, making it a preferred choice for many [112]. Moreover, studies indicate that RATS can result in less postoperative pain, lower mortality rates, shorter hospital stays, reduced chest tube duration, and fewer postoperative pulmonary complications compared to VATS. It has also been linked with better quality of life outcomes following lung cancer resections [113].

The rise of RATS has been largely driven by the advent of technologies like the DaVinci system (Figure. 2.5), which facilitates safer and more minimally invasive procedures [114]. This technique has been utilized in a variety of cases, from lung cancer resections to the management of intrathoracic goitres and pulmonary sequestration [115, 116].

Port placement in RATS presents a critical set of challenges that significantly influence surgical access, instrument manoeuvrability, and overall surgical outcomes (Figure. 2.6) [33]. A foremost challenge is achieving ideal port placement to facilitate effective triangulation and instrument movement within the constrained space of the thoracic cavity. This is especially pivotal in RATS, where strategic robotic

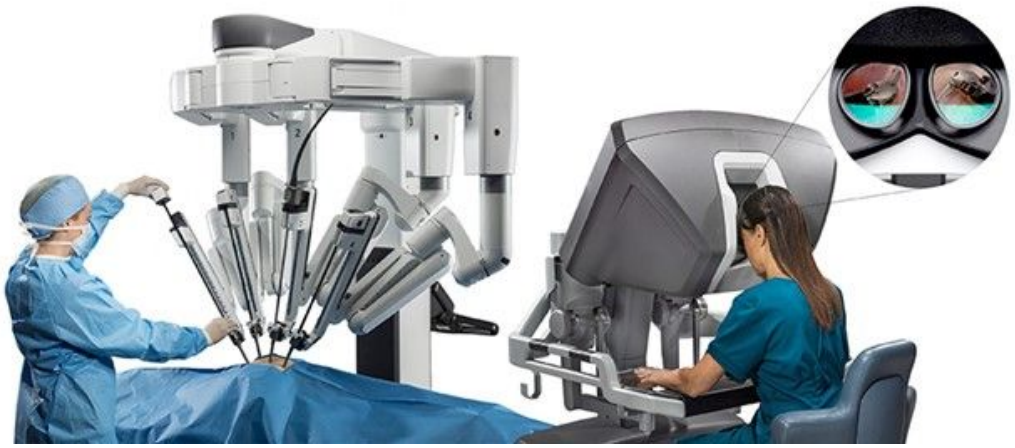

**Figure 2.5:** An illustration of porting the DaVinci Xi system into the thoracic cavity of a patient (on the left), and a surgeon controlling the robot's movements by using the console (on the right).

arm positioning is essential for navigating anatomical structures and executing precise surgical manoeuvres [34]. Additionally, creating adequate distance between the robotic arms is a necessary consideration when placing ports, particularly in patients with smaller chest cavities. This helps to prevent instrument clashing, ensuring a smooth operation.

A separate challenge is adapting port placement to cater to individual patient anatomy variations such as scoliosis, pectus excavatum, or intrathoracic herniation of abdominal viscera. These variations can affect port positioning, often requiring adjustments to secure optimal surgical access and manoeuvrability [35].

Accurate 3D reconstructions from CT scans are crucial for effective preoperative planning and optimal port placement. However, accurately placing these ports in vivo can be challenging due to variations in patient-specific anatomy and intraoperative factors [32]. Moreover, the shift from traditional open surgery or VATS to RATS can pose a learning curve for surgeons. They may face difficulties in determining effective port placement strategies for robotic procedures. To overcome these challenges, training and experience are key in optimizing the surgical approach in RATS [117].

## 2.5 Size-Matching of Donor and Recipient in Lung Transplantation

Lung transplantation is a highly intricate procedure where the matching of donor and recipient organ sizes is paramount for successful outcomes. This process in-

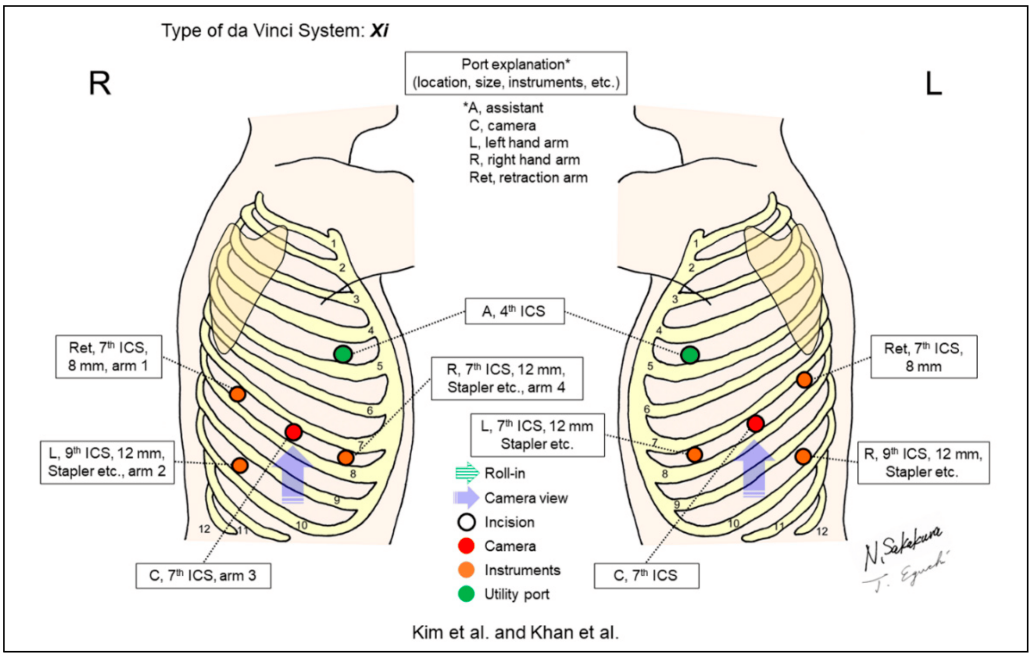


**Figure 2.6:** An example of port placement for each individual arm of Da Vinci for right upper lobectomy using the robotic stapler[1].

volves a detailed assessment of the total lung capacity (TLC) and chest volume of both parties to ensure compatibility. The significance of size matching in lung transplantation has been underscored in numerous studies, which have consistently highlighted its impact on post-transplant outcomes, specifically rejection burden, bronchiolitis obliterans syndrome, and overall survival [37, 36, 38, 118, 39].

The process of size matching becomes even more challenging in pediatric lung transplantation. Smaller children often wait longer for size-matched donor lungs compared to adults [119]. Achieving optimal size matching for pediatric recipients is a significant hurdle in lung transplantation, and size mismatching can lead to increased mortality, especially in preadolescent patients [120]. Potential risks are also associated with using pediatric donor lungs for adult recipients due to size-based tidal volumes and height mismatch [121].

In some instances, lobar lung transplantation is a viable solution for pediatric patients who have been on the waiting list for an extended period of time and are in need of immediate transplantation. Also, lobar lung transplantation often involves urgent small recipients who may face difficulties in obtaining size-matched lungs promptly [122, 123]. The use of size-reduced lung transplantation in children and small adults further necessitates meticulous size matching, with various methods proposed to achieve optimal matching [124].

Several methods exist for evaluating donor-recipient size matching, such as pre-

dicted total lung capacity (pTLC), X-ray sizing, and CT volumetry. However, these methods face many challenges in terms of accuracy and effectiveness. A significant issue is the lack of comprehensive literature detailing the current practices and the impact of size matching on outcomes [39]. This lack of data can hinder the decision-making process during organ donor offers.

### 2.5.1 Predicted Total Lung Capacity (pTLC)

The pTLC ratio is a critical metric in lung size matching. This ratio is calculated using formulas based on sex, height, and age, and is a cornerstone in current lung size matching procedures [38, 36, 118]. The accuracy of pTLC calculations is vital for assessing lung size compatibility, which is a key contributor to the success of lung transplantation procedures [39]

Moreover, using pTLC as a lung size proxy may not always accurately reflect the functional lung volume, leading to a discrepancy between anatomical size and functional capacity [125]. This discrepancy can result in suboptimal size matching. Similarly, the reproducibility and reliability of CT volumetry, a method seen as a promising technique for assessing lung volume, require further validation [126].

For men, the predicted TLC in litres can be calculated using the European Respiratory Society (ERS) formula [127, 128]:

$$\text{pTLC (liters)} = (7.99 \cdot \text{height in meters}) - 7.08 \tag{2.1}$$

**7.99** is a coefficient that represents the increase in predicted Total Lung Capacity (in litres) per meter increase in height. It indicates that for every meter increase in a male's height, the predicted TLC increases by 7.99 litres before any adjustments. This value reflects the strong relationship between a person's height and lung volume, with taller individuals typically having larger lung capacities. **-7.08** is subtracted from the height-based prediction before the final calculation is made. The coefficient serves as a baseline adjustment that shifts the entire prediction equation up or down. In practical terms, this adjustment accounts for factors not directly related to height that can influence lung volume. For example, it helps ensure that the equation provides realistic estimates for individuals at the extreme ends of the height spectrum, where a simple proportional increase might not accurately reflect physiological realities.

For women, the predicted TLC in litres is estimated by:

$$\text{pTLC (liters)} = (6.60 \cdot \text{height in meters}) - 5.79 \tag{2.2}$$

**6.60** is a coefficient that indicates the increase in predicted Total Lung Capacity (in litres) for each meter increase in height for females. It suggests that for every meter increase in a female's height, her predicted TLC increases by 6.60 litres before any adjustments. The value is slightly lower than that for males, reflecting the general trend that females, on average, have smaller lung volumes than males of the same height, partly due to differences in body composition and thoracic cavity size. **-5.79** is a constant subtracted from the height-based calculation and serves as a baseline adjustment for the female predictive model. This adjustment accounts for non-height-related factors influencing lung volume and ensures the equation provides realistic estimates across the range of female heights. It adjusts the baseline predicted TLC downward to better align with the typical lung volumes observed in females.

### 2.5.2 X-ray Sizing and Computed Tomography Volumetry

Techniques like chest X-ray sizing and computed tomography volumetry can provide data for more optimal matching and reduce complications [129, 130] (Figure. 2.7 & 2.8). However, the precision of chest X-ray lung height measurements is a concern. Errors in these measurements could lead to size-mismatched lung transplant procedures, negatively affecting postoperative outcomes [131].

Predicted total lung capacity by using computed tomography ($TLC_{CT}$) volumetry has emerged as a promising technology in this field. It facilitates size matching by allowing for a more precise comparison of a transplant recipient's lung volume with that of a donor's pTLC [126, 132]. This method has shown efficacy in downsizing oversized grafts in brain-dead donor lung transplantation, with a significant correlation observed between the calculated size matching and the ratio of the recipient's chest volume to the donor's lung volume [132]. In another study, $TLC_{CT}$ showed smaller predicted volumes than pTLC, and it was more apparent in obstructive lung disease that recipients were struggling with [38]. Therefore, both the difference between $TLC_{CT}$ and pTLC, as well as lung disease patterns of candidates should be considered in lung size matching for transplantation. Although 3D-CT volumetry is considered a promising technique for assessing lung volume, more robust evidence is required to establish its superiority over traditional methods like pTLC measurements through pulmonary function tests.

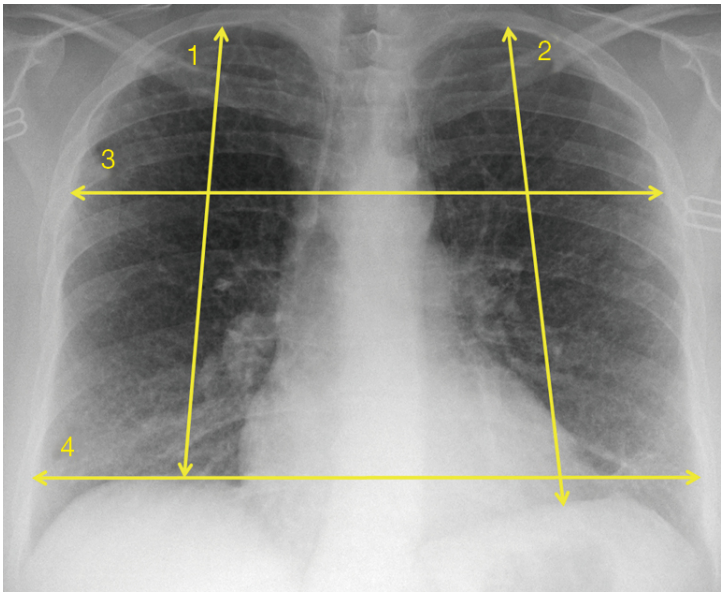


**Figure 2.7:** An example of lung measurements performed on donor and recipient chest radiographs to optimize matching. The lungs are measured from the dome of the right hemidiaphragm to the apex of the right lung **1**, the dome of the left hemidiaphragm to the dome of the left lung **2**, the width of both lungs together at the level of the aortic knob **3**, and the width of both lungs together at the level of the higher hemidiaphragm **4** [2].

In conclusion, while predicted total lung capacity and other methods provide valuable frameworks for lung size matching in transplantation, there is a clear need for further research, standardization, and development of more accurate and reliable techniques. This will enhance the success rates of lung transplantation procedures and improve post-transplant outcomes for recipients.


**Figure 2.8:** A visual representation of lung segmentation for volumetric estimates (in orange) for the left and right lung in Syngo.via Pulmo 3D (Siemens Healthineers, Germany).

Chapter 3

# IKEM VRLab: Clinically Scalable VR System for Surgical Planning†

In this chapter, we present our platform IKEM VRLab, a clinically scalable system developed to aid pre-operative planning for various organs. Our system is deployed on the commercially available standalone headsets Meta Quest 3 and Pro and developed in the Unity 3D Engine (Unity Technologies, USA) [134], providing an immersive VR platform where surgeons can plan the operation on an organ based on patient-specific data from medical imaging. Different surgical strategies can be evaluated and visualised before performing the intended operation/resection on the patient and prospective resection proposals and estimates of the volume of remaining parts of the organ can be calculated.

Central to our approach is the system's flexibility and scalability that allows remote distribution of patient-specific 3D reconstructions from a centralised secured location while maintaining its capacity to meet the demands of a large transplantation clinic of Institute for Clinical and Experimental Medicine (IKEM) (Figure. 3.2 for a system overview). Our system can adapt to new surgical techniques and supports the integration of a variety of surgical planning tools. Additionally, it fosters collaboration between medical professionals by sharing detailed surgical plans and patient data in real-time, thus facilitating multidisciplinary team discussions and decision-making processes via the implemented collaborative components.

†The contributions of this chapter were published in Springer Visual Computer [133] - some postliminary elements of this chapter are under review in the Springer Virtual Reality Journal with the title IKEM VRLab: VR System for Surgical Planning of Liver Resections.

Our *two* specific contributions include:

- We developed a VR system specifically tailored for scalable clinical use and deployment, supporting collaborative efforts within a single clinic or in international multidisciplinary settings. The system supports the planning of complex surgeries by creating a centralised patient data distribution system, a VR platform with a collaborative network component, and a set of optimisation tools to support the visualisation of complex patient data. The system is designed to be usable across different medical fields by supporting the integration of toolkits to enable a variety of surgical procedures.

- We developed and applied a novel approach for validating volumetric properties of models segmented from CT imaging converted for a VR environment to quantify possible deviations from the ground truth volume and establish the accuracy of our 3D model conversion algorithms.

## 3.1 System Architecture

The system is based on the Unity Engine [134], a popular platform for developing applications for Virtual Reality. Unity provides robust tools and the flexibility required for creating complex scenarios and interactions. This allowed us to create a detailed and immersive virtual environment that is the foundation of IKEM VRLab.

### 3.1.1 Collaborative surgical planning environment

The premise of our approach is a collaborative surgical planning environment for the clinical evaluation of patient organ reconstructions (from CT and MRI scans) that can be joined remotely by several VR users or observed by PC users, enabling involvement of supporting medical staff. The VR application consists of two environments: A main menu and a surgical planning room. The main menu provides the user with options to select patient data files for examination and set visualisation options for the surgical planning room (Figure. 3.1). A Patient Data Controller component downloads JSON-formatted patient data previously uploaded to the distribution portal. Following data parsing, button elements are instantiated in the UI canvas for each patient separately, containing information such as patient's name, file name, and a variable assignment that will serve as an identifier for the

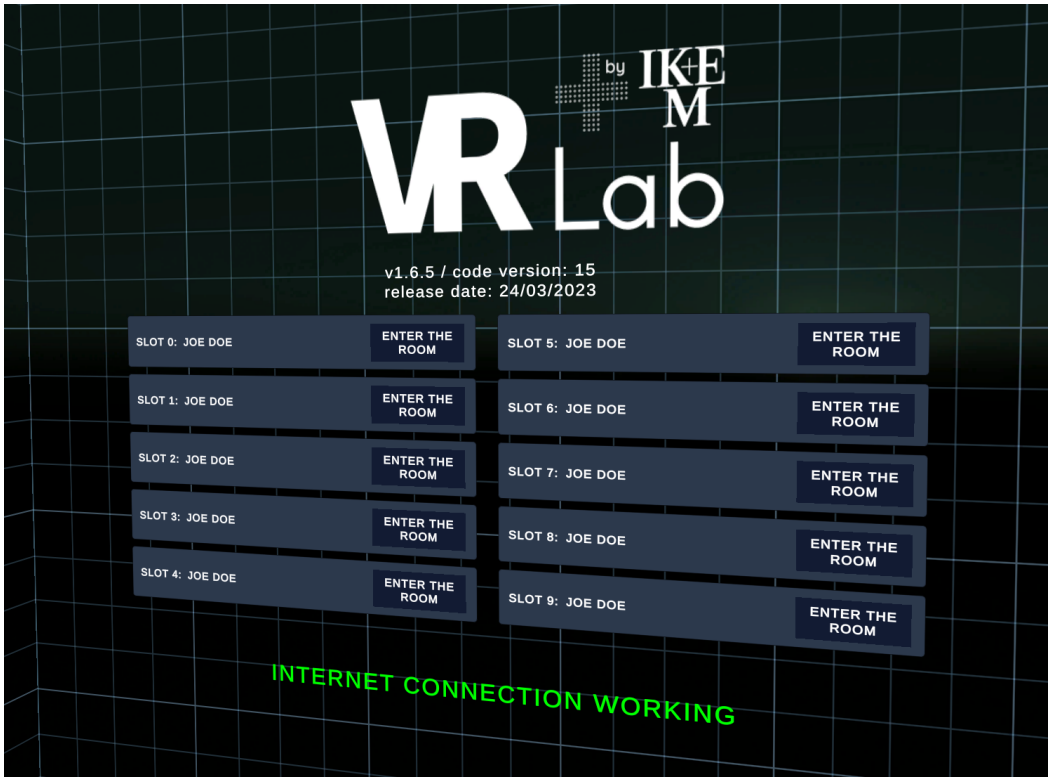


**Figure 3.1:** A screenshot of the *Main Menu* scene with a UI rendering of all available patients currently available on the distribution portal.

virtual room; this enables remote users to identify the same patient case on another device, when multiple users are joining the same room where they can interact with each other (Figure. 3.2).

The surgical planning room is a box-shaped 3D environment, with dimmed lighting to minimize ocular strain. At the centre of the room, the 3D model of the manipulated organ in addition to other information are loaded at runtime fetched from a central database (see Subsection 3.1.5). This data is processed by a custom OBJ URL importer that re-constructs the organ 3D model at a 1:1 real-world scale. The environment employs Photon Network [135] components for synchronising interactions across multiple users and incorporates Photon Voice for remote communication. Photon components are crucial for enabling the collaborative surgical planning environment described in this section. The VR application includes a main menu and a surgical planning room. Photon Network components synchronize interactions across multiple users in real-time, allowing surgeons and medical staff to collaborate remotely. Photon Voice facilitates remote communication by enabling audio conversations, essential for discussing complex surgical plans. The Photon Voice Network transmits users' voices, recorded by the Recorder component from the user's microphone, to other users, creating a virtual environment where

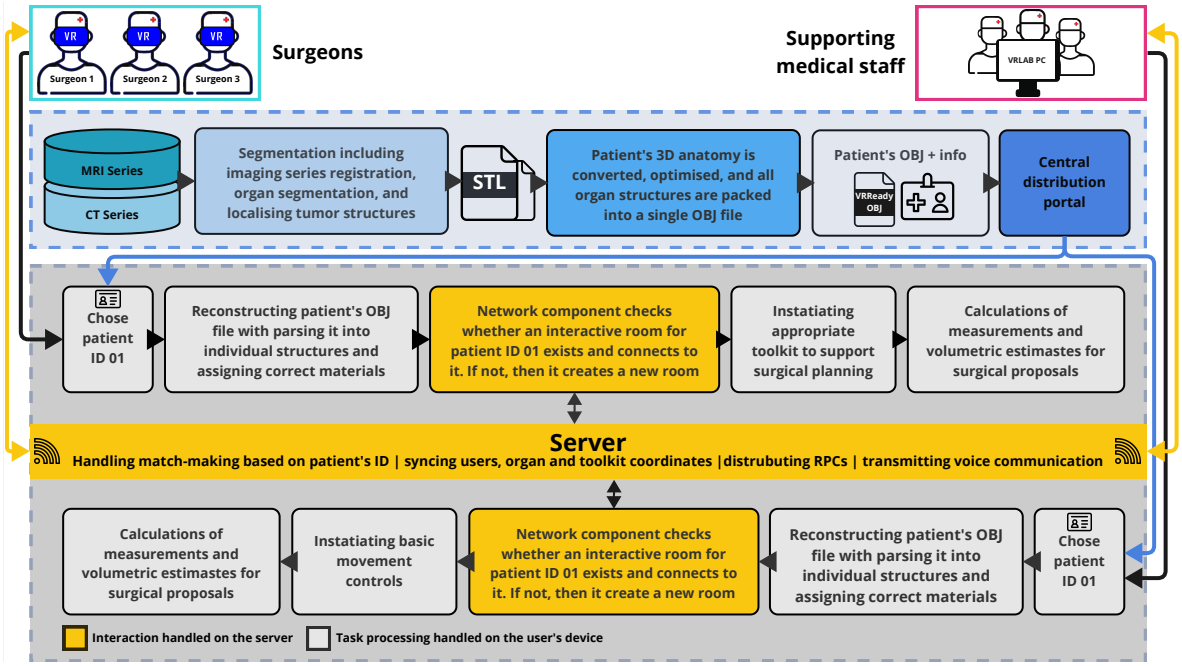


**Figure 3.2:** Overview of VRLab system's architecture. It showcases the pipeline of patient data segmentation, optimisation and distribution (blue coloured). Black arrows from *surgeons* (VR app) and *supporting medical staff* (desktop app) groups visualise the flow of different steps that the application performs when selecting the same patient at different platforms from the main menu. The yellow line visualises the synchronisation between users, allowing interactive collaboration. The interaction between VR users (surgeons) is synchronous, while the users connected via desktop application have no controls regarding the surgical planning process and can only move around, observe, and discuss the procedure via integrated voice chat.

participants can converse as if they were in the same room.

Virtual avatars have been implemented to ensure coordination between multiple users sharing the same virtual environment (up to 20, currently). These avatars are spawned for each user when joining the virtual room. An avatar consists of a sphere corresponding to the head of the user with a VR headset model attached indicating the direction of the other user's head. Additionally, models of hands are visualised so users can point to areas of the patient's anatomy to each other.

Surgeons not sharing the same physical environment with their colleagues when discussing cases or investigating and planning surgical procedures require audio chatting capabilities. Therefore a Photon Voice plugin has been implemented to provide users with such functionality. Recorder and Photon Voice Network components implement the transmissions of users' voices. The Recorder component records the audio from the user's microphone and distributes it to other users via the Photon Voice Network component. The audio source is located at the centre of the user's avatar head. Therefore, the origin of the sound appears to follow users

as they move.

The system also places a strong emphasis on security to ensure patient data is protected. All patient data, including 3D reconstructions and accompanying health information, is uploaded to a centralized, secure location. The uploading, storage, processing, and distribution of this data are handled via a web portal and centralized repository, which employs multiple security measures. More details are described in Section 3.1.5.

### 3.1.2 3DUI

Users interact with the reconstructed organ mesh using VR controllers, which are tracked in 3D space. Users are able to grab, move, rotate, and scale the organ mesh as if they were handling a physical object. The application is controlled through a triad of button sets: Hand Triggers, Index Triggers, and the App Menu Button (Figure. 3.5). The organ, serving as the primary focus in the visualisation, is manipulated via either Index Trigger. To grab the organ mesh, the user brings a VR controller near a mesh and holds the Primary Index Trigger. The mesh then "attaches" to the controller, allowing the user to move it around. To rotate or scale

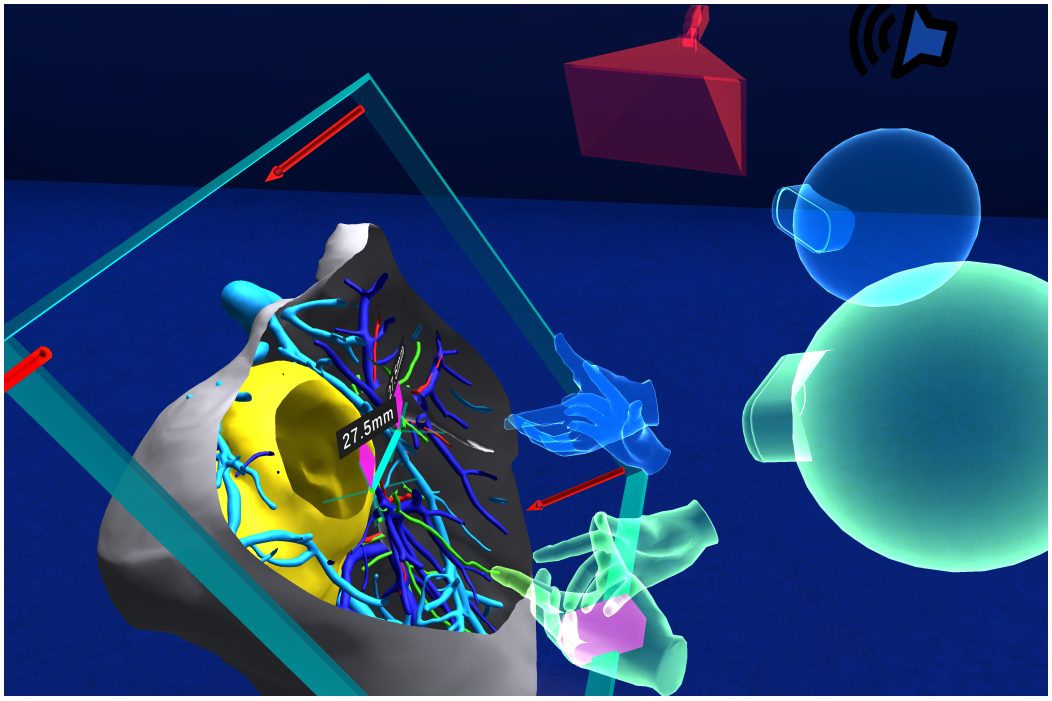


**Figure 3.3:** Two VR users (blue and green avatars) and one PC observer (red camera in the background) discussing placement of a liver tumour (yellow) and its relationship to surrounding structures such as portal vein (dark blue), hepatic vein (light blue), biliary tree (green), and hepatic artery (red) while not being together in the same physical room.


**Figure 3.4:** A screenshot of the control panel displays the patient information board, the layer system, and the panel showcasing the volumetric properties of various organ structures (specifically different liver segments and tumours). Additionally, it features a set of control buttons below the layer system: *mute* (green), *reconnect* (blue), and *main menu* (grey).

the mesh, the user can use both controllers in a gesture similar to stretching or shrinking an elastic object. To ensure optimal user awareness when interacting with other UI elements of imported toolkit supporting particular surgical planning, we have implemented a control scheme organized in a contextually *colour-coded* manner: Integrated tools for surgical planning are represented by transparent purple elements, indicating that the Hand Trigger controls any such element.

Users can interact with different tools independently, eliminating concerns about inadvertently moving organ structures or tools into undesirable positions. For example, holding a segmentation with the left hand by holding the left Index Trigger and manipulating a tool by holding the Hand Trigger on the right controller. However, if necessary, the user can activate both buttons concurrently on the same controller to interact with both the organ segmentation and the tool. This helps

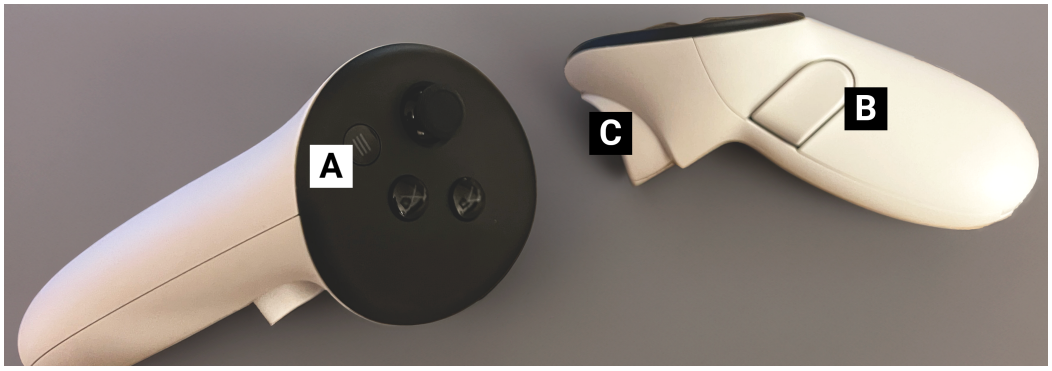


**Figure 3.5:** A picture of Meta Quest Touch controller with App menu button (A), Hand Trigger (B), and Index Trigger (C).

a user to grab and manipulate the organ mesh without affecting an already set clipping plane.

The user also has access to a layer system composed of a set of On&Off toggle buttons for individual organ structures that are instantiated upon the OBJ import (Figure. 3.4). Each button controls the visibility of the structure within the environment, and the state of the buttons is synchronised by making Remote Procedure Calls via the Photon network. The control panel is spawned on the left or right hand based on user's preference when pressing the Start Button. The desired Action can be selected by a *virtual laser pointer*; selection is confirmed using the Index Trigger. The control panel can be also used to mute the voice chat, reset the room to default settings, or return to patient selection (Figure. 3.2). Any progress made during surgery planning is then reflected on any new user entering the VR room by fetching the room cache stored onto a centralised server.

### 3.1.3 VR-ready model optimisation

It is crucial for virtual reality applications to maintain a balance between visual quality and computational efficiency. By reducing the number of polygons without losing critical details, the performance of virtual reality applications is enhanced, a requirement for stable frame rates and realistic user interaction.

The output of our CT and MRI data fusion and segmentation pipeline is an STL 3D model. While STL is efficient for certain applications, this format can be limiting for detailed real-time visualization and manipulation in VR, due to its structure and disconnected triangle faces. In contrast, the OBJ format offers better support for intricate structures, detailed textures and simpler data exchange [136]. The VR optimisation process begins with the conversion of the 3D models to OBJ using trimesh [137]. To then ensure that the model's polygon count is reduced

while preserving its fine geometric details, we employ the quadratic decimation algorithm (using vtkQuadricDecimation from the vtk library) [138]. This step is fundamental in reducing computational demands and enhancing the performance of models in virtual reality. The target number of vertices for each model is a parameter that depends on the required visualisation fidelity of each anatomical structure. For example, a liver model shell may have a lower vertex count compared to its vascular structures that can be represented with much higher amount of vertices to maintain their complex geometry.

### 3.1.4 System optimisations for standalone VR deployment

Scene lighting is a blend of "pre-baked" and real-time lights. The scene's ambient lighting, such as the walls, ceiling and floors, is calculated using pre-computed light transport "baked" light, into a single 1024x1024 pixels lightmap - helping reduce the number of draw-calls when static batching is enabled). Objects which share the same material, as well as the lightmap, are drawn in the same draw-call. Lightmaps are generated by the Progressive CPU Renderer [139]. Pixel light count is set to 1, to maintain high performance on stand-alone VR headsets [140]. Global illumination is processed using the Shadow Mask lighting mode [141]. Lighting the dynamic objects is based on real-time calculations. In order to avoid unnecessary real-time light ray casting onto static models, layer-based filtering is used. Real-time shadow casting is disabled as it would lead to increased draw-calls and polygons due to the high-res organ segmentation.

### 3.1.5 VRLab Secure Patient Data Distribution Infrastructure

The uploading, storage, processing and distribution of 3D patient data and accompanying health information to the VRLab application is facilitated via a web portal and a centralised repository. During data upload, the user is prompted to enter a patient identifier, along with basic patient data and clinical diagnostic information, directly from the Picture Archiving and Communication System (PACS). The user is then asked to upload a 3D reconstruction of the patient data. The 3D reconstruction is stored in an OBJ file format, while patient information in JSON format.

The web application is written in Python using the Django framework [142]. Authentication is handled using an internal Active Directory service, and user data is isolated based on individual access permission flags. All metadata and models, are secured by an individual secret token withing the VRLab application on the device

and accessed using a custom API. Several docker containers (running on Debian Linux), including a web application, nginx and a database, which communicate with each other using the docker-compose configuration facilitate the distribution system for patient reconstructions to VR headsets

OBJ URL importer with API key validation serves the purpose of transferring patients' 3D anatomical data from a centralised server securely. We divided the algorithm into several steps, which we executed sequentially in Unity. First, the component loads the OBJ file from the downloaded model and splits it into lines. Then we processed each row and extracted the necessary information about vertices, normals and triangles. We then created an empty game object to serve as a container for all the reconstructed anatomical structures. We then created a mesh object and populated it with the vertex, normal and triangle data from the loaded file. Next, a game object is created for the mesh and added it to the placeholder for anatomical data. This is followed by material assignment to individual substructures from the single OBJ files base on keywords predefined in the name of the structures. The whole process allowed us to load and process single OBJ model containing all anatomical data of patient's organ structures in Unity from a URL and display them in the immersive scene. The GameObject is destroyed after the user exits the VR session or turns off the headset.

## 3.2 Volumetric Validation of VR-ready 3D models in VRLab

Optimising a mesh by reducing its triangle count may inadvertently affect its estimated volume. In this study, we aimed to validate that the volume estimates provided by our platforms for VR-optimized 3D models generated from CT data organ segmentations accurately reflect the actual volume of the organ.

We first designed a phantom organ that could be scanned using CT (Figure. 3.6.A). The phantom consisted of twelve containers of various shapes and volumes, enabling comprehensive testing of the segmentation algorithms used for different geometric configurations. We 3D printed the phantom striving for maximum volumetric precision: the exact volume of each container was measured and recorded to provide reference data (ground truth - GT).

Each container was filled with a mixture of water and Iomeron 400 mg/ml, an injectable solution used to simulate the contrast imaging of vascular tissues in CT. The ratio of the mixture was optimised so that the Hounsfield unit (HU) values in the scanned container area fell within the range of 150 to 250 HU, corresponding to

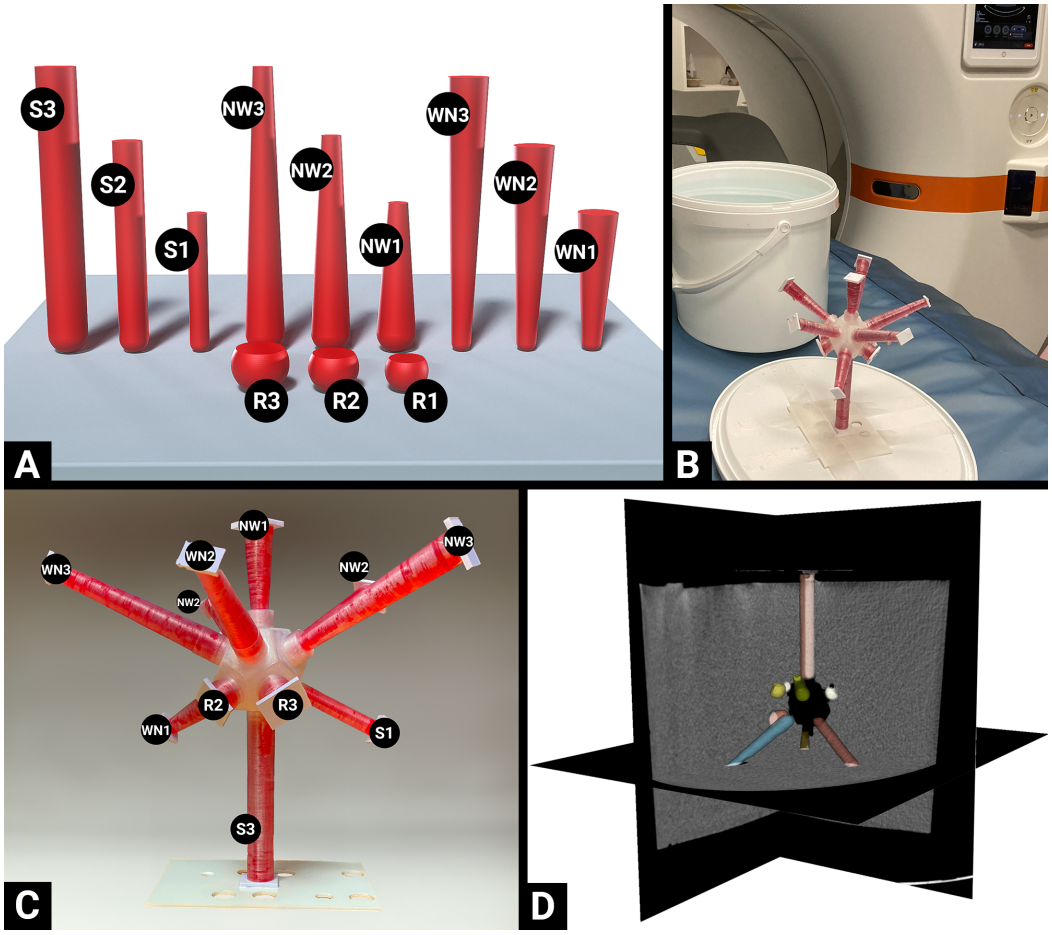


**Figure 3.6:** A digital representation of the inner shape of individual containers (A). Assembled containers into a phantom (C), which was then mounted onto the lid of a 10-litre bucket filled with water (B). A representation of segmented containers filled with a contrast fluid (D). R stands for rounded containers, S for straight cylindrical containers, WN (wide to narrow) for cylindrical containers starting with a wider diameter at the root of the rig than on the outer end, and NW (narrow to wide) representing cylindrical containers with a narrower diameter at the root of the rig with a wider diameter at the outer end. The added number represents size, a smaller number equals to smaller version of that type of the container and vice-versa.

the typical contrast properties observed in vascular structures in a clinical setting when contrast solution is applied.

The containers were mounted into a custom rig oriented in various directions, effectively simulating the diversity of anatomical positions of large and small vessels in the abdominal cavity (Figure. 3.6.C). This rig was mounted on the lid of a container filled with water, whose oval shape resembled the human body's trunk, whilst the water simulated the physical properties of the average human tissue, particularly in the absorption and scattering of X-ray radiation, which was crucial for realistic testing and calibration of CT systems (Figure. 3.6.B).

The phantom was then scanned on a CT device using the same scanning protocol and equipment as used during clinical examinations to ensure the comparability and relevance of the results. Subsequently, we performed segmentation of the scanned data using a thresholding method, with each container identified and marked (Figure. 3.6.D). We then calculated the volumes of the structures using the Scalar Volume module calculation model (3D Slicer software) computed from the number of voxels multiplied by the volume of a single voxel - values were computed only for parts of segments that overlapped with the scalar volume.

The individual segmentations of the containers were then exported in STL format. Each model was optimized and converted to an OBJ format according to our protocol (Section. 3.1.3), with larger containers representing larger vessels having a target polygonal count of 8500, while smaller containers had a target polygonal count set to 2500. This optimization procedure was carried out to ensure that the resulting models (i) were consistent with the geometric complexities of real segmented vessels, (ii) accurately represented real anatomical structures and, (iii) were compatible with the performance requirements to render them in VRLab.

The measurements for individual containers in the VR environment were obtained by implementing a real-time volumetric calculation based on dividing the mesh into a set of tetrahedra, where each triangle of the mesh formed the base of a tetrahedron and a reference point, usually the origin of the coordinate system, was chosen as the vertex. We calculated the volume of each tetrahedron using the scalar triple product, which is a mathematical operation based on the determinant of a matrix composed of the coordinates of the triangle's vertices. It was necessary to use the absolute value of the results to account for the possible negative orientation of the triangles relative to the reference point.

The volume $V$ of the mesh is calculated as the sum of the volumes $V_i$ of all its triangles. The final volume is then multiplied by 1000 to gain a volumetric representation in milliliters, a standard unit in liver surgery.

Considering a triangle with vertices at $P_1$, $P_2$, and $P_3$, where the coordinates are $P_1 = (x_1, y_1, z_1)$, $P_2 = (x_2, y_2, z_2)$, and $P_3 = (x_3, y_3, z_3)$, we can calculate the volume $V_\triangle$ of this triangle using the determinant of a 3x3 matrix formed by these coordinates. The volume is one sixth of the absolute value of this determinant:

$$V_{\triangle} = \frac{1}{6} \left| \det \begin{pmatrix} x_1 & y_1 & z_1 \\ x_2 & y_2 & z_2 \\ x_3 & y_3 & z_3 \end{pmatrix} \right| \tag{3.1}$$

The explicit algebraic expression for the signed volume of a triangle in 3D space is:

$$V_{\triangle} = \frac{1}{6}(-x_3y_2z_1 + x_2y_3z_1 + x_3y_1z_2 - x_1y_3z_2 - x_2y_1z_3 + x_1y_2z_3) \tag{3.2}$$

To compute the total volume $V$ of the mesh, we sum the absolute values of the volumes of all triangles comprising the mesh:

$$V = \sum_{i=1}^{n} |V_i| \tag{3.3}$$

where $n$ denotes the number of triangles in the mesh.

The analysis of observed volumetric measurements was overall very positive regarding the accuracy and consistency of volume measurements across two different ways of volume estimation. When comparing volumes measured onto the CT segmented imaged by 3D Slicer Scalar Volume module and VRLab volumetric calculation based on the Signed Volume of a Triangle against reference values (Ground Truth - GT), most results closely align with GT, indicating high precision in our segmentation and measurement techniques (Table. 3.1).

The volumes measured in 3D Slicer and VRLab consistently matched or were very similar for most containers (R1, R2, R3, S1, S2, S3, WN1, WN2, NW1, NW2, NW3). In containers NW2 and NW3, the CT and VRLab measurements slightly exceeded GT, pointing to potential slight overestimation. The result highlights the successful data transformation between these platforms with insignificant accuracy loss in some cases according to the participating surgeons during the evaluation of IKEM VRLab in liver resection planning (Chapter. 3).

In a comparative study of 12 containers using two volume estimation methods, the Repeated Measures of One-Way ANOVA indicated statistically significant differences across the methods and GT, with an F-value of 6.579 and a p-value of

**Table 3.1:** A table comparing the ground truth measurements of individual containers to volumetric estimates from 3D Slicer Scalar Volume plugin and from VRLab.

| Container | GT (ml) | Scalar Volume 3D Slicer (ml) | Error Rate GT vs. Slicer (%) | VRLab (ml) | Error Rate GT vs. VRLab (%) |
|---|---|---|---|---|---|
| R1 | 0.75 | 0.77 | 2.67 | 0.77 | 2.67 |
| R2 | 1.15 | 1.14 | 0.87 | 1.14 | 0.87 |
| R3 | 1.75 | 1.77 | 1.14 | 1.77 | 1.14 |
| S1 | 1.10 | 1.11 | 0.91 | 1.11 | 0.91 |
| S2 | 3.75 | 3.77 | 0.53 | 3.77 | 0.53 |
| S3 | 8.80 | 8.86 | 0.68 | 8.87 | 0.80 |
| WN1 | 2.80 | 2.87 | 2.50 | 2.87 | 2.50 |
| WN2 | 4.10 | 4.12 | 0.49 | 4.11 | 0.24 |
| WN3 | 5.25 | 5.20 | 0.95 | 5.21 | 0.76 |
| NW1 | 2.50 | 2.58 | 3.20 | 2.58 | 3.20 |
| NW2 | 3.85 | 3.97 | 3.12 | 3.97 | 3.12 |
| NW3 | 5.05 | 5.08 | 0.59 | 5.09 | 0.79 |
| Error Rate Mean | | | 1.47 | | 1.46 |
| Error Rate SD | | | 1.07 | | 1.08 |

0.0237. However, when specifically examining the differences between GT and the other two methods through Tukey's Multiple Comparisons Test, the results were as follows: GT vs Scalar Volume from 3D Slicer yielded a mean difference of -0.032 with an adjusted p-value of 0.067, and GT vs VRLab showed a mean difference of -0.034 with an adjusted p-value of 0.0509. Neither of the comparisons reached statistical significance, indicating that the variations in volumetric measurements between GT and Scalar Volume calculations from 3D Slicer and VRLab were not statistically significant at the 0.05 alpha level.

Chapter 4

# OrthopedVR: Clinical Assessment and Pre-operative Planning of Paediatric Patients with Lower Limb Rotational Abnormalities in Virtual Reality†

Rotational abnormalities of the lower limbs are a relatively common orthopaedic problem (Figure. 2.1). The estimated incidence rate of patients suffering from this pathology is approximately 5.8 per 100 000, and this incidence rate increases in patients 10 - 17 years old. A misaligned joint axis (Figure. 2.2) can lead to joint overloading, the onset of exercise pain, and cause early-onset osteoarthritis. Medical diagnosis of rotational abnormalities requires quantifying the rotational profile of the whole limb both by clinical examination and imaging techniques, preferably by computational tomography (CT) examination. Surgical treatment of these defects depends on the degree of deformity [25] and the patient's age [26].

In this section, we investigate how VR can be used to examine patients' anatomy and visualise surgical outcomes for de-rotational corrective procedures such as the femoral, tibial, and tibial-tuberosity osteotomy. We design and implement a VR system, OrthopedVR, where surgeons can simulate "breaking" the bone and adjusting the rotational profile in each bone segment separately. New segment angles are calculated and the post-operative change in angle is visualised. We achieve this

†The contributions in this chapter were published in the Springer Visual Computer, presented at Computer Graphics International 2023 [133] and recognised with Visual Computer **Best Paper Award**. It was also published and presented at IEEE VR 2023 [143].

by designing an application-specific 3DUI and integrating it in collaborative VR.

Our system was inspired by medical specialists' growing demand for VR visualization tools [20]. As standalone VR hardware becomes more affordable, 2D CT and magnetic resonance images (MRI) transformed into 3D models can be viewed and manipulated stereoscopically in an immersive environment, improving (i) medical judgment, (ii) clinical training, and (iii) operation planning [16]. We specifically focus on VR surgical planning, that enables surgeons understand pathological and anatomical spatial relationships, boosting surgical confidence [17]. As complex surgical procedures and training of future surgeons requires teamwork [40, 144], OrthopedVR also supports VR collaboration and remote consultation with colleagues. We evaluate our VR system based on surgeons' performance when determining bone incision locations and lower limb rotational profile angles in VR, compared to surgical planning using standard clinical digital imaging and communications in medicine (DICOM) viewers for axial CT images. Our study confirms VR's practical benefit in lower limb clinical assessment planning.

Our *three* specific contributions include:

- We developed a toolkit, OrthopedVR, enabling surgeons to examine 3D reconstructions of CT scans of patients suffering from rotational abnormalities and patellar mal-tracking in an immersive, multi-user, collaborative environment.
- To facilitate this, we extended the UI with an application-specific, hybrid 3DUI combining contextual and static UI designs. The 3DUI controls the surgical planning simulation by providing incision positioning, post-incision leg re-alignment, and post-operative angles calculation and visualisation.
- We performed a quantitative and qualitative evaluation for corrective osteotomy planning of the lower limbs in VR. Four expert orthopaedic surgeons endorse our methodology.

## 4.1 Architecture

OrthopedVR, provides surgeons with a VR environment where they can rehearse an osteotomy beforehand, based on real patient measurements, and visualise its outcome. Various angle correction amounts can be appraised and visualised before operating on the patient. A surgeon first indicates the anticipated incision plane. Our system then recalculates the geometry of the segmented bones and generates two superimposed bone segments that can be manipulated independently and then

fused back, in a collaborative manner. OrthopedVR is implemented in Unity3D (Unity Technologies), and deployed on Meta Quest 2 headsets.

We leveraged the multi-user capability from the IKEM VRLab platform in OrthopedVR. The collaborative virtual environments enable surgeons to work on patient cases jointly, increasing their ability to understand a case and treat it effectively. Additionally, the implementation of collaborative mode provided respondents with adequate VR training by the study coordinator before they were asked to evaluate our system (Figure. 4.1). At the start of the VR training session, respondents are able to observe the instructor interact with the 3DUI elements in the VR environment, but also practice the controls themselves.

The user enters the VR room with the patient's reconstruction, where all interaction happens. A 3D model of the patient's lower limbs hovers in the centre of the room. Following preliminary testing, we chose colours for the background and the different osseous structures to maintain a strong perceived contrast and enhance their distinctiveness. We avoided using brighter colours (the natural beige colour of bones), as they strained users' eyes during preliminary testing.

The main task that must be performed in VR is bone cutting and repositioning based on bone segment angles. To do so, the user grabs a *Cutting Cube* using the controller, which defines the position and direction of the cutting plane. The plane has six degrees of freedom (6-DoF). We devised a whole set of different 3DUIs, to aid the cutting process decision making, which we present in the next section.

### 4.1.1 3DUI

Our application-specific 3DUI (Figure. 4.2) combines multiple UI principles [145] to aid with decision making and information visualisation, and is only controlled with two physical buttons, Index Triggers and Hand Triggers. We combine three different UI design paradigms to enable users make treatment-related decisions and actions whilst having access to all required information at all times. The dynamic UI maintains relevant items/options visible and ready to select/view depending on the surgery simulation state, *without* tedious searching in non-intuitive scroll-view menus.

#### 4.1.1.1 Contextual UI

A contextual UI enables direct interaction with the lower limbs, appearing where an incision is being performed. The contextual UI model is based on OVR Unity

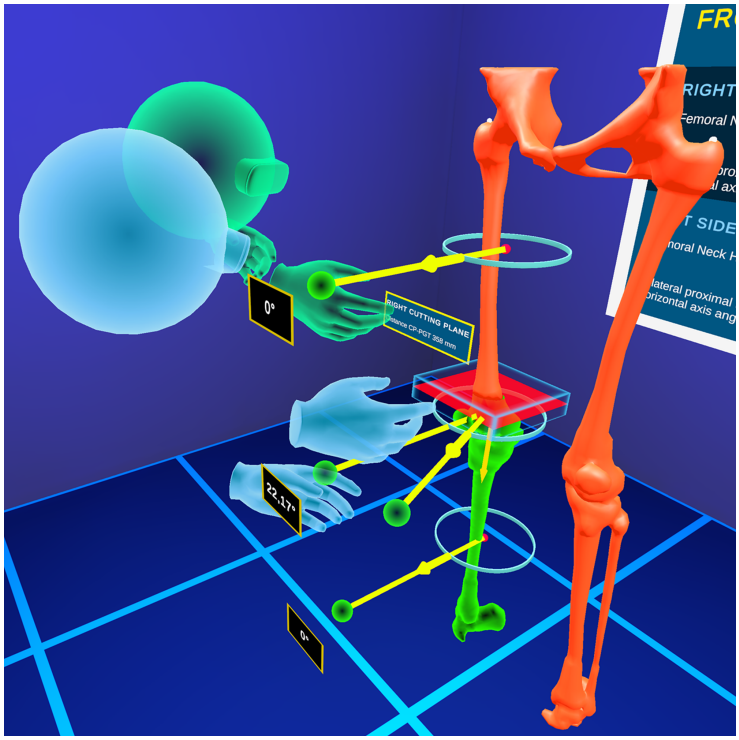


**Figure 4.1:** A study coordinator (green avatar) and the respondent (blue avatar) training on a collaborative osteotomy before the beginning of the evaluation session.

integration. The user adjusts the rotation of the limb segment by touching the limb and rotating the wrist. The interaction algorithm utilizes a combination of gesture recognition, inverse kinematics (IK), and rotation and translation calculations. Using data from the VR controllers, the system identifies and interprets the user's gestures to apply corresponding transformations to the 3D model. The IK algorithm from the OVR Avatar calculates the necessary joint angles to achieve the desired limb segment positioning, ensuring realistic and intuitive manipulation. The system applies quaternion-based rotation calculations to avoid gimbal lock and ensure smooth, continuous adjustments. The OVR Grabber function from the OVR Unity integration ensures user's manipulation with the incision plane and different lower limb segments to adjust the rotational angle. A protractor (Figure. 4.2.A) indicates the rotation angles achieved for each bone segment. This UI provides essential data for decision-making, increasing situational awareness when manipulating bone structures.

#### 4.1.1.2 World-positioned UI

A World-positioned UI displays key patient/procedure-related data that should be available at all times, collected during the clinical examination, e.g., rotational angles measured in different locations on both lower limbs (Figure. 4.2.B). This UI is purposefully fixed, always-present. Fixed position rendering ensures the UI remains in a constant position relative to the user's viewpoint. Real-time data binding algorithm updates the displayed information dynamically as new measurements or adjustments are made. The world-positioned UI parses JSON and loads data from the distribution portal (Section. 3.1.5), ensuring that all relevant patient data is accurately displayed and updated.

#### 4.1.1.3 Dynamic control panel UI

This is a point-and-click control panel, dynamically updated, visible at all times, *attached* to the left controller (user's left hand - for right-handed users; can be swapped for left-handed users) providing immediate access to the most essential functions (Figure. 4.2.C). Pressing the Secondary Index Trigger selects the indicated task. The UI includes dynamic content management, raycasting for selection, event handling, coordinate tracking, and Photon Network integration. The control panel uses a state management component to update the available options based on the current context of the surgery simulation. Raycasting algorithms enable precise selection of UI elements by casting a ray from the controller to determine which button the user is pointing at. Once a call-to-action (CTA) button is selected, event-handling algorithms trigger the corresponding functions essential to bone-cutting and other planning tasks. Individual CTAs are connected to remote procedures via the Photon Network, ensuring that all information is transmitted across different users during the collaborative session.

### 4.1.2 Collaborative osteotomies

The collaborative mode in OrthopedVR allows multiple surgeons to participate in the osteotomy planning and rehearsal. The system synchronizes actions such as cutting, rotating, and repositioning bone segments in real-time across all connected users. This synchronization is achieved through a combination of server-client architecture, real-time data streaming, and conflict resolution. A central server coordinates all interactions with clients (user devices), sending and receiving updates to ensure a consistent experience. Algorithms for conflict detection and resolution

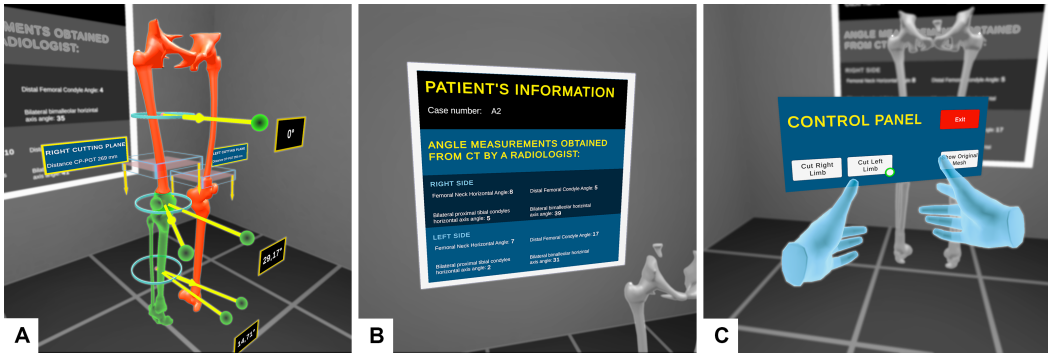


**Figure 4.2:** (A) The contextual 3DUI providing bone-cutting actions and relevant information visualisation. (B) The world-positioned UI, omni-present, communicating essential information. (C) Dynamic control panel UI, attached to the one hand of the user and controlled with their other hand, containing context-specific actions that get dynamically updated.

manage simultaneous inputs from multiple users, prioritizing actions and maintaining system stability.

To perform an osteotomy in a collaborative VR environment and calculate accurate rotational angles, we address several technical challenges, such as the complex synchronization required between meshes and environment states:

- The system architecture relies on Photon Network to manage the connections between multiple users. Upon starting the application, the system initializes the Photon Network connection, assigning each user a unique *PhotonView* identifier to manage their actions and synchronize data across the network.
- When a user initiates a bone cutting operation, they interact with the *Dynamic Control Panel* to trigger the cutting process. The system first ensures that the user has control over the object to be cut by requesting ownership through the network. This is achieved using ownership transfer protocols in Photon Network, which ensure that only the user who initiated the cut can control the slicing process.
- Once ownership is confirmed, the system broadcasts a RPC to all connected clients to perform the cutting calculation. This RPC mechanism ensures that the calculation of the intersection of the slicing plane with the bone model is synchronized across all users. The RPC invokes an algorithm that calculates the intersection points by checking the positions and orientations of the slicing plane and the bone mesh.
- The incision algorithm performs an exclusion check of the intersecting vertices in the limb vertex list. Two vertex lists are created in the intersection plane,

and checks are performed to establish on which side of the cut the final *original* vertices lie. Then two new meshes are created from each vertex list. New vertex normals are then calculated along with their boundaries and tangents for accurate lighting. Different materials are assigned to each segment: a green material indicates the split-off part that should be rotated (orange material means fixed).

- The newly created bone segments are instantiated as separate game objects in the Unity scene using Photon Network's object instantiation methods. These objects are tagged and assigned layers for further interaction and manipulation. The Photon instantiate method is used to create these objects across the network, ensuring that all users have an identical view of the newly created bone segments with Photon View ID assigned.
- To manage the real-time synchronization, the system utilizes Photon Network to handle the transmission of user actions and updates. When new objects are instantiated or when their positions and states are updated, these changes are transmitted to all connected users using Photon Network's state synchronization features. This ensures that all users see the same state of the VR environment.
- Conflict resolution algorithms are employed to manage simultaneous actions by different users. These algorithms prioritize actions based on the order of execution and ownership transfer, ensuring that no conflicting operations occur. For example, if two users attempt to cut the same bone simultaneously, the system resolves the conflict by allowing only the first user's action to proceed while the second user's action is deferred or cancelled.

## 4.2 Evaluation

We evaluated our VR system both quantitatively and qualitatively.

### 4.2.1 Materials & Methods

Quantitatively, our focus was on surgeons' examination performance when manipulating patient CT data on a standard desktop DICOM viewer (as in a picture archiving and communication system, PACS) compared to our immersive 3D reconstruction of the data in OrthopedVR. Our objective performance metric was task completion time for each case and method of assessment. Task completion time serves as an excellent proxy to assess the respondent's spatial understanding

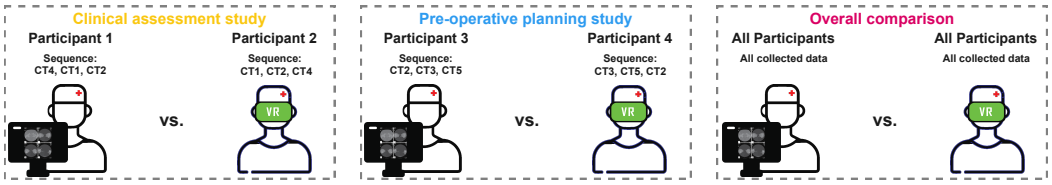


**Figure 4.3:** We split the evaluation cohort in two groups of two, enabling us to draw a plethora of conclusions, despite the limited cohort and dataset size. In the clinical and pre-operative studies we directly compared performance between respondents using a DICOM viewer and OrthopedVR on three cases. All of the data collected from the testing session were then included in the overall comparison of the DICOM viewer vs OrthopedVR, regardless of the study type. Note that the illustration of the testing sequences does not follow the exact order of how respondents viewed the individual cases; the order was randomised for each participant.

of the unique pathological anatomy of the patient. Our goal was not only to measure how much time our technique saves, compared to PACS, but rather establish, in combination with the qualitative questionnaires and user feedback that significantly less cognitive resources are required to diagnose and plan a surgery in VR, versus 2D viewing. System data such as CPU and GPU utilization and average FPS count were also recorded.

Qualitative evaluation data were collected in the form of post-session questionnaires and feedback, particularly focusing on the usability of our 3DUI. An additional, conventional UI usability study with non-experts would not provide valuable data for our purposes, as members of the general population without experience in derotational osteotomies, would not be able to evaluate the UI in the context of surgical planning. More specifically, the qualitative questionnaire is designed to assess user experience when using OrthopedVR for osteotomy planning. We obtained feedback on the visual fidelity, user interface, multi-user interaction capabilities, the quality of the 3D data reconstruction, and the perceived performance of the VR simulation among other things. We also gauged the potential of VR in pre-operative orthopaedic assessment and planning, and assessed the willingness of users to adopt and recommend VR technology for pre-operative planning to colleagues and trainees, thus predicting the potential acceptance and uptake of the technology in the orthopaedic community. Participants responded using an extended Likert scale (1 = "very negative" to 10 = "very positive"). Participants were also asked for insights outside of the pre-set questions.

### 4.2.2 CT data acquisition

Following ethical approval by our department, we obtained five anonymised data sets of patients indicated to undergo lower limb corrective surgery from our country's national health system. The Modified Perth Protocol used in the NHS only records the areas of the proximal femur, femoral condyles, and taulus from an axial view (0.4-0.6mm slice thickness in coronal view, 0.4-0.5mm in sagittal view, and 3.3-3.6mm slices) to reduce X-ray radiation dosage. Due to the missing CT data between the proximal femur, femoral condyles and the taulus, we model the missing structures synthetically. This was required to provide doctors with a realistic 3D model enabling them to locate anatomical features, but no leg joint data were interpolated, or joint angles where affected. We present our bone interpolation/optimisation technique in the next section (4.2.2.1). The CT data were segmented using 3D Slicer based on the master volume range on the Yen's threshold method and using the Robust Statistics Segmenter [146, 147]. Our CT data segmentation and processing was validated by a Lead Consultant Musculoskeletal Radiologist specialising in diagnostic, interventional musculoskeletal and sports imaging (collaborator).

#### 4.2.2.1 Mesh augmentation & optimisation

Due to the aforementioned limitation of missing CT data between the proximal femur, femoral condyles and the taulus, it is necessary to model the missing structures synthetically. This is essential to provide doctors with a realistic 3D model enabling them to locate anatomical features. The remodelling does not affect or adjust the original bone parts as recorded on CT, but rather only adds structures in-between them. This additional geometry helps visualise how different angle changes in various areas of the leg affect one-another. We used a mesh of the lower limb generated from an open-source contiguous CT stack, as the base mesh for the remodelling of the in-between structures. The modelling filling process is performed in Maya (Autodesk, USA), (mean data preparation time 1h 36m (SD=0h 24m).

3D Slicer produces 3D models with dense topology containing millions of polygons and saves them into a .stl CAD format. Due to the noise and artefacts that are present in the CT slices, significantly more *unnecessary* polygons are generated. Importing such 3D models with dense topologies in VR significantly impacts the rendering performance. To ensure a well-performing VR experience, data first go through a re-meshing and decimation process. We used IKEM VRLab's mesh optimisation tools (Section. 3.1.3) for processing and editing 3D triangular meshes.

By using our surface simplification tool based Quadric Error Metrics, we unify neighbouring vertices that share the exact coordinates and reduce the polygon count of the segmented 3D models [148]. After applying this procedure, we obtain an optimised model made of just a few thousands of vertices instead of hundreds of thousands. During software testing, we observed that the model of the entire structure of both lower limbs decreased in polygon count more than 90 times, from 755,644 to 8,234 polygons. That ensures stable performance during run-time on the Meta Quest 2. We studied the possibility of accidentally deforming the anatomical structures, thus decreasing anatomical accuracy, and we found no significant proportional changes in the optimised model. Optimised models from our optimisation tool are exported in the .obj file format. Following the mesh augmentation and optimisation processes, the collaborating radiologist validated the reconstruction by utilizing segmentation software to overlay the 3D reconstructed mesh over the CT volumetric data. This process ensured that possible geometrical deviations in the 3D model compared to the CT image were detected. No inaccuracies were detected in the 3D reconstruction by the radiologist.

### 4.2.3 Participants

According to the most recent report of our national register for knee osteotomies, 49 surgeons are registered in the UK healthcare system [149]. Due to the complicated and invasive nature of derotational procedures, these types of surgeries are only performed by a very limited number of individuals with a vast experience in the field. Despite the scarcity of experienced specialists in derotational osteotomies, we managed to recruit 4 experienced orthopaedic surgeons (8.16% of the professional body in the UK) averaging 20 years of experience in the field (SD=2.36), mean age 50 years (SD=2.87). Two surgeons out of four are performing corrective osteotomies regularly. Two surgeons focus on primary and revision hip and knee replacement and one of them partly performs corrective osteotomies. None of them had previous experience with VR. The doctors were not involved in the development process of our system and were not aware of its functioning.

### 4.2.4 Procedure

CT scans of five pediatric and young adult patients suffering from patellar maltracking either caused by femoral or tibial rotational abnormalities were selected, processed (Section. 4.2.2.1) and were used for the evaluation. To make the most of our evaluation cohort we split the participants into two groups of two, each group

running their own study (Figure. 4.3). The *first* group of participants (clinical assessment study) comprised one surgeon with experience in hip and knee replacements and some corrective osteotomy experience, and one surgeon with experience in hip and knee replacements, and experience in indicating patients with rotational abnormalities for expert surgeons primarily focusing on this area. The first group's objectives were to examine and set diagnoses based initially on the axial CT images and later on 3D reconstructions of the CT data in VR, and provide us with a direct comparison regarding decision-making between different methods (Section. 4.2.5.1). The *second* group of participants (pre-operative planning study), including two exceedingly experienced osteotomy surgeons was used to provide a direct comparison in decision-making for surgical intervention and surgical planning between different cases and assessment methods *with* and *without* prior examination of CT images (Section. 4.2.5.2). Participants of this group had to explain their surgical plan.

### 4.2.5 Clinical assessment study & pre-operative planning study

During the first part of each study, participants were shown patient data on a desktop computer using a DICOM viewer with radiological annotations including femoral horizontal axis angle, femoral condylar horizontal axis angles, tibial condyles horizontal axis angles, and bimalleolar horizontal axis angles (Figure. 2.3). Patient data presentation order was randomised for each participant and method. Participants were not aware that the cases presented in Orthoped VR or in the DICOM viewer could be of the same patients. For each patient case, we asked participants to establish a diagnosis and indication for a surgical procedure (in addition to a surgical plan for the pre-operative planning study). We recorded task completion time and their diagnosis.

Before the second part of each study (evaluation in Virtual Reality), each participant underwent a tutorial session in collaborative VR with the session coordinator, during which they were trained on how to interact with the user interface and perform incisions on a 3D model of the lower limbs specifically for training (not included in the testing set). Then, during the examination of patients' 3D reconstructions in VR, participants were again asked to establish patients' diagnoses. The task completion and details of the diagnosis were recorded for each patient's case. After the clinical assessment in OrthopedVR, participants were asked to fill up the qualitative questionnaire. This post-session questionnaire followed an informal feedback discussion probing the participant's experience with the virtual reality system to specifically indicate its benefits and potential issues before implementation into clinical medicine.

#### 4.2.5.1 First group: Clinical assessment study

The intent of the clinical assessment study was to compare task completion times of Participant 1's performance of setting patient's diagnoses based on the CT images prior to the visualisation in OrthopedVR, and Participant 2 being only able to use OrthopedVR, and to compare overall task completion times spent examining and diagnosing on a desktop CT DICOM viewer *and* by using OrthopedVR.

Participant 1 was presented with CT data of five patients. Participant 2 was presented CT data of only three patients' prior to the VR examination. This was done in order to be able to compare task completion times of a participant who *was* able to examine CT data prior to the visualisation onto the OrthopedVR system, and a participant who *was not* provided CT images beforehand with an exemption of a single case. Participant 2 only saw three out of five cases in order to limit their possible bias when directly comparing both participants' performance per case using different methods, i.e., we wanted to ensure that they did *not* see all cases in both systems. Participant 1 *was* presented all five cases in both methods for us to observe changes in understanding of the patients' anatomy if cases are seen in both systems.

#### 4.2.5.2 Second group: Pre-operative planning study

The purpose of the pre-operative planning study was to compare task completion times of Participant's 3 performance of surgical planning on the CT images prior to the visualisation in OrthopedVR and Participant 4 only being able to use OrthopedVR.

Participant 3 was presented all five cases for clinical evaluation on the desktop DICOM viewer and later on the OrthopedVR system. Participant 3 also performed an examination of CT 3D reconstructions in the OrthopedVR system in a different randomised order to eliminate any learning effects. Participant 4 was presented with three cases each for clinical evaluation on the desktop DICOM viewer and in the VR system with one case overlapping between both examination methods. As in the case of the Clinical assessment study group, presenting just three cases for each method to Participant 4 was done to minimize bias and learning effects due to them seeing a patient's case with a different visualisation method when comparing each participant's performance per each case.

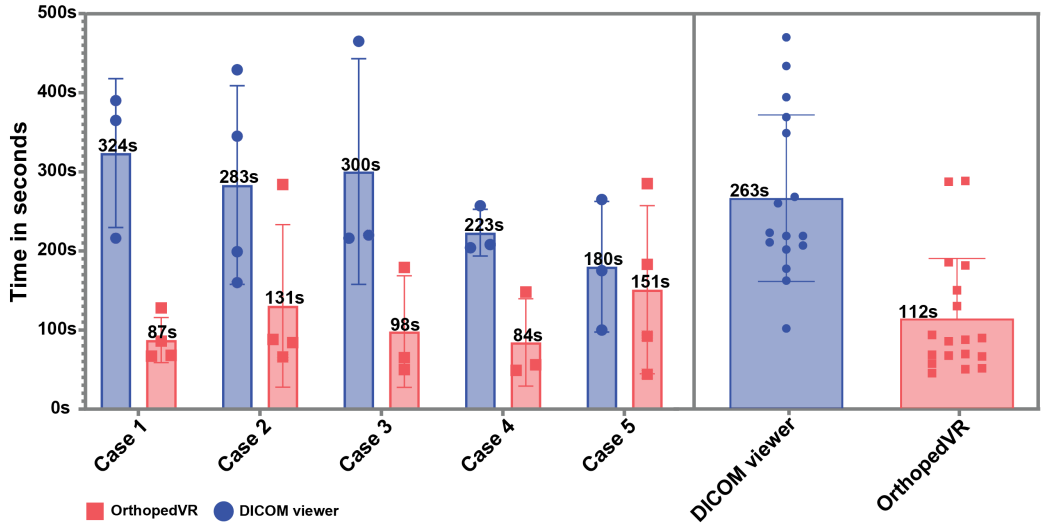


**Figure 4.4:** Task completion times for each case in DICOM viewer vs VR (left), and aggregated performance data across all datasets (right).

## 4.3 Results & Discussion

### 4.3.1 Quantitative measurements.

Task completion times of all participants and study groups for desktop-CT versus VR strongly indicated that participants completed the tasks much faster in VR. Mean completion time in VR was shorter (mean=1m 52s, SD=0m 29s) in contrast to examinations performed on the desktop DICOM viewer (mean=4m 23s, SD=1m 44s) (Figure. 4.4). We tested the difference of the completion times over all participants and both study groups for desktop-CT versus OrthopedVR using a non-parametric Mann-Whitney U test due to log-normal distribution reported by Shapiro-Wilk test. A Mann-Whitney test indicated statistical significance in task completion times differences (DICOM viewer (Mdn=218s) vs OrthopedVR (Mdn=85s), U=30, p=.0001). These results, taken together with very positive user feedback (see next subsection), establish that VR indeed enabled a better understandings of patients' pathological anatomy in the OrthopedVR system.

#### 4.3.1.1 First group: Clinical assessment study

Task completion times analyses indicate a better understanding of patients' anatomy when in VR, and improvement in decision-making. Participant 1 assessed three selected patients' CT scans on a desktop DICOM viewer. Participant 2

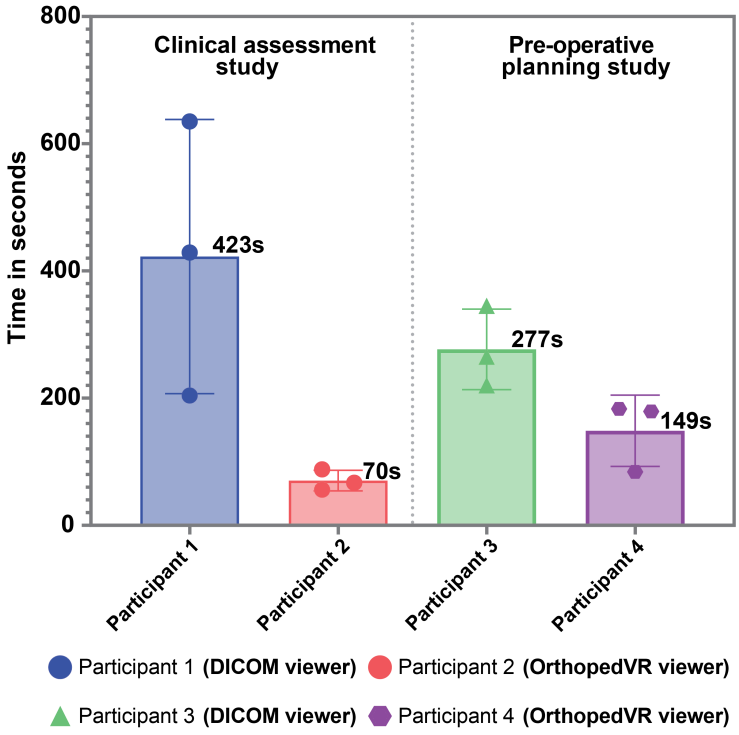


**Figure 4.5:** Performance data for each participant when grouping them by method. VR has a clear advantage in all cases.

examined the same three selected patients' 3D reconstructions in OrthopedVR without being able to examine CT datasets in the DICOM viewer beforehand. Our measurements indicated that Participant's 2 understanding was strengthened from the 3D reconstructions (Participant 1: mean=7m 3s, SD=3m 36s vs Participant 2: mean=1m 10s, SD=0m 16s) (Figure. 4.5). Participant's 2 decision-making was 6x faster in OrthopedVR than Participant's 1 decision-making on the DICOM viewer. Participant's 1 average total task completion time for setting on a diagnosis for all 5 patients in OrthopedVR (mean=3m 25s, SD=1m 15s) improved by 46.3% in comparison to the average total task completion time while examining all patients' data in the DICOM viewer (mean=6m 22s, SD=3m 22s). Comparing average task completion times across both participants in OrthopedVR (mean=2m 14s, SD=1m 30s) and desktop DICOM viewer (mean=4m 58s, SD=3m 8s) showed a 55% difference (more than 2x) between methods in favour of OrthopedVR.

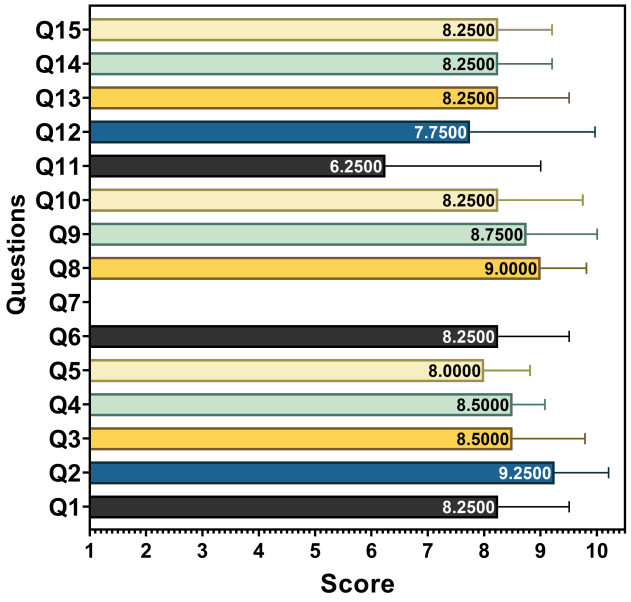


**Figure 4.6:** The results of the qualitative questionnaire (10 is better) (Section. 4.3.2). Please note that Q7 was an open-ended question (also see Appendix A. for the full questionnaire).

#### 4.3.1.2 Second group: Pre-operative planning study

The results of the pre-operative planning study provided us with insights on how experienced surgeons could benefit from surgical planning in an immersive VR environment. We observed much shorter task completion times for Participant 4 during the clinical examination and surgical planning in OrthopedVR (without being able to first examine CT images) (mean=2m 29s, SD=0m 56s) compared to Participant's 3 examination and planning in the DICOM viewer (mean=4m 37s, SD=1m 3s), overall a 46,2% difference in decision-making time (Figure. 4.5). During the clinical examination and surgical planning of all patients' data, Participant 3 performed 77,3% faster in OrthopedVR (mean=1m 5s, SD=0, 17s) than in the DICOM viewer (mean=4m 46s, SD=1m 19s).

When using 2D CT scans, the surgery planning appeared to be faster than the clinical assessment (again, for 2D CT scans). However, this trend is reversed in VR: it is faster to do the clinical assessment than to plan the surgery. We attribute this to the greater experience of respondents in the "Surgical Planning" group. However, it was expected that the surgical planning itself will take more time in VR than clinical assessment, as the surgeons were asked to provide a more comprehensive report on how they would proceed.

#### 4.3.1.3 VR system performance

OrthopedVR running on the Meta Quest 2 had consistently stable frame rates throughout clinical testing. The CPU utilization of the device was low (mean=20%, SD=5.76%) and the GPU utilization was moderate (mean=50.75%, SD=9.99%). Frames-per-second (FPS) were locked to a maximum of 72 FPS during testing, supported by our optimisation methods (mean=71.8 FPS, SD=1.3 FPS).

### 4.3.2 Qualitative measurements

Responses to the questionnaires support that Participants felt that OrthopedVR offered a better understanding of lower limb alignment and rotational profile in comparison to isolated 2D axial CT images (mean=8.25/10, SD=1.5) (Q10) (Figure. 4.6). They agreed that such a VR system can play a significant role in orthopedic assessment (mean=9/10, SD=0.81) (Q8). The majority of the participants felt neutral, and one participant felt positive about reducing their reliance on conventional radiological manual measurement of angles on CT images (mean=6.25/10, SD=2.75, min.=3, max.=9) (Q11). Participants further indicated that VR-based orthopaedic planning will be used in the future (mean=8.75/10, SD=1.25) (Q9). They shared a positive feedback relating to the increased reproducibility of lower limb rotation profile angle measurements as part of pre-operative planning and reduced variation in angles related to human factors (mean=7.75/10, SD=2.21) (Q12). Based on the respondents' feedback, use of VR software in conjunction with radiology reports could improve the surgical planning, precision, and post-operative outcomes for the patients (mean=8.25/10, SD=1.25) (Q13).

They were positive about them being confident that VR should be incorporated in future clinical practice (mean=8.25/10, SD=0.95) (Q14), and they would recommend VR rotational profile alignment software for pre-operative planning to their colleagues and trainees (mean=8.25, SD=0.95) (Q15). Participants found the collaborative functionality in OrtopedVR useful for training and cooperation (mean=8.5/10, SD=1.29) (Q3). Participants also stated that they appreciated more the collaborative tutorial they underwent before the testing session of OrtopedVR with the study coordinator than they would have a pre-recorded video tutorial (mean=8.5/10, SD=0.57) (Q4). Participants found the VR environment visually appealing (mean=8.25/10, SD=1.25) (Q6).

Participants appreciated the contrast between the anatomical structures of the patient and the darker background. Participants did not complain during the testing for any strain on their eyes. Participants also indicated general satisfaction with the visual performance during the osteotomy planning (mean=8.25, SD=1.25) (Q1).Participants showed positive feedback towards the combination of *Contextual*, *World-static*, and *Dynamic control panel* UIs (mean=8/10, SD=0.8) (Q5). Participants also rated that the application was perceivably stable during their individual testing session (mean score=9.25/10, SD=0.95) (Q2).

#### 4.3.2.1 Setup Time Costs

The VR setup requires a shorter amount of time (compared to desktop) for initializing the system, loading patient data, and entering the collaborative virtual environment. The VR system allows for immediate manipulation and interaction with 3D models, making it more efficient for real-time surgical planning. Users find the intuitive nature of VR controls and the immersive environment conducive to faster setup and preparation.

In contrast, the desktop approach is more time-consuming, particularly when loading patient data on a PACS. Pulling a large volume of high-resolution images takes significantly longer. Additionally, while the learning curve for desktop systems may be currently easier due to familiarity, the process of reconstructing and manipulating 3D volumetric reconstructions from 2D slices is inherently slower and more labor-intensive compared to the VR approach. Overall, the VR system provides a more streamlined and time-efficient setup process for surgical planning.

### 4.3.3 Conclusion

Reflecting upon the quantitative and qualitative study results, the reconstruction of patients' CT data into an immersive environment has an undoubtedly positive impact on diagnosis and surgical planing. Our framework enables surgeons to essentially rehearse a surgery before performing it and try out different parameters and observe the result. Moreover, OrthopedVR, works based on the current *limited* clinical protocols of our health system, without requiring any additional data or radiation dosage.

This is the first study, to our knowledge, that concentrates on improving surgical planning during orthopaedic procedures of the lower limbs, whose current gold standard for diagnosis and pre-operative planning is only a CT scan, an anterior-posterior X-ray, or a physical examination of the patient by an orthopaedic doctor.

### 4.3.4 Limitations

A limitation of this study is the amount of available datasets of patients suffering from rotational abnormalities of the lower limbs. Obtaining pediatric cases was exceedingly difficult as our national body reports only 620 cases between the years of 2014-2017 and 70% of patients were between 40 and 55 years of age [149]. These abnormalities are not that widely diagnosed in the younger population as patients are often told to wait until they are candidates for knee arthroplasty despite the fact that knee osteotomy could delay the progression of arthritis. As a result of this, we were only able to gather data from 5 cases. A second limitation stems from the fact that due to current clinical protocols attempting to reduce radiation exposure, there exist no post-operative CT datasets serving as a ground truth comparison for the pre-operative planning. We relied on the experience of the four surgeons to validate their outputs. We did not ask the surgeons to cross-validate each other as their preferred operating approaches (angles and incision technique) to treat mal-tracking differed substantially depending on their personal preference.

## 4.4 Chapter Summary

We presented OrthopedVR, a toolkit for IKEM VRLab implementing an application-specific 3DUI to (i) visualise rotational abnormalities of the lower limbs and (ii) enable surgeons first rehearse a derotational osteotomy in VR. Our quantitative and qualitative evaluation showed beyond doubt that immersive surgical planning in VR can be beneficial for more accurate understanding of structural abnormalities, the patient's pathological anatomy, efficient surgical planning and improved clinical outcome. OrthopedVR can function based on existing clinical screening protocols without requiring additional data or radiation exposure. To our knowledge, this is the first system and study to improve surgical planning for lower limb orthopaedic procedures, whose gold standard for diagnosis and pre-operative planning is only a CT scan, an anterior-posterior X-ray, or a physical examination by an orthopaedic doctor.

Based on extensive discussions with the experienced surgeons, future work could involve: (i) creating a virtual model enabling an understanding of the effect of additional interventions on patella tracking, e.g., as the distance between the lower pole of the patella and the tibial tuberosity remains the same, the femoral condyle moves around that point; It would thus be beneficial for surgeons to be able to view the knee in an extension, 30, 60, 90, and 120 degrees of flexion and observe the relation of the patella to the trochlear groove. (ii) Provide the ability for surgeons

to mix and match techniques to gain an understanding of what happens with each intervention and how interventions affect one another. One surgeon also suggested the implementation of medial patellofemoral ligament reconstruction into the VR simulation. (iii) Further work on tailored CT protocols, to improve the overall quality and reduce time for producing 3D models for simulated VR environments. This would also allow to validate our approach on a large sample of patients data including post-operative screening serving as the ground truth. Finally, future work could also validate our approach on a larger sample of patient data as well as to compare the results of the VR pre-operative planning to actual post-operative CT screenings, which, however, will require a fundamental change of the clinical data acquisition protocols in our health system.

Chapter 5

# Clinically Scalable VR System for Surgical Planning of Liver Resections†

Liver resection, essential in liver cancer treatment, involves a variety of surgical approaches based on the nature, size, and location of the tumour. The five-year survival rate for individuals with primary and secondary liver cancer who do not undergo surgical resection is only around 3%. However, if surgical resection is performed and results in negative margins (no cancer cells can be found at the edge of the removed tissue, suggesting that the entire cancer has been removed), this rate improves, increasing to between 20% and 30% [150, 151]. The challenge in this procedure is to remove enough tissue to ensure clear margins thus avoiding macroscopic and microscopic tumour involvement at the resection line, while also preserving as much healthy liver tissue as possible to reduce the risk of liver failure. Planning the surgery involves identifying the important blood vessels that are necessary for maintaining healthy liver tissue and determining their proximity to the tumour(s) [152, 153].

Standard clinical pre-operative planning gathers abundant patient-specific data from various imaging modalities, yet medical specialists predominantly rely on 2D screens to examine 3D structural data from CT and MRI scans, neglecting advanced 3D visualization techniques. This practice, highlighted in surgeries like oncologic liver surgery, can lead to confusion due to the sheer volume of images to analyze. While 3D PDF-like formats attempt to address this and are used conventionally, they lack the depth cues crucial in medical assessment. 3D printing

†The contributions of this chapter are under review in the Springer Virtual Reality Journal with a tentative title "IKEM VRLab: VR System for Surgical Planning of Liver Resections".

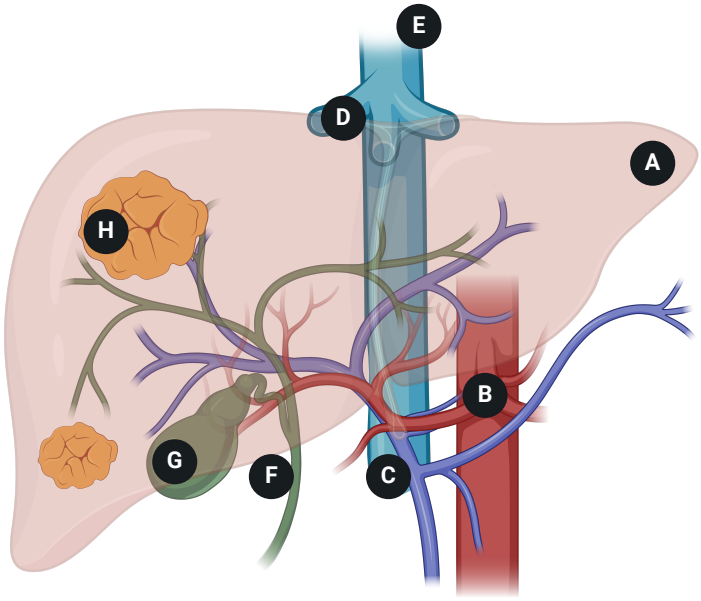


**Figure 5.1:** A simplified graphical representation of liver anatomy with (A) liver contour, (B) hepatic artery, (C) portal vein, (D) hepatic vein, (E) vena cava, (F) bile duct, (G) gallbladder, (H) tumour. Created with BioRender.com.

organs offers tactile feedback, but its high operational costs and time constraints pose challenges for real world applications. Integration of VR surgical planning into clinical workflows faces hurdles like scalability issues, complex UIs, and lack of portability, hindering efficient usage in medical practice [50, 154, 155, 55, 56, 57, 61].

In addition, previous academic research on VR applications specialised in surgical planning have primarily used standardised qualitative feedback questionnaires and users' statements [18, 40, 15], lacking quantitative data from clinical settings. Particularly for liver resections, it is very important to quantitatively examine the efficacy of VR to ascertain error-free decision-making.

In this chapter, we present a extension toolkit for IKEM VRLab. This system extension, as corroborated by our evaluation study, supports surgeons' decision-making in liver surgery planning using VR versus standard clinical visualisation tools including DICOM (Digital Imaging and Communications in Medicine) viewers and point-cloud based volumetric visualisations. The system also improves surgeons' ability to choose the most suitable surgical approaches and understand patient anatomy. IKEM VRLab liver toolkit further supports VR collaboration and remote multidisciplinary team consultations.

We thoroughly evaluated our system, aiming to establish VR's effectiveness in enhancing surgical planning, particularly in reducing miss-indications for procedures and improving procedural feasibility by analyzing surgeons' performance and feed-

back within the VR environment compared to standard clinical medical imaging. As part of our study, we also introduce our modified version of Igroup Presence Questioner (IPQ), which can be used as a standardised way of measuring qualitative data about UI and medical visualisation. Our quantitative and qualitative evaluation studies confirmed VR's practical benefit in liver resection planning.

Our *two* specific contributions include:

- We designed a joint CT and MRI acquisition protocol to support highly detailed reconstruction of patient-specific liver anatomy. We also created and implemented a toolkit into the VRLab system to support the indication for specific liver resection procedures, including real-time volumetric estimates, clipping and measuring tools while considering anatomical and non-anatomical liver resection.

- We performed a comprehensive quantitative evaluation of the study's methodology with 6 experienced abdominal and hepatic-biliary surgeons during 60 instances of examining real patient cases. Evaluation also includes a qualitative component including our modified IPQ, termed IPQ-XRMSE designed to capture the nuances of how medical professionals interact with XR applications in clinical contexts to ensure that findings are grounded in practical and real-world surgical scenarios.

## 5.1 Architecture

We designed, developed and integrated a Liver Resection Planning VR Toolkit into IKEM VRLab. In this section, we present the specifics of the developed liver toolkit, followed by a thorough evaluation in the next section. Specifically, this section delves into the process of data acquisition and segmentation for liver surgery planning. We present our protocol to optimize image acquisition for 3D segmentation through a combination of CT and MRI imaging phases to accurately reconstruct the vascular and billiary branches of the liver. These models are then introduced to the IKEM VRlab environment, where surgeons can navigate, plan, and simulate liver resections with a high detail and realism in a collaborative setting.

### 5.1.1 Data acquisition

To acquire CT imaging, we used a Siemens Neoatom Alpha scanner (Siemens Healthineers, Germany). For MRI imaging we used a Siemens Magnetom Avanto 1.5T scanner. To obtain high quality organ reconstructions from the 3D segmentation process we developed in collaboration with a radiologist (collaborator) a modified CT and MRI acquisition protocol. The modification does not affect data acquisition time. In the modified protocol, the CT imaging is being used to acquire the liver tissue, vascular systems, tumours, and lesions whereas the MRI imaging provides us with images of the biliary system and in the instance of substandard CT acquisition, with detailed images of tumours. The modification does not affect data acquisition time in the case of MRI or patient radiation dose in the case of CT. More specifically:

The 3D reconstruction is based on the CT arterial and venous phases, where arterial and venous branches are filled with contrast fluid and are imaged in separate image series. The primary key parameters is keeping CT voxel slice thickness between 0.6 mm to 1 mm increments between slices to achieve an overlapping imaging series thus preventing gaps and an *art-factor* - when either an operator or software are required to approximate shapes between individual slices using interpolation.

To obtain imaging of the biliary and pancreatic ductal systems, we used magnetic resonance cholangiopancreatography (MRCP) with heavily weighted T2 images in the coronal or axial plane. The ideal slice thickness of the images is between 1.0 and 1.5 mm, preferably with isotropic voxel. When a more detailed imaging of tumorous structures were needed, we utilized the T2 MRI (T2-weighted magnetic resonance imaging) with the HASTE (High-Speed Acquisition with Turbo spin Echo) and FS (Fat Suppression) and non-FS techniques to acquire fast images with minimal motion distortion. These images are acquired in the axial plane with voxel thickness $\leq$ 7 mm.

### 5.1.2 Liver anatomy segmentation

Our three-dimensional reconstruction of liver structures includes liver tissue, hepatic vein, portal vein, hepatic artery, and in some cases also hepatobiliary ducts and is based on data registration and fusion of different CT and MRI imaging series to ascertain imaging all liver structures. Image registration of the CT series acquired during venous and arterial phases enables accurate segmentation of most of the vascular branching during a single segmentation process and for most patients' cases this combination appropriately displays all regions of interest in a single 3D model.

When surgeons require a visualisation of the bile ducts then the fusion will also include the MRCP series. To achieve this, we use a multi-modal image registration approach. The registration process aligns images from different modalities (CT and MRI) and phases (venous and arterial) using rigid transformations. Initially, rigid registration aligns the images based on their overall structure using mutual information as the similarity measure, ensuring precise alignment of anatomical features across different images.

We employ surface-based modelling for the reconstruction process. Surface modelling is more suitable for VR visualisation compared to e.g., volumetric (voxel) rendering, as it is both more computationally efficient in rendering complex anatomical structures and provides a clearly detailed representation of organ boundaries and lesions [156, 157]. The key benefit of using a surface-based model by segmenting CT and MRI data is that it simultaneously allows visualising all structures of interest, even for structures like liver anatomy, where the tissue densities of vascular, biliary, and tumorous formations are very similar and can not be individually isolated using e.g., thresholding in volumetric rendering. Surface-based models also support easy interactive editing and refinement of the boundary of segmented structures, enabling deformable surface models even on mobile devices [133].

The segmentation process begins with a pre-processing step, where anisotropic diffusion filters are applied to the CT and MRI images to enhance the quality of the input data by reducing noise while preserving edge details. This step ensures that small anatomical details are preserved while reducing the impact of image artifacts. Following pre-processing, an initial segmentation is performed using a combination of region-growing and morphological operations. The region-growing algorithm starts from seed points placed within the liver tissue and expands outwards based on intensity similarity, while morphological operations such as dilation and erosion help refine the boundaries by closing gaps and removing small, irrelevant structures.

To segment the liver imaging data for subsequent visualization in virtual reality, we used MeVis Liver Suite (MeVis Medical Solutions AG, Germany). MeVis Liver Suite is certified as a medical device under Medical Device Regulation, guaranteeing its safety and reliability for use in medical practice. It supports medical diagnosis and planning of surgical procedures on livers containing algorithms for automated liver lobe, bile ducts and vascular structures segmentation. Tumour or lesion segmentation can be manually performed by a radiologist. The software incorporates non-linear segmentation methods based on morphological gradients and regional minima which allows segmentation of objects based on the topology of their surfaces, and shape-based segmentation, which uses shape information to

segment anatomical structures. We used a combination of these algorithms with manual segmentation validation and correction by expert collaborators to process CT and MRI data of the liver, achieving the most accurate segmentation and 3D model creation for the evaluation study of our system (see Subsection 3.2).

Manual segmentation validation and correction are critical steps in our workflow. Expert radiologists review the automatically segmented structures and make necessary adjustments using interactive tools provided by MeVis Liver Suite. These tools include live-wire and paintbrush editing methods, which allow for precise boundary adjustments. Live-wire segmentation uses edge detection and shortest path algorithms to allow the radiologist to quickly and accurately define segment boundaries by snapping the contour to the strongest edges in the image. Paintbrush editing enables direct manual correction by allowing the radiologist to paint over the segmentation mask to add or remove regions. The combination of automated algorithms and expert validation results in highly reliable and detailed liver segmentations, suitable for surgical planning and VR visualization.

The workstation used for segmentation tasks was equipped by an AMD Ryzen Threadripper PRO 5965WX CPU, 128GB DDR4 3200MHz RAM, NVIDIA RTX A5500 24 GB GDDR6 GPU.

### 5.1.3 Liver Resection Planning Tools

Once a patient's case liver 3D model is loaded from the remote server, materials are assigned to the generated visualisation using colours consistent with the ones used in anatomical atlases, i.e., the liver is grey, tumours and lesions yellow, the arterial vascular system is red, the portal vein branches are dark blue and the hepatic vein branches are light blue. The biliary tree is in dark green (Figure. 3.3 & 5.2.A). Individual liver segments are coloured in a variety of salient colours, so that boundaries between individual segments are easily discernible (Figure. 5.2.B). A Clipping Plane and an Interactive Ruler are also visualised. Each segmented part can be individually serialised and updated over the network ensuring the accurate synchronisation of positions and orientations of these objects across other users.
**Clipping Plane**. The Clipping Plane tool enables users to "cut" into liver structures and remove structures behind the plane. The clipping plane can be controlled when grabbed with either Hand Trigger by the purple-coloured rectangle. This allows the user to have all anatomical structures concurrently visible but see vascular overlapping or vascular supply inside of the tumour by shifting the Clipping Plane. This enables navigating through a stack of CT or MRI data in three degrees of freedom instead of scrolling through an imaging stack in one locked axis. Our al-

gorithm processes all mesh vertices, establishing which ones are behind the clipping plane (thus visible), removing the rest, and then generating new triangles to make the mesh watertight.

**Interactive Ruler**. An initial assessment of the patient pathological anatomy is followed by the doctor attempting to get a sense of the extent of a particular tumour or lesion, or the length of a specific vascular structure in real-world units. The interactive virtual ruler tool was designed to be easily manipulated within the VR environment, allowing users to measure distances between points of interest on the liver model (Fig. 5.2.C). The ruler is equipped with a dynamic scaling feature, which automatically adjusts the ruler's scale based on the organ scaling. This ensures that measurements remain accurate regardless of the user's perspective or position within the VR environment. It is also controlled by Hand Triggers using purple-coloured grab points.

**Estimation of liver remnant.** When a surgeon is considering a particular resection procedure, liver remnant and resection volumes play a crucial role [158, 159]. We have implemented (and thoroughly validated, Section. 3.2) the volumetric calculation from surface models to compute the volume of a portion of a complex 3D mesh object lying behind a user-specified cutting plane when examining tumours and lesions (Figure. 5.2.D) or based on the volume of individual liver segments when the user is enabling/disabling the visualisation of specific liver segments in the case of anatomical resection (Figure. 5.2.B). Our algorithm extracts the meshed vertices and triangles and then transforms the mesh into a new representation as a set of triangular prisms. It then sifts through each triangular prism verifying that all its vertices are positioned behind the specified cutting plane before calculating its volume. The remaining volume estimation is displayed above the segmented part.

Our algorithm recalculates the volume after every action allowing for interactive movement and rotation of the mesh and the cutting plane in the scene. This functionality is invaluable for a detailed investigation of the liver's structure and to explore the impact of a series of hypothetical surgical procedures. Our method of volume calculation provides high precision for closed, non-self-intersecting meshes, and handles complex shapes effectively, such as the volume of a liver partitioned by a plane, which is pivotal for surgical planning and assessment.

## 5.2 Evaluation

To evaluate our pre-operative planning platform, we performed 3 separate studies. The first one aimed to validate that the volume our platforms estimates for the VR-

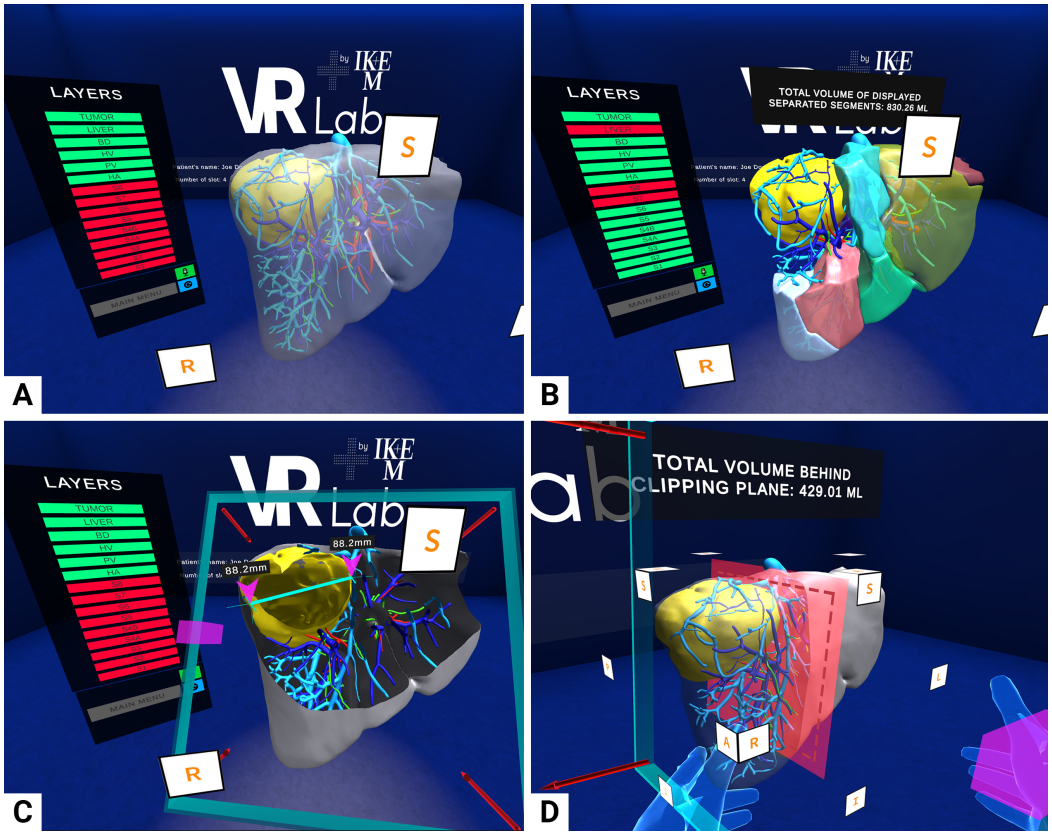


**Figure 5.2:** Visualisation of liver structures including tumour with the layer system pop-up menu on the left (A). Visualisation of remaining liver segments after virtual segmentectomy of segments 7 and 8 with displayed remaining volume above the organ (B). Deployment of ClippingPlane and Interactive Ruler during an inspection of interior liver structures and measuring the extent of the tumour to surrounding tissues (C). Virtual resection planning by using a cutting plane with a remaining real-time calculated volume displayed above the organ (D).

optimised 3D models generated from CT data organ segmentations, corresponds to the actual volume of the organ. The second study evaluated the effectiveness of VR planning to assess the feasibility of a variety of surgical procedures during liver resection and to reduce miss-indications for procedures. The study compared the accuracy of correct indication for a certain type of procedure and its time efficiency in VRlab versus standardised medical visualisation tools. The third study employed the System Usability Scale (SUS) and our modified version of the Igroup Presence Questionnaire (which we call IPQ-XRMSE and an example of the questionnaire is available in the Appendix B.) to evaluate the usability of our system [3, 160, 161]. The SUS evaluated the system's overall usability with scores ranging from 0 to 100, with higher scores indicating better usability (an example is available in Appendix C.). At the same time, the IPQ-XRMSE focused on assessing the level of immersion, realism, and involvement experienced by medical experts.

Aiming to assess our platform's capability to handle real-world clinical scenarios effectively, we complement our evaluation by looking into system performance metrics such as virtual room instantiation time, communication latency between users in collaborative mode, and frames per second (fps) achieved during visualisation.

### 5.2.1 Liver Resections in VR

In this section we present our evaluation of the effectiveness of VR planning to assess the feasibility of a variety of procedures during liver resection and to reduce miss-indications for procedure. Specifically, we aimed to compare the effectiveness of standardised clinical visualisation (SCV) against our immersive environment of VRLab in enhancing surgeons' performance, understanding, and perception of depth in patient-specific anatomy. CT and MRI scans of 10 infants, young adults, and adults suffering from tumorous formations in livers (HCC, ICC, renal cell carcinoma, hepatoblastoma, adenoma, echinococcosis) were selected and processed according to our protocol (Section. 5.1.1).

#### 5.2.1.1 Participants

Six qualified liver surgeons participated in the study. We selected only experienced surgeons who meet the criteria of having a minimum of ten years of experience (Mean = 17, SD = 7.49). Three participants are attending surgeons and three participants were surgical fellows. All surgeons have extensive experience in performing surgeries related to the field of abdominal and hepatobiliary surgery in question, ensuring that they have a deep understanding of the tasks and challenges involved. In addition, two of the surgeons have previous experience with the use of VR technology in their surgical practice, providing a valuable perspective on the benefits and limitations of the technology.

#### 5.2.1.2 Design

Each surgeon participated in 2 sessions where 5 cases were presented in the SCV tool, Jivex DICOM Viewer (VISUS Health IT GmbH, Germany) and another 5 cases in VRLab (Figure. 5.3). At least 7 days separated the two sessions. For each case presented either in SCV or VRLab, participants were given a form with questions on patients' anatomy and the surgical approach they would indicate. The indication options were resection or transplantation (inoperable).

**Case selection.** We selected *closed* (i.e., past) cases for which we had the ground truth data (procedural decisions and outcomes) serving as ground truth. First, we examined the database for patients who had undergone liver resection, transplantation, or were contraindicated for any surgical procedure because of their specific anatomy. Each of these patients had detailed information about their diagnosis, indication or contraindication for the procedure and other relevant information that provided us with important data sources and benchmarks for our research purposes. Two senior surgeons carried out the selection process to ensure the reliability of our research results. For each patient, we had a set of either available CT scans and, in some cases, also MRIs.

**Randomization.** Each patient case was assessed 3 times in VRLab and 3 times in SCV. We used a balanced incomplete block design to construct a sequence of cases that ensures each case is presented to each respondent once, either in VRLab or SCV and that no two respondents see the same sequence of cases. When selecting resection, the following question was asked about the type of resection they would perform: right hepatectomy, right extended hepatectomy, left hepatectomy, left extended hepatectomy, left lobectomy (segment 2 + 3), resection of segments 6 + 7, segmentectomy of particular segments, non-anatomical resection of segments, central resection, or associating liver partition and portal vein ligation for staged hepatectomy (ALPPS).

The form also included critical clinical patient data to perform the assessment, such as the type of the tumour and the patient's age, and biometrics. We also included the percentage of each segment of the total liver volume. When available, we included 3D volumetric reconstructions from the radiologist when participants were planning procedures using SCV. To ensure a fair comparison, participants were not provided with the option to visualise individual liver segments in either the SCV or VRLab settings. This approach was chosen to isolate the impact of the immersive VR environment's added depth and spatial orientation capabilities without the influence of segment-specific visualization.

The quantification of participants' performance in each examination environment is based on comparing surgeons' performance across both methods and all patient cases. In the forms participants had to fill out after each case, we recorded their approach and indicated the specific procedures they would have performed. We also recorded task completion time for each patient case and used the examination method. The questions were anonymously given to the leading senior surgeons who performed the procedures on the patient's cases and served as mentors to their younger colleagues. Raters then evaluated the anonymous forms completed by the participants. We then compared the error rates and task completion times

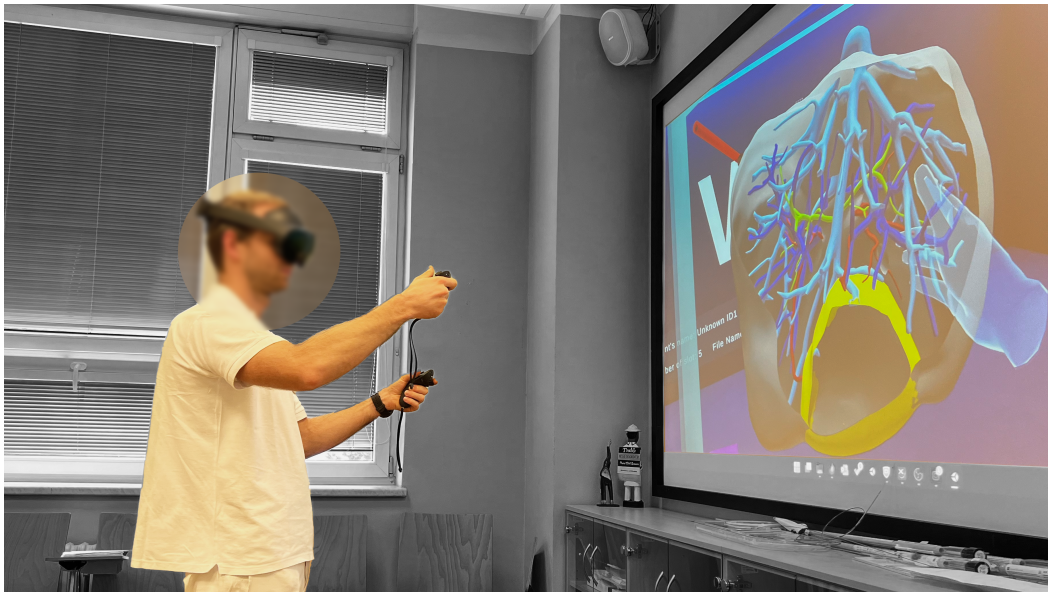

**Figure 5.3:** A photo of a participant carrying out an anatomical assessment and procedure indication. The projector screen on the right broadcasts what is seen in the VR planning room using a VRLab PC Spectator Client to observe participants' action within VRLab.

collected data across cases and evaluation methods to establish a direct comparison between decision-making in VR and on SCV.

### 5.2.2 System Usability study

Following the second evaluation session, participants responded to questionnaires regarding the system's usability, realism, and involvement in surgical planning that assesses the degree to which the user feels engaged and absorbed in the virtual environment during their decision-making process. We employed the standard 10-question SUS and our adjusted version of Igroup Presence Questionnaire, Igroup Presence Questionnaire for XR Medical Software Evaluation (IPQ-XRMSE). During each evaluation session, we also collected surgeons' impressions of the VR system by using the think-aloud evaluation protocol [162].

To analyse the computational performance of the system in clinical conditions (which can directly affect usability), we recorded the virtual room instantiation while downloading deployed patients' 3D reconstructions from the internal centralised server, network consumption of the application, and FPS during the visualisation. IPQ-XRMSE's purpose is to provide us with a more detailed understanding of the level of immersion, realism, and involvement experienced by medical experts when testing VR medical apps, focusing on their ability to explore, manipulate, and effectively engage with medical visualisations. The IPQ-XRMSE consists of

13 questions separated into 3 subgroups (Immersion, Realism, Involvement) with a rating scale from 1 "not at all confident" to 7 "completely confident" and score is reverted in some questions to prevent *straight-lining* bias. Questions structured into the subgroups are presented below with respective rating scales with questions 1, 2, 7, and 12 having reverted score scale.

## 5.3 Results

We now present the results of our studies, evaluating the performance of surgeons in two different examination environments: VRLab and SCV, focusing on the validity of their decisions in each environment and the time taken to complete those examinations. We also present the results of our system evaluation study.

### 5.3.1 Liver Resections in VR - Accuracy

We collected data from 60 cases, 30 in each environment, with both VRLab and SCV encompassing a range of scores stretching from 0 to 100. Assessors did not know which method they were scoring. For a flawlessly correct procedure indication, respondents were given 100 points. In case of a minor mistake 30 to 50 points were removed based on whether the respondents would remove more or less of liver tissues than was necessary in the particular case. No points were given to respondents when indication was not at all correlated with procedures considered by the board of senior experienced surgeons for that particular case. When analyzing the mean scores, we observed a notable difference between the two environments. The mean score in the VRLab environment was significantly higher (mean = 66.67, SD = 42.60), in contrast to a lower mean in the SCV setting (mean = 38.50, SD = 48.27). This difference indicates a potential edge in performance when using VR.

To further understand the distribution of the scores since neither VRLab nor SCV scores adhered to a normal distribution, as indicated by the Shapiro-Wilk test results (VRLab W=0.7045, PACS W=0.6474), both yielding p-values less than 0.0001, we employed the Mann-Whitney U test. This test revealed a significant difference in case indication scores between the VRLab and SCV environments, with a p-value of 0.0486. The test, being two-tailed, also accounted for the overall direction of differences. The sum of ranks was 1039 in VRLab and 791.5 in SCV, and the Mann-Whitney U value stood at 326.5, establishing the significant divergence in performance scores between the two settings.

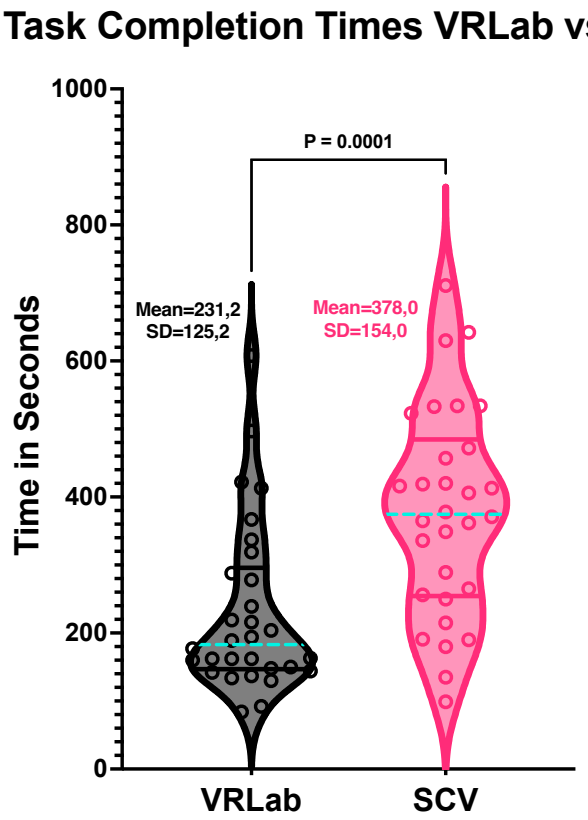


**Figure 5.4:** The violin plot illustrates task completion times for the VRLab and SCV systems during surgical planning. VRLab demonstrates a mean time of 231.2 seconds (SD=125.2 seconds), indicating more efficient and consistent performance when compared to SCV which exhibits a mean time of 378 seconds (SD=154 seconds), suggesting greater task completion time overall and higher variability. The p-value of 0.0001 confirms the statistically significant difference between the systems. The light-blue-dotted line in each violin plot represents the median (median VRLab=184, median CSV=374.5).

### 5.3.2 Liver Resections in VR - Time Efficiency

Data was collected for 30 cases in each environment (60 case in total). The shortest task completion time recorded during a patient case examination and procedure indication was in VRLab (84 seconds), less than the shortest task completion time in SCV (99 seconds). The longest task completion time observed was 608 seconds in VRLab and 711 seconds in SCV, leading to a range of 524 seconds in VRLab and 612 seconds in SCV.

The mean task completion time in VRLab was 231 seconds, which is notably lower than the mean of 378 seconds observed in SCV. This suggests that tasks were completed quicker in the VRLab environment. The standard deviation in VRLab was 125 seconds, compared to 154 seconds in SCV, indicating a greater variability in the SCV environment.

The Shapiro-Wilk test for normal distribution yielded different results for the two environments. The VRLab data, with a W value of 0.8471 and a p-value of 0.0005, did not follow a normal distribution. However, the SCV data, with a W value of 0.9797, showed a p-value of 0.8182, suggesting a normal distribution as it passed the normality test with an alpha level of 0.05.

Further analysis using the Mann-Whitney U-test revealed a significant difference in task completion times between the two environments, with a p-value of 0.0001. The test was two-tailed, and the sum of ranks was 661.5 for VRLab and 1169 for PACS, with a Mann-Whitney U value of 196.5. The median task completion time in VRLab was 183.0 seconds, significantly lower than the median of 374.5 seconds in PACS. The actual difference between these medians was -191.5 seconds.The median task completion time for the SCV is estimated to be between 76.00 and 228.0 units higher than that of the VRLab group with a 95.04% level of confidence.

### 5.3.3 System Evaluation

We now present the results of our evaluation to assess VR's effectiveness in medical simulation, using IPQ-XRMSE and SUS, specifically aiming to gauge the immersive experience and usability of the VRLab system from the perspective of medical professionals. The *IPQ-XRMSE* examined three core aspects of the VR experience: Immersion, Realism, and Involvement. The average scores for these dimensions indicated robust engagement with the VR environment (Figure. 5.5). *Immersion*, with a score of 6.75 (SD = 0.56), *Realism*, at 6.59 (SD = 0.35), and *Involvement*, scoring 6.32 (SD = 0.42).

Our system achieved a total score of 93.125 in SUS, indicating excellent user experience and ease of use - according to the standard benchmark for SUS, where a score of 75 and above indicates excellent usability. The aspects of ease of use, integration of functions, and user confidence were all rated highly, with questions concerning the system's ease of use, learnability, and user confidence in operation receiving particularly strong scores (Figure. 5.6). The questions related to complexity, consistency, and learning curve, while showing lower values, still indicated very positive user experience.

#### 5.3.3.1 Post-evaluation session interviews

During the course of the software testing interviews, a diverse range of feedback was provided by the respondents, each contributing unique insights into the software's efficacy and potential applications. One of the respondents articulated how the

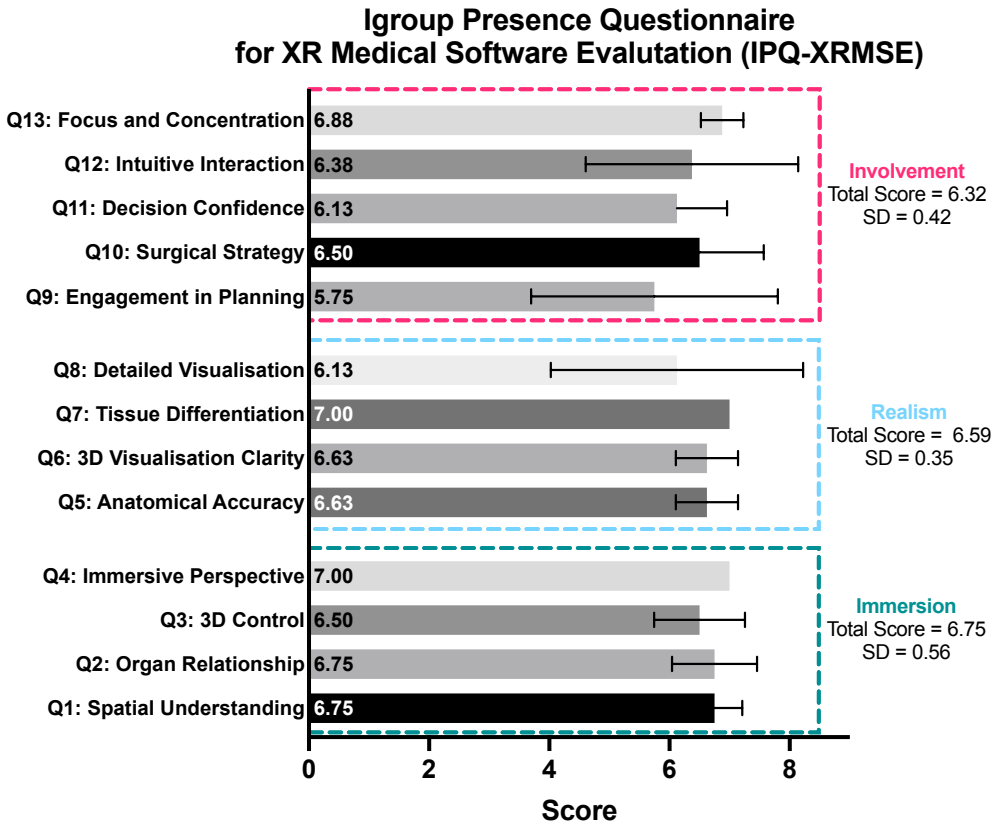


**Figure 5.5:** Mean score for each individual question asked in IPQ-XRMSE with total score for Involvement, Realism, and Immersion shown on the right side.

software instilled a greater sense of confidence and comfort in their work. This respondent noted a marked increase in decision-making speed, attributing this improvement to the heightened certainty felt when using the tool.

Another respondent emphasized the software's significant advancement over existing technologies, such as 3D PDFs and similar 3D reconstructions displayed on 2D monitors. They pointed out the added depth provided by the software, which, in their opinion, led to enhanced preoperative preparation. The high accuracy of the projections was also highlighted, with the respondent acknowledging that "everything made logical sense" when using the tool, thereby underscoring its intuitive design.

The third respondent focused on the clarity of data presentation offered by the system. They expressed a preference for surface data segmented over data rendered using volumetric rendering reconstruction typically presented by radiologists. This preference underscores the software's ability to present complex data in a more comprehensive way, which could be particularly beneficial in medical imaging and diagnostics.

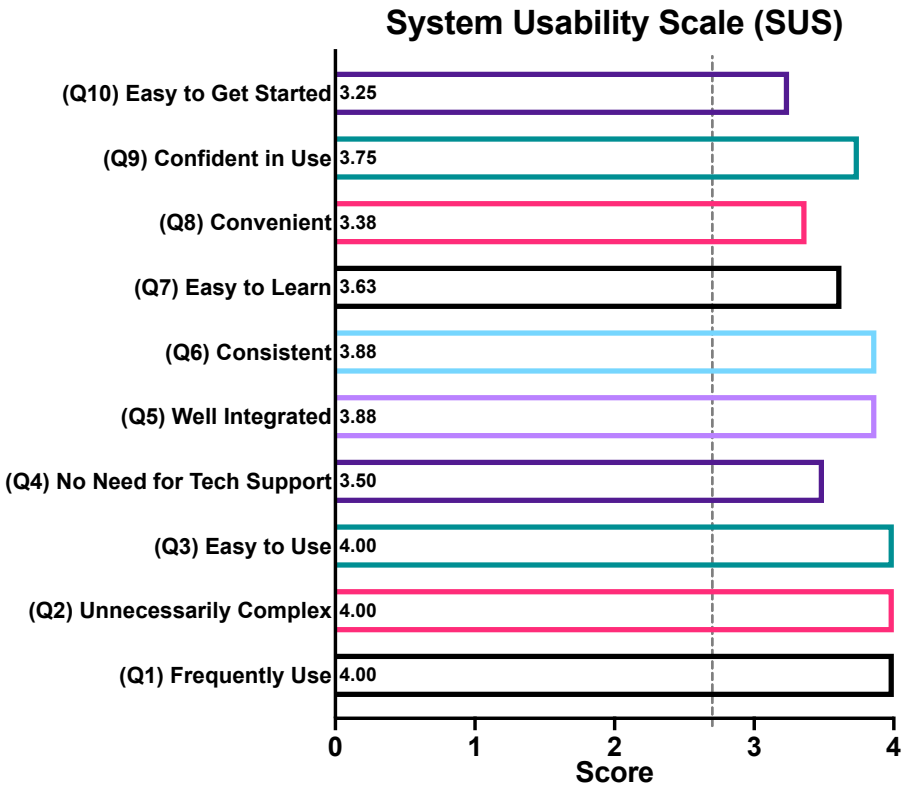


**Figure 5.6:** Mean scores for individual questions in the SUS questionnaire. The dotted vertical line at 2.72 points represents the average of 68 points for SUS (the sum of individual scores is converted to the total SUS score by multiplying by 2.5, resulting in 93.123 points [3, 4]), indicating excellent usability.

Another interviewee provided insights on the broader implications of the system's implementation. They suggested that wider adoption of this software could decrease miss-indications for procedures and increase predictability during complicated surgeries. This perspective highlights the software's potential to enhance individual surgical outcomes and contribute to overall improvements in surgical standards and patient safety.

Finally, the last respondent commented on the depth of visualization provided by the system. They noted that the system offers an enhanced depth of view compared to traditional 3D visualization on computer or tablet screens. This feature could be especially beneficial in fields where depth perception and spatial awareness are critical, such as in certain surgical or diagnostic procedures.

#### 5.3.3.2 Application technical statistics

The application efficiently loads and reconstructs patient-specific OBJ files and generates an examination room on the Photon Cloud within VR swiftly (Mean =

1.69 s, SD = 0.937 s, Internet link Down = 200 Mbps, Up = 1.7 Mbps, Latency = 4 ms). Analysis of 244 real cases reveals an average file size of 7.81 MB per patient (SD = 0.516 MB). This efficiency enables quick initiation of collaborative VR planning rooms, crucial for medical applications. The mean value of frame rate measurements is 75 FPS (SD = 0.3) on Meta Quest 3 (IKEM VRLab has a maximum frame rate locked on 75 FPS). The data traffic of the implementation of collaborative functionality consumed by IKEM VRLab over the period of one month, providing visualisation for 19 patient cases, and with a total of 2 hours and 37 minutes that users spent in the app was 20.88 Mb.

### 5.3.4 Clinical deployment

VRLab has been successfully deployed in clinical settings for liver surgery planning and is integrated into the daily workflow of the surgical team. The deployment process begins at a multidisciplinary seminar where surgeons indicate the patients for whom they require VR visualization in the IKEM VRLab.

When making an imaging examination request, surgeons include a prescription for image acquisition according to the VR CT/MR protocol. Once the imaging data is processed, a team consisting of anatomical 3D modelers and radiologists creates the segmentation of the liver structures. Upon completion, the segmented models are uploaded onto the distribution system.

Surgeons receive an email report and a text message notification indicating that the patient's VR examination is ready. They primarily use Meta Quest 2 and Meta Quest 3 headsets to conduct these examinations. These headsets are available in their offices, pre-operation areas, at home, or other locations.

Screenshots taken from the VR examination are uploaded to a machine inside the operating room and are displayed there during surgical procedures.

Since implementing device analytic tools in August 2022, the application has been used in surgical planning for 105 hours. The mean quarterly number of devices using VRLab was 18.44 devices (SD = 4.95). The collaborative planning was instantiated from 7 countries from Europe, North America, and South America. Since the first clinical deployment of VRLab in May 2021, we have utilized VRLab in over 302 patient cases. The IKEM VRLab with liver section toolkit has been substantially appreciated in pediatric liver resections (Figure. 5.7).

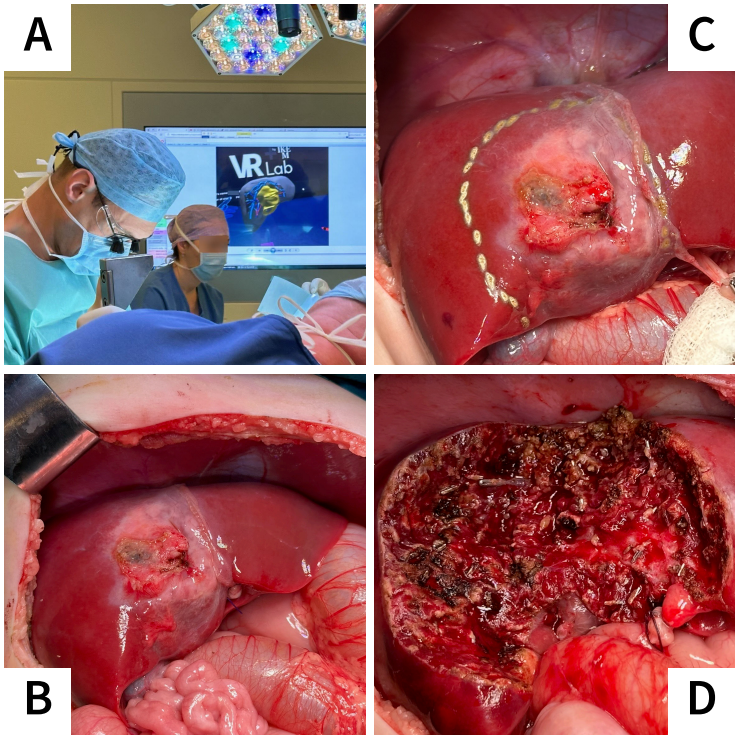


**Figure 5.7:** A screenshot of pediatric patient's anatomy taken in IKEM VRLab being displayed, providing surgeons with information about critical vascular structures in the operation room during a liver resection (A). A pediatric liver with a centrally located tumour (B). Marked resection line, partly into segment 3 in the left lobe, at the interface of the anteromedial and posterolateral segments of the right lobe, preserving part of segment 8 and segment 4a, with a small part of the middle hepatic vein (C). Patient's liver after resection with the central part of the liver being removed (D). (Source: Institute for Clinical and Experimental Medicine)

## 5.4 Discussion

Our findings highlight a pronounced variance in surgeons' decision-making and task completion time efficiency between VRLab and traditional SCV environments. The statistically significant higher mean performance scores in VRLab indicate the advantage of VR technologies in enhancing surgical performance, providing compelling evidence that VR can be a superior tool for surgical planning.

The task completion time analysis results indicate a statistically significant difference in task completion time efficiency between VRLab and SCV environments. The VRLab environment demonstrated a shorter mean task completion time and a lower variability compared to SCV. This efficiency, mirrored in average and median completion times, further underscores the advantages of VR technology in surgical planning and practice.

The responses to specific questions from the IPQ-XRMSE further fortify these

findings. Questions related to *Immersion* (1-4) yielded scores that consistently touched the upper echelons of the scale, signaling a powerful sense of being "in the moment" within the VR environment. In terms of *Realism* (questions 5-8), the participants rated the VR application favorably in its accurate representation of anatomical structures and spatial relationships. Though slightly lower in scores compared to the other two, the *Involvement* aspect (questions 9-12) still showcased a meaningful engagement and confidence in decision-making within the VR setup. The total score from the SUS is considered to be within the range of excellent usability *(benchmark $\geq$ 80)*. This score demonstrates the system's effectiveness and user-friendliness in a demanding medical simulation context. The results from both IPQ-XRMSE and SUS point to a highly immersive, realistic, and engaging experience the VRLab system provides, coupled with an excellent level of usability. These findings further underscore the potential of VR technology as a valuable tool in medical education and training, offering an effective platform for simulating complex medical scenarios.

Finally, the feedback from the one-on-one interviews with respondents collectively suggests that the software represents a notable advancement in the field of preoperative preparation and medical imaging. Multiple respondents mentioned that, in their opinion, the implementation of the system could lead to clear indications or contraindications for patients suffering from initially indicated inoperable lesions. Its ability to provide enhanced depth perception, accurate data representation, and improved decision-making confidence holds promise for its application in various medical disciplines.

**Limitations.** In this chapter, several constraints must be considered while illuminating the benefits of VRLab in liver resection surgical planning and training. The limited sample of surgeons (n=6) and patient cases (n=10) might affect generalisability. This small cohort is mainly due to the scarcity of hepatobiliary surgeons experienced in such complex resections. Additionally, case selection was stringent, excluding those previously operated on or diagnosed by participating surgeons, and focusing instead on unique cases challenging the expertise of less experienced surgeons assisting in the study. Moreover, case selection was prioritized based on indications for procedures based on anatomical landmarks over the properties of the lesion itself (e.g., type of cancer), further constraining the study sample. While ensuring relevant and challenging cases, this deliberate selection process also limited the potential pool of study cases.

The use of the SUS also has limitations. While valuable for assessing usability, these tools may not cover all aspects relevant to the complex context of surgical

planning. Tailoring these questionnaires more specifically (as we did with IPQ-XRMSE) to the surgical context or developing new tools designed for this purpose could yield more comprehensive and context-specific insights.

## 5.5 Chapter Summary

We presented a toolkit for IKEM VRLab for surgical procedure indication of liver resection in a clinical setting. We run a unique set of evaluation methods for XR medical applications to examine the potential of XR in reducing miss-indications for procedures and improving procedural indications. Our research systematically explored not only qualitative but also quantitative metrics of VR applications in surgical environments, thereby marking a significant step in the realm of XR medical technology and surgical practice.

The data reproducibility and scalability of IKEM VRLab with liver resection toolkit for clinical use are among its most important contributions. With its successful implementation in over 300 cases to date, the application has demonstrated not only its effectiveness in diverse clinical scenarios but also its robustness and reliability. The ability to consistently replicate results across different cases and settings highlights the application's potential as a scalable solution in clinical practice. This aspect of the study is particularly significant, as it suggests that the VR system can be effectively integrated into various clinical environments, enhancing the surgical planning process across a broad range of cases. The extensive application of this system in real-world cases further reinforces its practical utility and potential for widespread adoption in the medical field.

Central to this study is the high calibre of participating surgeons, whose expertise and qualifications add substantial credibility to the findings. The surgeons, with extensive experience in hepatobiliary surgery, provide profound and practical insights. Their contributions are particularly valuable given the real and unusual cases they handled, further accentuating the study's relevance and applicability.

The study's methodology, focused on a comprehensive evaluation of VR technology, reveals a notable improvement in decision-making and procedural accuracy when VR is utilized. This is contrasted with traditional clinical visualisation methods, highlighting VR's enhanced capabilities in complex surgical planning. The findings suggest that VR augments the surgeon's understanding of intricate anatomical structures and potentially reduces the likelihood of procedural miss-indications. This is a crucial aspect, as the reduction of complications is a primary objective in any surgical intervention, particularly in high-stakes environments such as

liver resection surgeries. The software was noted for its improved depth perception and accuracy over traditional 3D technologies. Additionally, its potential to reduce complications in complex surgeries and offer a more detailed visual experience compared to standard 3D visualizations was emphasized. The respondents highlighted its ability to boost user confidence, speed up decision-making, and provide clearer data presentation. This collective feedback points to the software's significant potential in advancing surgical outcomes and diagnostics in other surgical fields, such as pancreatic resection, as some respondents suggested. The involvement of actual patient cases and the collaboration with experienced surgeons in clinical trials add a layer of practical validation.

Future research in this field should include a longitudinal study to assess the long-term impact of VR planned surgical procedures focusing on the patient recovery times, blood losses during surgery, and quality of life post-surgery. This would provide valuable insights into the practical benefits and potential limitations of the system, informing its continued development and refinement. Moreover, as some of the respondents suggested, expanding the IKEM VRLab's functionality to pancreatic resection would increase its applicability. Lastly, we suggest creating an extension of this system that could interactively present patient's anatomy at different stages while undergoing chemotherapy allowing to assess operability as the patient progresses throughout the treatment or when patient's are put on long-term watchful waiting.

In conclusion, this chapter represents a significant leap forward in the integration of VR technology in the surgical practice of abdominal surgeries. It opens new routes for enhancing surgical precision and patient outcomes, with the potential to transform how surgeries are planned and executed. The promising results obtained pave the way for future research, which will be crucial in establishing VR as a standard tool in the surgical toolkit.

Chapter 6

# IKEM VRLab in Surgical Treatment of Lung Disease†

In thoracic medicine, managing lung cancer and performing lung transplants for patients with end-stage diseases pose significant challenges. This chapter explores early-stage surgical treatment for lung cancer, specifically, the role of IKEM VRLab-assisted Robotic-Assisted Thoracoscopic Surgery (RATS) in improving patient outcomes. It also proposes late-breaking work on size matching for lung transplantation, a critical option for those with terminal lung disease.

**Lung Cancer and Early-stage Surgical Treatment**

In 2020, lung cancer accounted for 11.9% of all new cancer diagnoses (excluding non-melanoma skin cancers) and 20.4% of all cancer deaths in EU-27 countries. It is therefore the fourth most common cancer (following prostate, breast, and colorectal cancers) and the leading cause of cancer death, with 200,000 deaths in the EU-27 [87].

The most common types of lung cancer are non-small cell lung cancer (NSCLC) and small cell lung cancer (SCLC) [165]. NSCLC accounts for approximately 85% of all lung cancer cases, with subtypes such as lung adenocarcinoma and lung squamous cell carcinoma being the most prevalent [166]. Adenocarcinoma is the most common subtype among NSCLC cases, followed by squamous cell carcinoma [167]. Research indicates that NSCLC is the predominant form of lung cancer, accounting for the majority of cases [168]. Adenocarcinoma, a subtype of NSCLC, is highlighted as the primary type of lung cancer, with a high incidence rate (Cai et al., 2020). On the other hand, SCLC is caused by smoking and tends to spread

†The contributions in the Section 6.2 of this chapter were published in the Perspectives in Surgery [163]. The contributions in Section 6.3 are published in a poster publication at ACM SIGGRAPH 2024 [164].

faster than NSCLC [165].

RATS lobectomies are becoming the standard of care for early-stage lung cancer. These methods have been validated as safe and oncologically radical. By adhering to the recommended procedures when implementing such techniques, minimally invasive thoracic surgery is safe, with decreased morbidity and a variety of cancers becoming operable.

The most common system used in RATS procedures Da Vinci Xi, having 4 robotic arms which can be equipped with operative instruments and a camera. Due to the nature of lobectomies, the placement of robotic *ports*, as well as ports for assisting surgeons and utility ports for inserting needed surgical material, is essential. The procedure of placing Da Vinci Xi ports for lung segmentectomy poses significant challenges due to a complex interplay of anatomical, physiological, and technical factors inherent to thoracic surgery. The human thoracic cavity, where lung segmentectomies take place, offers limited space. Properly inserting and positioning the robotic arms requires precise control to avoid damaging internal structures. The proximity of vital organs and blood vessels increases the risk of inadvertent injury if the arms are not carefully managed. Determining the optimal locations for the robotic ports is thus crucial for successful surgery. Furthermore, incorrect placement can limit the range of motion of the robotic arms, potentially making it difficult to reach certain areas or perform specific manoeuvres. Surgeons must thoughtfully balance the tradeoff between wide coverage and accessibility against the risk of causing trauma to the entry points or internal structures.

Over and above basic arm and port positioning for most surgeries, as described in the related work (Section. 2.4), the lung's intricate anatomy, characterised by multiple segments each with its own vascular and bronchial structures, requires even more accurate port placement. Potential arm clashing can disrupt the surgical flow, requiring adjustments that can prolong the procedure and increase the risk to the patient. Another challenge is correct placement when dealing with a collapsed lung or unusual pathological anatomy. Making matters worse, the surgeon's field of view is restricted to what the robotic camera can see. Unexpected repositioning can take critical structures or areas out of view, requiring adjustment of the camera and potentially leading to disorientation or loss of situational awareness.

Thus for optimal port placement, limitations in imaging technologies are the major culprit. Accurate 3D reconstructions from CT scans are crucial for effective preoperative planning and optimal port placement. While pre-operative imaging, such as CT scans, provides detailed anatomical insights, it may not always offer the required level of clarity. This inconsistency can hinder a surgeon's ability to navig-

ate the surgical field, especially when identifying and preserving critical structures within the lung.

**Lung Transplantation for Patient's Suffering with End-stage Disease**
Lung transplantation, an extremely complex procedure, is frequently the last resort for patients with end-stage lung disease. The most common ailments requiring a lung transplant include chronic obstructive pulmonary disease (COPD), cystic fibrosis (CF), idiopathic pulmonary fibrosis (IPF), pulmonary fibrosis, bronchiectasis, and pulmonary hypertension [169, 170, 171].

COPD is the leading cause of lung transplantation globally. It accounts for a significant proportion of all lung transplants [172, 169, 170, 171]. It has high post-transplant survival rates [173, 174, 171]. IPF has also emerged as a major reason for lung transplants, with many procedures being performed for this condition [175, 176]. CF is the primary reason for lung transplants in pediatric cases (third most common in adults), while pulmonary hypertension is the second most common cause for infants and children needing lung transplants [177, 178].

For a transplant donor-recipient size-matching process, current size-matching methods take into account parameters such as the donor's and recipient's height, weight, and thoracic dimensions. The goal is to ensure the transplant is neither too large nor too small for the recipient's chest cavity. When predicted accurately, size matching can improve the ventilation and perfusion of the transplanted lung and reduce the risk of complications and transplant rejection. These complications may include atelectasis (lung collapse), pneumothorax (air in the chest cavity), and pleural effusions (fluid in the chest).

Even more advanced size-matching methods, such as chest X-rays, computed tomography (CT) scans, and regressive predictive lung volume models, may not adequately capture the dynamic and three-dimensional nature of the thoracic cavity. As a result, these methods can lead to suboptimal outcomes. Size-matching is particularly challenging in pediatric patients. Smaller children often wait much longer for size-matched donor lungs compared to adult patients. To address this issue, various methods have been proposed, such as considering the differences in body weight and height ratios between the donor and recipient. Consequently, while the importance of current size-matching is widely recognized, limited data exist on its specific impact on post-transplant outcomes.

**IKEM VRLab Lung toolkit**

In this chapter, we present two toolkit extensions for IKEM VRLab specifically tailored to correspond to the requirements of lung lobectomies and transplantations. Specifically:

- We first present an extension to the data processing pipeline of IKEM VRLab to facilitate imaging data processing specifically for the lung toolkits.
- We then develop an augmented reality (AR) lung toolkit designed to assist with the preoperative placement of robotic arms during RATS procedures. Our objective was to explore the potential of using AR to project patient-specific data, derived from segmented CT scans, enhancing the accuracy and comfort of surgeons and support staff during the process of robotic arm port localisation. The toolkit aims to enable surgeons visualize a patients' internal structures during port placement and mark those locations on patients' bodies for better navigation of the physical robotic arms.
- We develop an additional IKEM VRLab toolkit to enhance the accuracy of size matching in lung transplantation. By creating a virtual environment where surgeons can manipulate and visualize the fit of donor lungs within the recipient's thoracic cavity, our system aims to provide a more intuitive and accurate method for size matching. The incorporation of VRLab into the lung transplantation process represents a paradigm shift in how surgeons approach size matching. Unlike traditional methods, VR allows for the exploration of the spatial relationship between the donor lung and the recipient's thoracic cavity in real-time, offering dynamic manipulation and assessment adaptive to to the unique anatomical features of each patient. Our approach not only aims to improve immediate post-transplant outcomes by reducing the incidence of size mismatch complications, but also has the potential to expand the donor pool by enabling more precise adjustments that accommodate a wider range of donor-recipient size discrepancies.

## 6.1 Data Generation of Lungs & Thoracic Cavity from CT

This section delineates our method for creating 3D reconstructions of patients suffering from lung tumours as well as lung transplant donors and recipients, from CT scans. Our method involves three stages, corresponding, but differentiated, to data

processing in the previous legs and liver toolkits: data acquisition, segmentation, and data conversion.

For our toolkit development, the patient's lung imaging data were recorded using CT. There was no set protocol prior to obtaining the imaging, as it was acquired from a variety of institutions across the country, however, we did set specific criteria in place to ensure useful, accurate data. For patient health reasons additional re-examination by CT was not recommended to avoid increased radiation exposure. The range for image slice thickness was between 0.8 to 1.5 mm with increments set to generate a continuous stack of images. For example, when slice thickness is 1 mm, the increment should be no more than 1 mm. We were primarily selecting imaging series when patients were breathing in (inhale phase) to get the maximum possible capacity of the lungs and expose the inner vascular structures. The resolution of the image reconstruction was never less than 512x512 pixels.

We segmented the obtained CT data using the Lung CT Analyser tool, which includes the Total Segmentator functionality in the 3D Slicer environment [179, 180, 181]. This software suite performs automatic identification and delineation of critical anatomical structures within the thoracic region, such as the lung lobes, heart, trachea, esophagus, aorta, vena cava, and the bone structure of the torso. The latter consists of the sternum, costal cartilage, ribs, vertebrae, spine, clavicles, and shoulders. Particular attention was paid to accurately locate the position and size of the diaphragm due to its crucial role in ensuring size compatibility between the donor organ and the recipient. Despite the inherent challenges associated with directly imaging the thin diaphragm (due to imaging techniques limitations), a practical approach was taken. The upper edge of the diaphragm was inferred based on proximate anatomical landmarks, specifically the liver and spleen, thus approximating the demarcation between the thoracic and abdominal cavities. Providing estimation of the diaphragm's edge is required for transplant surgeons during size-matching evaluation.

When segmenting data of patients that would undergo a RATS procedure for tumour removal, vascular structures, including pulmonary veins, pulmonary arteries, and lesions, were segmented semi-automatically by using region-growing and thresholding methods. For lung transplant recipients, we prioritised CT series obtained at the peak of inhalation to ensure the lungs were fully expanded. However, the acquisition of donor data posed certain limitations, primarily due to the inability to standardize the respiratory phase of the donors, compounded by the heterogeneous nature of imaging protocols across different institutions. Typically, donor scans were received in native phase before any radiocontrast has been administered, which reflects the pragmatic challenges encountered in real-world clinical

settings

To expedite the transformation of segmented data into a format suitable for both implemented toolkits based on IKEM VRLab's framework, we developed a plugin that converts data from 3D Slicer's export files (STL) to the standard OBJ format used by IKEM VRLab. Initially, the system scrutinizes the export files, categorizing and structuring individual skeletal components into coherent layers. These components are then integrated into unified substructures, ensuring each pulmonary lobe remains distinctly partitioned. The abdominal cavity is depicted as a single layer, incorporating the intestine, colon, spleen, and liver, thus defining the physiological barrier. In contrast, entities such as the heart, aorta, vena cava, esophagus, tumor, and trachea are preserved in separate layers. Following this, during the optimization phase, individual structures are refined based on a predefined polycount model to ensure compatibility with the default parameters of the IKEM VRLab environment. This optimization ensures the seamless integration of 3D models into the VRLab platform.

## 6.2 Initial Experience in Deploying Augmented Reality when Porting DaVinci Xi Robotic Arms during Robotic-Assisted Thoracoscopic Pulmonary Segmentectomy

In this project, we created a toolkit for IKEM VRLab to be used as an augmented reality (AR) system during the placement of robotic arms before a RATS procedure, enabling surgeons to see the patients' internal structures while placing ports and to mark places on the patients' bodies for better navigation of the physical robotic arms.

This work was done in collaboration with the Faculty Hospital Motol that has performed 126 robotic anatomical lung resections since the robotic program initiation in August 2020, reaching the status of a proctoring and case observation centre. The centre started a robotic segmentectomy program after completing 70 robotic lobectomies.

To provide a preliminary evaluation of this concept, we deployed the system during two RATS procedures and collected feedback from performing surgeons, assisting surgeons, anesthesiologists, and nurses through questionnaires and post-operation interviews.

The contributions of this project are twofold:

- We extended IKEM VRLab in AR for RATS procedures, introducing an AR-based system that projects patient-specific, CT-derived anatomical data onto the patient during surgery. This advancement not only facilitates the precise placement of DaVinci Xi robotic ports but also enhances the surgeon's spatial understanding in a complex anatomical landscape.
- We conducted comprehensive evaluations through both quantitative data from questionnaires and qualitative insights from post-operative interviews with medical staff. The findings substantiate the system's effectiveness in improving surgical planning, execution, and educational aspects, as confirmed by surgeons, anesthesiologists, and nurses who participated in the initial trials.

### 6.2.1 Technical Implementation

The core of the system is based on the IKEM VRLab system (Chapter. 3). For the AR visualisation, we employed a Microsoft Hololens 2. Several modifications and integrations are necessary to adapt the IKEM VRLab system for use with Microsoft HoloLens 2 and leverage the potential of augmented reality in robotic arm port planning and for RATS lobectomies. This adaptation involves altering the existing VR rendering system, which is primarily designed for use with Meta Quest headsets and developed in the Unity 3D Engine, to incorporate AR capabilities facilitated by HoloLens 2. This process includes integrating the Microsoft Mixed Reality Toolkit (MRTK) and migrating the application to a new platform (Universal Windows Platform). The toolkit offers out-of-the-box support for spatial awareness, gesture and voice commands, and advanced interaction models that are essential for AR applications.

### 6.2.2 UI and Interaction Adaptation

Meta's integration relies heavily on the use of hand controllers for interaction within the VR environment. Transitioning to MRTK involved adapting to a hands-free interaction model that utilizes hand tracking and gesture recognition, as well as voice commands available in the HoloLens 2. This required redesigning the user interface and interaction mechanisms to accommodate hand gestures for actions previously performed with controllers, such as selecting, grabbing, rotating, and scaling 3D models.

The transition also involved rethinking the feedback mechanisms. In VR, feedback is often provided through visual cues and haptic feedback from the controllers. In an AR context with the HoloLens 2, visual feedback remains crucial, but haptic

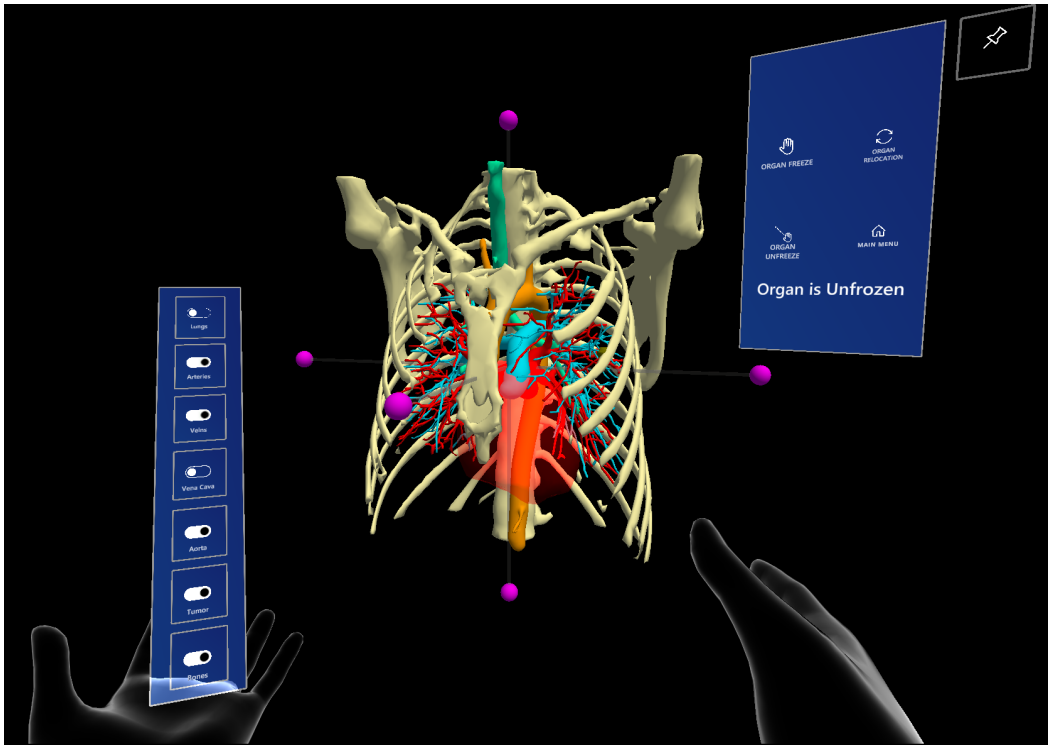


**Figure 6.1:** A screenshot from the Augmented Reality environment with the layer system hovering above the left hand, the patient's 3D reconstruction in the centre, and the control panel hovering on the right side. The purple dots placed around the 3D reconstruction are additional grabbing points to support easier manipulation when a user is trying to register the reconstruction on the patient's body.

feedback is absent. Therefore, we decided to implement audio-based cues audible every time the user decides to use a gesture, manipulate the organ model or interacts with elements on a UI panel.

The first UI panel the user interacts with is a slot selection panel connected to IKEM VRLab's distribution system, where the user can pick a particular patient (Section. 3.1.5). Following the AR environment's instantiation with the patient's 3D anatomical reconstruction in view, the user is provided with a levitating control panel, which can be moved and pinned as required to improve comfort. When the user moves within the operating theatre, if the distance of the control panel is greater than 1 meter, the panel unlocks and starts following the user. This prevents losing essential controls when large motions are performed - e.g., walking from one side of the operating table to the other. The control panel can also be used to reset the location of a patient's organ, useful when inspecting a model in the pre-operation room and then walking into the operating theater to avoid leaving the patient's reconstruction in the other room. The patient's 3D reconstruction can also be *frozen* in the environment to prevent unwanted movement. The anatomy

layer system described in Section 3.1.2 is transformed into a small bar-shaped panel, which appears after using a gesture in the form of the user looking at his/her left palm. The user can toggle each button and turn ON & OFF a particular anatomical structure.

MRTK integration enabled us to implement natural hand gestures to interact with the patient's 3D reconstruction, such as rotating or moving the 3D model. For example, the surgeon might use a pinch gesture to select a part of the anatomy and a drag motion to move it. When the user moves far away from a model (thus the model cannot be grabbed within hand reach), a laser pointer coming from the centre of the palm can be used as a *lasso* and, with a pinch gesture, bring the model closer. MRTK also supports visualisation of the user's hands as an overlay (Figure. 6.1). That ensures that the user has a clear idea of where exactly the position of their hands are with respect to the real physical environment but also the augmented environment. Without this implementation, the user's hands would have been *always* hidden *behind* the rendered elements in the AR as the display is physically closer to the eye than the hands.

### 6.2.3 Pre-deployment

Before the operation, the surgeon must register and calibrate the digital anatomical structures to ensure they are accurately superimposed over the patient's real body. The user can interactively modify and control the segmentation of anatomical structures using gestures and a control panel. This includes the ability to zoom in, zoom out, rotate, and pan the visualized structures. The surgeon's judgment, based on his experience and knowledge of the anatomy, is a key part of the process. However, we facilitate registration by including not only the patient's pulmonary anatomy but also bone and cartilage structures such as the rib cage, sternum, clavicles, and shoulder blades to provide surgeons with solid, not deformable reference points for accurate superimposition of the digital anatomy over the patient.

### 6.2.4 Evaluation Trials

In this section we provide details on the initial, exploratory trials of our system as tested during two RATS lung segmentectomy procedures. The system's efficacy and usability were assessed while used in two surgeries performed on two female patients, aged 45 and 48, both diagnosed with tumours in the upper lobe of the left lung (Figure. 6.2). The evaluation aimed to measure the system's impact on

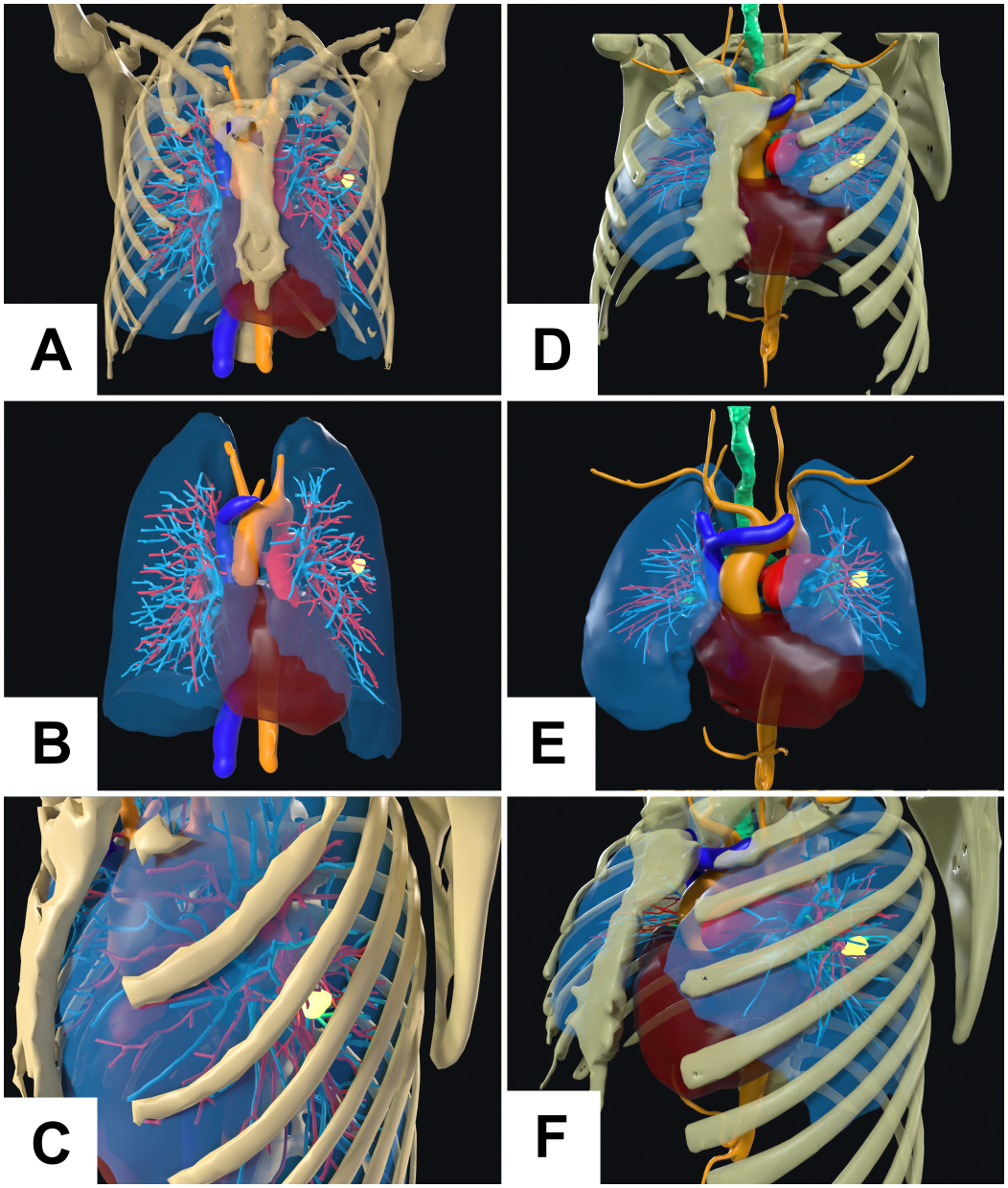


**Figure 6.2:** These renders show patients 1 and 2's 3D reconstructions, which were segmented using Total Segmentator and region-growing. The A, B, and C are renders of patient 1's reconstruction, followed by patient 2's anatomical renders in D, E, and F. Colouring is standardised for both reconstructions according to general anatomical atlases: pulmonary arteries are in light blue, pulmonary veins are in red, the aorta is in orange, vena cava is in dark blue, the heart is represented by dark red, and in green is the oesophagus. The tumours are in emissive bright yellow colour, especially noticeable in the left lungs in pictures C and F.

surgeons' decision-making, its integration into the surgical workflow, and the overall satisfaction of the medical team with its features.

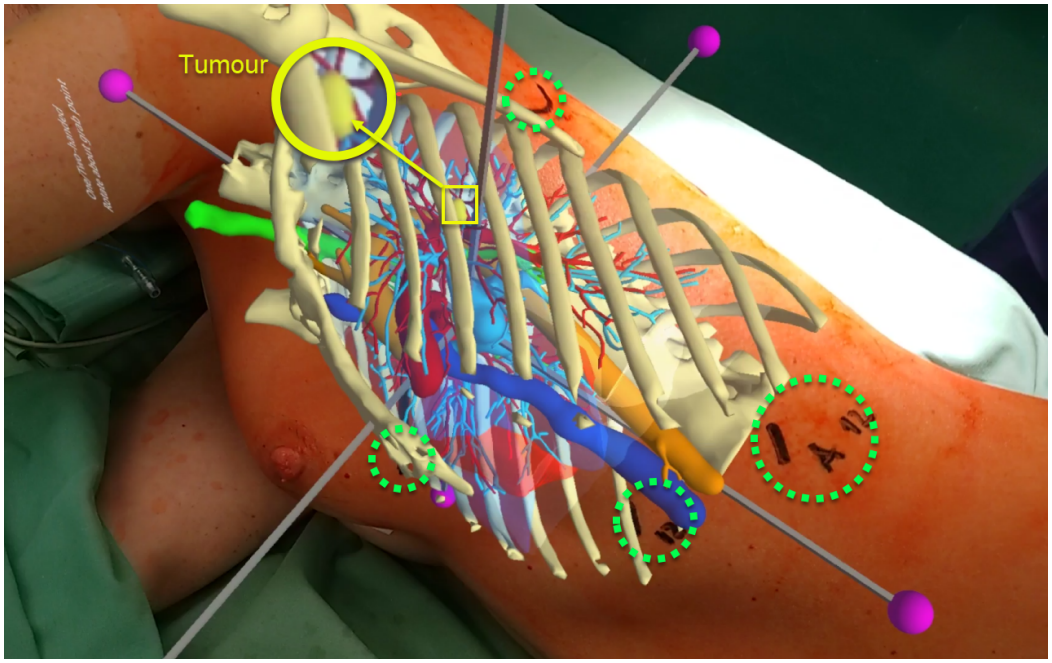


**Figure 6.3:** An image obtained during a trial while head surgeon is indicating port placement points for robotic arms of the surgical robot daVinci Xi at the University Hospital Motol in Prague. Green dotted circles highlight the marks for the individual ports. The yellow rectangle highlights the tumour's position inside the chest, while the yellow circle is a magnification of the rectangle.

#### 6.2.4.1 Patients' Details

**Patient 1**: A 45-year-old female with a tumour in the upper lobe of the left lung measuring 10 mm by 13 mm by 12 mm, with a volume of 1.2 ml as measured on CT. **Patient 2**: A 48-year-old female with a tumour in the upper lobe of the left lung measuring 14 mm by 14.22 mm by 14.42 mm, with a volume of 1.315 ml. Both patients were in stable conditions under anaesthesia throughout the procedures.

#### 6.2.4.2 Surgical Team Composition

The surgical team was composed of five experienced surgeons, two anesthesiologists, and two nurses. Three surgeons were local surgical consultants, and two were visiting from other institutions where they were introducing the RATS program for lung segmentectomies. This diverse group of medical professionals provided a comprehensive perspective on the system's performance across different roles within the surgical environment.

#### 6.2.4.3 System Utilization

Before the surgical procedures, the lead surgeon had the opportunity to review a 3D reconstruction of the patients' anatomy through the IKEM VRLab system. This pre-operative planning phase included tactile localization of anatomical structures and the strategic placement of Da Vinci Xi robotic ports.

During the surgical procedure, the lead surgeon utilized an augmented reality headset for real-time visualization of the patient's anatomy. Once the lead surgeon correctly registered patients' 3D reconstruction onto their bodies using bone reference points, the surgeon started marking the chosen insertion marks onto the body using a marker (Figure. 6.3). Once the lead surgeon decided on the insertion points (Figure. 6.4), the visualisation was shared with the team to discuss the proposed plan and prepare for any potential shift to open surgery in case of rupture and sudden bleeding (Figure. 6.5). The anesthesiologists and nurses also interacted with the system, gaining insights into the procedural steps and required tools, enhancing the collaborative effort and preparedness of the entire team.

#### 6.2.4.4 Evaluation Methodology

During both trials, we employed the think-aloud protocol. The lead surgeon, deriving the plan and locations for optimal ports, shared the proposal with the rest of the surgeons. During this discussion, we recorded the surgeons' comments and feedback. We extended this evaluation to the anesthesiologists and surgical nurses. Immediately after the surgical procedures, we held group conversations with the entire staff present during the surgery to collect feedback on whether this proof-of-concept system brings significant improvements and increases the staff's comfort and confidence. We also evaluated whether the development of this concept should be continued and how it could be further enhanced. For supporting staff members, we wanted to evaluate their level of understanding in terms of medication, required tools and procedure timeline.

Following the surgery, we distributed two specialized questionnaires to the involved parties: one for the surgeons and another for the auxiliary medical team. These questionnaires aimed to collect initial feedback on our system's impact on surgical workflows, its usability, the benefits perceived by the supporting medical staff, and suggestions for further improvements.

Both surgeons and the support medical staff were asked to evaluate the clarity of the 3D patient reconstructions (Q1), the system's contribution to cross-disciplinary education (Q2), its accuracy in mirroring real-life conditions (Q3), and its overall

effect on the surgical procedure's quality (Q4). The survey for surgeons was more comprehensive, including additional questions on whether the system improved port placement comfort (Q5), aided in the precise localization of tumours (Q6), and enhanced their understanding of the patient's vascular and bronchial structures (Q7). Respondents rated each question on a 10-point scale, with 0 being the lowest and 10 being the highest rating (an example of the questionnaire is available in the Appendix D.).

**Figure 6.4:** A photo of the lead RATS surgeon wearing a Microsoft Hololens 2 while using the AR visualisation of the patient's reconstruction superimposed onto the patient's body to determine the best locations for port placement.

### 6.2.5 Results & Discussion

We now present results collected during the two aforementioned RATS procedures. The total surgery time of *patient 1* was 2 hours and 4 minutes, while *patient's 2* was 2 hours and 54 minutes.

The integration of IKEM VRLab into RATS surgical procedures demonstrated considerable potential to enhance the efficiency and efficacy of lung segmentectomies.

**Figure 6.5:** A photo of the lead RATS surgeon with a visiting surgeon to share his port placement plan before the procedure.

These advancements have garnered positive feedback from various members of the medical team, as evidenced by their responses during the think-aloud protocol, questionnaires, and post-operative interviews.

The collected data from the questionnaires indicate overall positive feedback from both surgeons and the support medical staff regarding the medical system in question, with all mean scores ranging from good to excellent on a 10-point scale.

For Q1, that assessed the clarity of the 3D patient reconstructions, the average score was 8.89 (SD = 1.54). Respondents found the reconstructions clear, with only a few respondents suggesting less clarity than others. In terms of the system's contribution to cross-disciplinary education (Q2), the mean score was 9.33 (SD = 1.12), reflecting a high level of agreement that the system is beneficial for educational purposes across different disciplines. The system's accuracy in mirroring real-life conditions (Q3) received a mean score of 9 (SD = 1). This tight grouping around the high mean suggests that respondents consistently agreed that the system represented patients' pathological anatomies with high fidelity. Q4 dealt with

the overall effect of the system on the quality of surgical procedures and scored the highest mean of 9.44 (SD = 0.73). This indicates a strong consensus that the system positively impacts surgical procedure quality.

For the surgeon-specific questions, Q5 regarding improved comfort during port placement received a mean score of 8.8 (SD = 1.64), indicating elevated comfort during the robotic ports placement. Q6, which inquired about the system aiding in the precise localization of tumours, had a mean score of 9 (SD = 1). This conveys a generally favourable view of the system's effectiveness in tumour localization. Lastly, Q7, which asked about the enhanced understanding of the patient's vascular and bronchial structures, also received a high mean score of 9 (SD = 1). This reflects a consensus that the system is effective in improving surgeons' understanding of complex anatomical structures.

We recorded the respondents' views on the proposed system's potential for day-to-day use. An anesthesiologist, for instance, reported a significant improvement in their ability to comprehend the scope and timeline of surgical processes. They highlighted how the system enabled them to understand the extent of the operation within just ten seconds. This quick assimilation of critical information is key to the system's potential to streamline the surgical workflow, thereby significantly optimising the preparatory phase of surgery. Additionally, the nursing staff have lauded the system for its educational value. They particularly emphasised its utility in training novice nurses, thanks to the clarity with which the surgical procedure is being presented, allowing less experienced staff to gain insights into complex surgical techniques and the operational sequence.

Surgeons commended the system's ability for swift tumour localization. They mentioned the straightforward registration between the 3D models and the patient's anatomy as a notable enhancement, as it significantly reduces the time normally spent on analyzing CT scans to pinpoint tumour locations and their relationship to anatomical landmarks, such as the intercostal spaces. Additionally, surgeons complimented the system's improved visualisation of vascular structures and their relation to tumours. By offering a detailed view of the tumour location, potential resection margin, and the distance from the adjacent segmentation boundary, the system aids surgeons in their preoperative planning process. This crucial information facilitates determining the extent of the resection necessary, simplifying the decision between a segmentectomy (removing a segment of a lung lobe) or a lobectomy (removing entire lung lobe). The system also provides an intuitive interface for surgeons to trace the relationship of the lesion to the vessels. This feature is integral to the surgical process as it aids in better localizing the lesion within the patient and in selecting an adequate resection margin. This is particularly import-

ant for sublobar resection, as the knowledge of the variations in the vascular and bronchial supply of a given patient is a key factor in the procedure's success. Furthermore, segmentectomies present a unique challenge due to the greater number of anatomical variations in vascular and bronchial branching compared to single lung lobes.

Further to the above, surgeons characterised the system as an invaluable tool for anticipating the movements required by robotic arms, thereby simplifying the process of port placement. Such predictive capabilities are vital in robotic-assisted surgeries, where precision and preparation are key. The system also provides the surgeons with a better understanding of the diaphragm's location. Surgeons also found the process of selecting suitable sites for trocar insertion during robotic lung resection, to be vastly simplified, a normally quite complex and time-consuming task. During the operation, the system allowed the surgeons to return to the specific anatomy of the patient's vessels and bronchi as often as required. The segment's viewing angle can be adjusted according to the real-time view during the operation resulting in better identification of individual vascular trunks and bronchi, thus significantly enhancing operation safety. Finally, it was suggested that the toolkit was extremely useful in guiding where to perform the incision lines and which vascular structures would remain - a feature particularly beneficial in conserving the patient's vasculature and ensuring that even the smallest vascular branches are taken into account during surgery.

### 6.2.6 Project Summary, Limitations & Future Work

This project centred on implementing AR to improve the placement of DaVinci Xi robotic ports during RATS procedures. Taking place at the Faculty Hospital Motol, this study is crucial as the precision required for port placement in thoracic surgery is complex and significantly impacts the surgical procedure's outcome. In addressing the primary challenge of port placement in the restrictive environment of the thoracic cavity, this project employs AR via the adapted IKEM VRLab system to project detailed, patient-specific anatomical information directly onto the surgical field. The system serves as a direct visual guide for surgeons, allowing them to see through the patient's skin and place ports accurately in real-time, avoiding critical internal structures and ensuring optimal reach and manoeuvrability of the robotic arms.

The study's main contributions focus on significantly enhancing the surgical process for lung segmentectomies. By facilitating precise port placement, the system aids surgeons in efficiently navigating the complexities of the chest cavity. This

process not only simplifies the operative workflow but also has the potential to reduce surgery time and improve patient safety. Surgeons are provided with a level of situational awareness previously unavailable, reducing reliance on traditional pre-operative imaging and allowing for a more dynamic and responsive surgical approach.

Feedback from the deployment of this system during initial RATS procedures at the hospital has been positive. Surgeons report a shift in port placement—a task that requires meticulous planning and often a degree of trial and error—into a more assured and swift process. Similar implementation has the potential to make RATS procedures more accessible and effective, contributing to the advancement of minimally invasive surgery.

The evaluation of this novel surgical system during lung segmentectomy procedures has demonstrated promising outcomes in terms of operational efficiency, team collaboration, and surgical accuracy. Further studies with larger sample sizes and varied surgical scenarios are recommended to validate these findings and explore the system's full potential in enhancing patient care and surgical outcomes.

Surgeons identified several areas for improvement in our current, preliminary system - mainly suggested adding functions that would allow the addition or subtraction of vessels and bronchus from lung anatomy. While the AR implementation enhances visualization, it relies heavily on the registration accuracy of both the hardware and the software. Any calibration or registration discrepancies between the AR system and the patient's actual anatomy could lead to inaccurate port placements.

Moreover, the limitations of using the Microsoft HoloLens in the operating room encompass various aspects that need to be addressed. Firstly, the device has a restricted field of view, which can hinder the surgeon's ability to perceive the entire surgical area [182]. This limitation can impact the precision and accuracy of procedures, potentially leading to errors. Moreover, ergonomic concerns arise due to the need for the device to be worn for extended periods, which may cause discomfort and fatigue for the user [183]. Additionally, potential latency issues in the system could affect real-time interactions and decision-making during surgery, emphasizing the importance of seamless integration with existing systems in the operating room [184]. Furthermore, the HoloLens's indoor and closed environment usage limitation restricts its versatility and applicability in various surgical settings [185]. The device's tracking performance, influenced by factors such as marker size, distance, and camera resolution, can affect its accuracy in surgical navigation tasks [186]. Integration challenges with other technologies and systems in the operating

room need to be carefully considered to ensure smooth workflow and compatibility [187]. The absence of validated measures and comprehensive evaluation instruments poses a challenge in studying the learning effects and outcomes associated with using the HoloLens in medical education and training [188].

The AR system's effectiveness also depends on the quality of the pre-operative imaging. Variations in CT scan quality across different institutions or due to the patient's specific condition can compromise the precision of the 3D reconstructions used during surgery. One potential solution could be the implementation of an adjusted CT protocol for lung screening. Another suggested enhancement is to extend the system's capabilities to include pre-placement of the robotic ports via a standard desktop computer or tablet application. Surgeons could then use the AR to display these on the patient in the operating room, bypassing the need to do this during the placement procedure while immersed in AR. In conclusion, additional studies are required to validate the clinical benefits of AR implementation in RATS procedures during lung-segmentectomy.

## 6.3 IKEM VRLab FittingRoom: Lung Transplantation Donor-Recipient Size-matching Between Adults and Children in Virtual Reality

In this section we describe our work on lung transplantations, a life saving procedure that is becoming increasingly common. This work was conducted in collaboration with the 3rd Surgical Clinic, 1st Faculty of Medicine, Charles University in Prague, and Motol University Hospital that are currently the only lung transplantation centres in the Czech Republic. Since 2018, based on an international agreement between the Ministries of Health, lung transplants have also been performed for patients from the Slovak Republic. Since the program began in 1997, specialists have performed more than 400 transplantations in adults and children. In 2023, According to the Czech Coordination Center for Transplantation, the transplant team of the 3rd Surgical Clinic performed 67 lung transplants.

Before a transplantation, the predicted total lung capacity (pTLC) ratio is frequently used to estimate lung size matching [189]. This method considers both the volume of the donor's lungs and the available space within the recipient's thoracic cavity [130]. However, in pediatric cases, size matching becomes more challenging as smaller children often face extended waiting times for size-matched donor lungs compared to adults [119]. Such mismatching can lead to increased mortality, particularly in preadolescent patients [120]. Therefore, the ratio of the recipient's chest volume to the donor's lung volume is crucial, especially after downsizing oversized grafts [132]. Current challenges in size-matching include the impact of the donor's age on graft failure and the risks associated with using pediatric donor lungs for adult recipients due to size-related tidal volumes and height mismatch [121]. Techniques like X-ray sizing and predicted volume from computational tomography ($TLC_{CT}$) have been employed to improve size matching and minimize complications [190, 130]. However, concerns remain about potential errors in measuring lung heights via X-ray sizing, potentially leading to size-mismatched lung transplant procedures [131]. While $TLC_{CT}$ shows promise in assessing lung volume, more robust evidence is needed [126].

In this section, we describe the development of a toolkit for size-matching in lung transplantation for IKEM VRLab, deployed in two cases of size-matching between adult recipients and child and adult donors. To evaluate our system we compared IKEM VRLab Fitting Room to the existing methods challenging their accuracy. Our immersive method was able to perform size matching for cases that current methods did not provide clear and definite answers. This project represents an

initial exploration but also potentially a stepping stone into further development of more personalised VR methods for lung transplant size-matching.

### 6.3.1 IKEM VRLab Fitting Room: Examining Donor-Recipient Size Compatibility

The Fitting Room is an extension toolkit within the IKEM VRLab scalable framework. This toolkit is specifically altered to cater to the complex needs of lung transplantation surgery and leverages interactive tools previously deployed in liver resection surgery planning (Section. 5.1.3) such as interactive clipping plane and ruler. The volumetric estimation tool was upgraded to provide volumes of individual lung lobes of donor's and recipient's lungs.

The VRLab Fitting Room generates a 3-dimensional, interactive model of both the donor's lung and the recipient's thoracic anatomy. This includes important structures such as the lobar distribution within the lugs, ribs, spine, vertebrae, costal cartilage, sternum, aorta, vena cava, trachea, and nearby organs like the spleen and liver to estimate the range of motion of the diaphragm since its visibility on the CT images is limited, providing surgeons with a detailed visual and quantitative analysis tool. This enables surgeons to evaluate the fit and volume compatibility of the donor's lungs with the recipient's thoracic cavity in an immersive environment contrary to to the current size-matching methods.

#### 6.3.1.1 3DUI

The UI heavily leverages the previously integrated in the based of the IKEM VRLab system and liver resection toolkit (Section. 3.1.2 & 5.1.3) and its previously integrated tools, such as the Clipping Plane, Interactive Ruler, and Volume Estimation methods. The use of a Clipping Plane facilitates detailed exploration of internal lobar anatomy by permitting sectional views of the lung model at any orientation, essential for perceiving spatial relationships and potential intrathoracic impediments in the recipient. The Interactive Ruler provides distance measurements within the virtual environment, thereby supporting the evaluation of the proportional compatibility of the recipient thoracic cavity and the donor's parenchyma (portion of the lungs involved in gas exchange).

The user interface is reminiscent of the original VRLab framework, but the surgeon sees two 3D CT reconstructions in this system. The surgeon manipulates 3D models of the donor lung and recipient thoracic cavity within the VR space in the

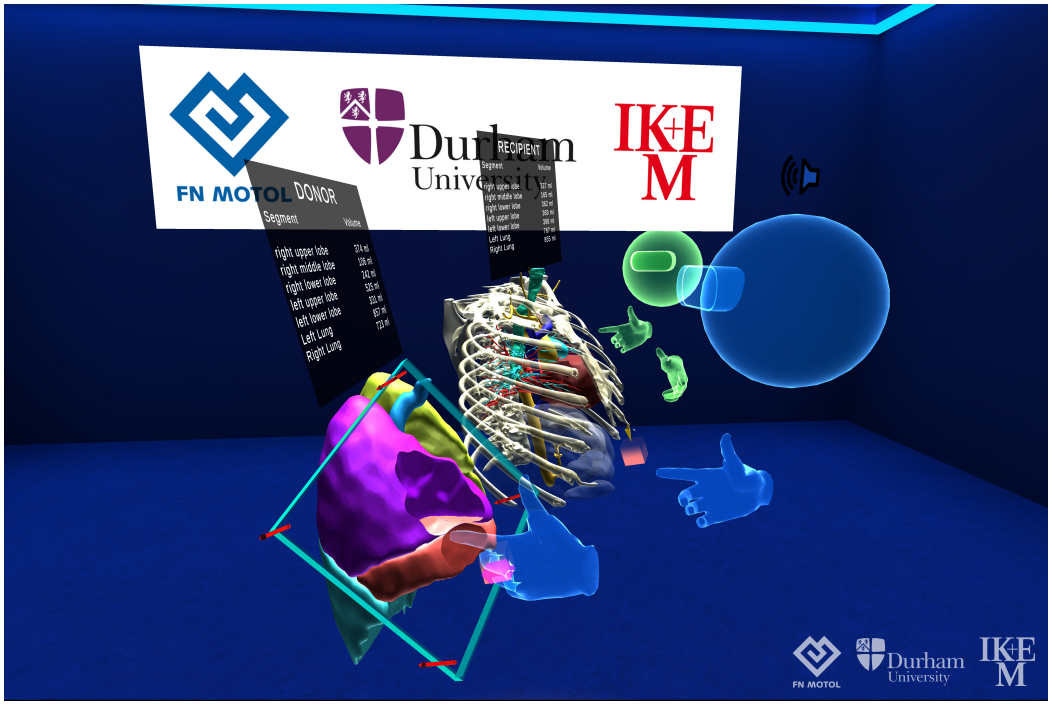


**Figure 6.6:** Showcasing our immersive environment of the Fitting Room, two users visually evaluate the donor and recipient's lung volumes and the recipient's thoracic cavity to determine anatomical compatibility with the donor's lungs. The user in blue is handling a cutting plane to examine the lobar borders in the right lung. The volumes of each lobe and the total lung volumes are displayed in millilitres above the reconstructions.

same way as in the case of the IKEM VRLab (Section. 3.1.2). We've modified the grabbing points for the 3D reconstructions to prevent accidental movement of the recipient's anatomy when adjusting the parenchyma within the recipient's chest. This modification involves control boxes placed in front of the patient's segmentation. When the user wants to manipulate a particular segmentation (donor's or recipient's), they must pass through a cube-shaped element with either the left or right hand to gain control over that 3D reconstruction. The system checks which hand the user used, allowing, for example, the user to hold the donor's parenchyma in the left hand and the patient's chest in the right hand. The surgeons can then virtually *place* the donor lungs within the recipient's thoracic cavity, assessing both fit and anatomical compatibility in terms of shape and size. The vivid colour differentiation of lung lobar anatomy aids in identifying and controlling the visibility of specific lung segments via the layer system (Section. 3.1.2).

We reused the previously implemented functionality from estimating liver segment volumes (Section. 3.2 & 5.1.3) to facilitate the computation of the volumetric properties of individual lung lobes for both the donor and recipient. This capability can be used in assessing the viability of transplantation, notably in situations where

partial lung transplantation is being considered. In the context of pediatric and small adult cases, the system's ability to selectively visualize and compute the volume of specific lobes (typically the middle and lower lobes of the right lung or the lower lobe of the left lung) and to subtract this from the total donor lung volume estimation, is crucial for pre-operative planning.

Since the core of the system is built on the scalable architecture of IKEM VRLab, the system supports real-time collaboration among multiple users from different medical centres (Section. 3.1.1). This can be helpful when a potential organ recipient is hospitalised in a remote district hospital under the supervision of an attending physician while the transplant centre is located elsewhere. This enables remote consultations and planning sessions between attending physicians and transplant surgeons.

### 6.3.2 Transplantation Size-matching: Case Reports

The IKEM VRLab Fitting Room system was evaluated twice, once post-operationally during a size-matching evaluation between a pediatric donor and two potential adult female recipients and once pre-operationally during a size-matching of an adult female donor and adult male recipient.

Traditional size-matching (based on height, weight, pTLC, pTLV, and $TLV_{CT}$) did not provide transplant surgeons with clear answers as to whether recipients are a right match to the donor's anatomy or whether one recipient is more anatomically compatible than another. The details about the individual cases, recipients, donors, and data collected from the size-matching instances are described below.

#### 6.3.2.1 Transplantation Size-matching Case 1:

**Donor and Recipient Details:**
In this case report on lung transplantation size matching, we delve into the compatibility between two potential recipients and a young donor. The first recipient (R1) is a 61-year-old woman suffering from pulmonary fibrosis. She has a body weight of 41 kg and a height of 159 cm. Chest X-rays, taken from a one-meter distance, show her lung heights to be 20.9 cm on the left side and 20.0 cm on the right, with a horizontal lung width of 23.4 cm. To ensure accurate measurements for lung size matching, chest X-rays in all instances were taken from a one-meter distance, standardizing image size and magnification.

The second recipient (R2), a 69-year-old woman, is dealing with Stage IV sarcoidosis accompanied by pulmonary fibrosis. Her weight is 69 kg, and she shares the

same height of 159 cm as the first recipient. Her chest X-rays indicate lung heights of 16.5 cm on the left and 15 cm on the right, with a horizontal lung width of 27.5 cm.

The donor is a 9-year-old boy (D1) who weighs 35 kg and measures 140 cm in height. His chest X-ray shows that his right lung is 14.2 cm high, his left lung is 14.9 cm high, and his horizontal lung width is 20 cm.

Assessing the compatibility between the donor and the recipients highlights potential challenges due to differences in the size of their lungs. For the first recipient, the donor's lungs may be relatively smaller, necessitating careful consideration of the transplant's feasibility and functionality. For the second recipient, given her wider lungs and larger body mass, adapting the smaller donor lungs could pose even more complex challenges.

**Size-matching by pTLC and TLC Estimates**

Pre-operationally, pTLC were calculated using the European Respiratory Society (ERS) formulas (Equation. 6.1,6.2) [127]. For R1, the calculated pTLC is 4.11 litres. For R2, the calculated pTLC was identical to R1's pTLC due to the same height of both potential recipients. Hence R2's pTLC was 4.11 litres as well. The D1's pTLC was estimated to be 4.11 litres. The pTLC ratio of D1 vs R1 was 0.87. The TLC ratio of D1 vs R2 was also 0.87. The 0.87 indicates undersizing of the donor's lung parenchyma to both recipients. Eberlein et al. (2013) categorized patients into "oversized" (pTLC ratio $> 1.0$) and "undersized" (pTLC ratio 1.0) groups [36]. Fraser et al. (2019) defined size mismatch as oversizing (donor-to-recipient pTLC ratio $> 1.2$) and undersizing (donor-to-recipient pTLC ratio $< 0.8$) [120].

For men, the pTLC in litres can be calculated using the formula:

$$\text{pTLC (litres)} = (7.99 \cdot \text{height in meters}) - 7.08 \tag{6.1}$$

For women, the pTLC in litres is estimated by:

$$\text{pTLC (litres)} = (6.60 \cdot \text{height in meters}) - 5.79 \tag{6.2}$$

Post-operatively, we employed sex-specific reference equations, including height and age, which were developed for total lung capacity by the Global Lung Function Initiative (GLI) with reference values for static lung volumes in individuals of European ancestry [191]. These equations are designed to calculate the median predicted value (M) (Equation. 6.3, 6.5), the variability around the median (S)

(Equation. 6.4, 6.6) considering factors like age, height, and sex. The equations make use of logarithmic transformations of age and height to align with the non-linear nature of lung function development and decline over one's lifespan. The terms "Mspline" and "Sspline" refer to age-varying coefficients which account for the non-linear changes in lung function with age.

The promise of employing age was to predict more accurate TLC in the pediatric donor and provide more accurate TLC for both recipients. Based on GLI's predictive model, R1's TLC is 4.8 litres, R2's is 4.89 litres, and D1's is 3.024 litres. The TLC ratio of R1 vs D1 is 0.63, while R2 vs D1 is 0.62.

**Table 6.1:** pTLC estimates in litres with donor-recipient ratios are presented at the bottom of the table.

| | **pTLC Total** |
|---|---|
| R1 | 4.7 |
| R2 | 4.7 |
| D1 | 4.11 |
| **Donor vs Recipient Ratios** | |
| Ratio D1 vs R1 | 0.87 |
| Ratio D1 vs R2 | 0.87 |

**Table 6.2:** TLC estimates based on GLI's model in litres with donor-recipient ratios are presented at the bottom of the table.

| | **GLI's TLC Total** |
|---|---|
| R1 | 4.8 |
| R2 | 4.89 |
| D1 | 3.02 |
| **Donor vs Recipient Ratios** | |
| Ratio D1 vs R1 | 0.63 |
| Ratio D1 vs R2 | 0.62 |

The GLI's TLC for males can be predicted using the equation:

$$\text{TLC} = \exp\left(-10.5861 + 0.1433 \cdot \log(\text{age}) + 2.3155 \cdot \log(\text{height}) + M_{\text{spline}}\right) \quad (6.3)$$

where log denotes the natural logarithm, age is in years, and height is in centimetres. $M_{\text{spline}}$ is an adjustment factor based on a spline model for age.

The variability around the median (S) for males is calculated as:

$$S = \exp\left(-2.0616143 - 0.0008534 \cdot \text{age} + S_{\text{spline}}\right) \quad (6.4)$$

$S_{\text{spline}}$ adjusts the standard deviation based on age.

The GLI's TLC for females is predicted with:

$$\text{TLC} = \exp\left(-10.1128 + 0.1062 \cdot \log(\text{age}) + 2.2259 \cdot \log(\text{height}) + M_{\text{spline}}\right) \quad (6.5)$$

The variability (S) for females is given by:

$$S = \exp\left(-2.0999321 + 0.0001564 \cdot \text{age} + S_{\text{spline}}\right) \quad (6.6)$$

**Size-matching by pTLV Estimates**

Another method we employed prior to final decision-making was a predictive Total Lung Volume (pTLV) model. Conventional methodologies such as pTLC or GLI's TLC predominantly rely on height and age comparisons between donors and recipients, which introduce significant variability in lung size matching and potentially negatively impact post-transplant outcomes. The study conducted by Konheim et al. [126] introduces an approach that utilizes three-dimensional computed tomography (3D-CT) volumetry to generate predictive equations for pTLV (Equation. 6.7), predicted right lung volume (pRLV) (Equation. 6.8), and predicted left lung volume (pLLV) (Equation. 6.9) [126]. This method aims to facilitate more accurate size matching by incorporating parameters such as age, gender, height, and race, which are identified as independent lung volume predictors.

The development of this model involved the retrospective evaluation of chest CT scans from a cohort of normal patients, from which predictive equations were derived. The study's rigour was further established through the validation of these equations in a separate patient group, comparing predicted lung volumes against actual volumes measured via 3D-CT volumetry. Additionally, an external validation compared predicted total lung volumes with total lung capacities derived from pulmonary function tests, illustrating strong linear correlations. This validation process underscores the potential of pTLV equations to offer a more refined tool for size matching in lung transplantation, aiming to mitigate the limitations associated with conventional size matching techniques and potentially improve transplant outcomes through a more precise matching process.

In the predictive equations for lung volumes (pTLV, pRLV, pLLV), the constants, such as 630.819 or 967.100, function as coefficients derived from the regression model. The intercept, for example, 630.819, sets the baseline for the predicted lung volume when the variables of age, gender, height, and race are zero. It serves to calibrate the model to the data at hand. The coefficient associated with gender, 967.100, reflects the adjustment to the predicted lung volume when the variable

changes — being male, which is encoded as 1, increases the predicted lung volume by 967.100 millilitres compared to being female. The height coefficient, 25.197, indicates a decrease in the predicted lung volume by 25.197 millilitres for each additional centimetre in height, suggesting an inverse relationship within the model's context. Race is another factor, with a coefficient of 713.838, which denotes that being African American (coded as 1) is associated with a 713.838 millilitre decrease in predicted lung volume relative to non-African Americans. Lastly, age, with a coefficient of 15.10, suggests that every additional year of age is linked to an increase of 15.103 millilitres in the predicted volume. These coefficients encapsulate the statistical relationships established in the study and are calibrated to the specific demographic characteristics of the sample population from which the data was drawn.

Deploying this models estimated volumes for R1 (pTLV = 4.30 litres, pRLV = 2.28 litres, pLLV = 1.99 litres), R2 (pTLV = 4.33 litres, pRLV = 2.30 litres, pLLV = 2.01 litres), and for D1 (pTLV = 3.99 litres, pRLV = 2.30 litres, pLLV = 1.91 litres). The pTLV ratios between R1 vs D1 is 0.93, and R2 vs D1 is 0.92). In this equation, we treated both recipients and the donor as non-African Americans. Furthermore, the sum of pRLV and pLLV in the donor exceeds the pTLV.

**Table 6.3:** pTLV estimates in litres with donor-recipient ratios are presented at the bottom of the table.

| | **pTLV Left Lung** | **pTLV Right Lung** | **pTLV Total** |
|---|---|---|---|
| R1 | 1.99 | 2.28 | 4.30 |
| R2 | 2.01 | 2.30 | 4.33 |
| D1 | 0.75 | 0.83 | 1.59 |
| **Donor vs Recipient Ratios** | | | |
| Ratio D1 vs R1 | | 0.93 | |
| Ratio D1 vs R2 | | 0.92 | |

Predictive equations for predicted total lung volume (pTLV):

$$pTLV = \frac{-630.819 + (967.100 \cdot \text{Gender}) + (25.197 \cdot \text{Height}) - (713.838 \cdot \text{Race}) + (15.103 \cdot \text{Age})}{1000} \tag{6.7}$$

Predicted right lung volume (pRLV):

$$pRLV = \frac{-383.300 + (507.864 \cdot \text{Gender}) + (13.316 \cdot \text{Height}) - (352.502 \cdot \text{Race}) + (9.083 \cdot \text{Age})}{1000} \tag{6.8}$$

Predicted left lung volume (pLLV):

$$pLLV = \frac{-257.539 + (460.948 \cdot \text{Gender}) + (11.834 \cdot \text{Height}) - (365.027 \cdot \text{Race}) + (6.150 \cdot \text{Age})}{1000} \tag{6.9}$$

- Sex: Female = 0, Male = 1
- Race: Non-African American = 0, African American = 1
- Height: Centimetres
- Age: Years
- pTLV, pRLV, pLLV: Litres

**Size-matching by $\text{TLV}_{\text{CT}}$**

We also utilized Siemens Syngo.via Pulmo 3D package (Siemens Healthneers, Germany) for TLV from CT imaging ($\text{TLV}_{\text{CT}}$). Prior to transplantation, both the donors and the recipients underwent CT examination. These scans capture detailed cross-sectional images of the thoracic cavity during the inhalation phase, which are crucial for the subsequent volumetric analysis.

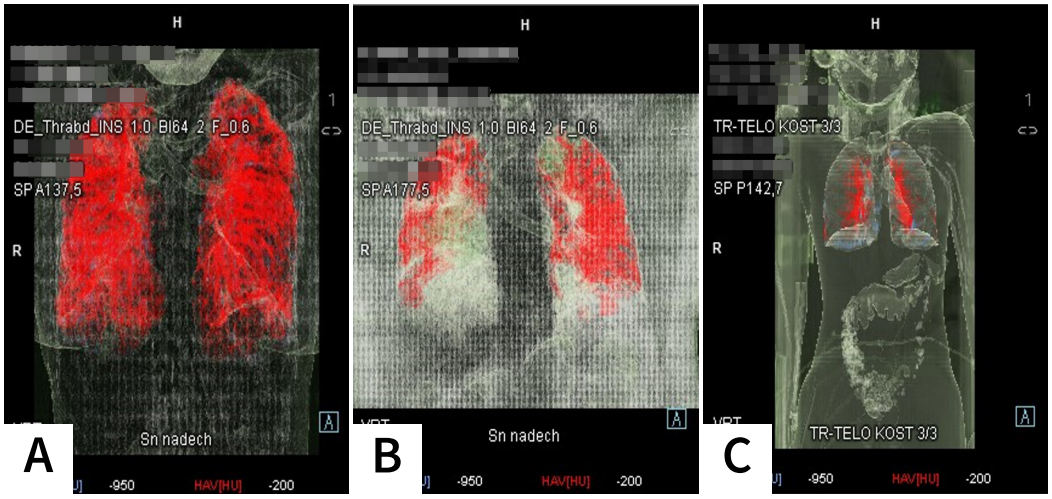


**Figure 6.7:** Lung segmentation during calculation of lung volume in Pulmo 3D for R1 (A), R2 (B), and D1 (C).

For recipients, the acquired CT images were imported into the Syngo.via software suite, where they underwent processing prior to the transplantation. This platform uses pre-trained algorithms for image segmentation, effectively distinguishing lung parenchyma from other thoracic structures. Pulmo 3D performed a 3D reconstruction with the lungs segmented to provide a virtual model of both recipients' lungs. This allows for volumetric analysis and visualization of the lung's structure in three dimensions. Pulmo 3D calculates the volume of each lung by tallying the voxels within the defined threshold for lung tissue. This volumetric assessment is done separately for the right and left lungs, offering detailed information pertinent to

either single or double lung transplantation. Syngo.via estimated $TLV_{CT}$ for R1 ($TLV_{CT}$ = 1959 ml, $TLV_{CT}$ Right Lung = 885 ml, $TLV_{CT}$ Left Lung = 1074 ml), and for R2 ($TLV_{CT}$ = 997 ml, $TLV_{CT}$ Right Lung = 392 ml, $TLV_{CT}$ Left Lung = 605 ml).

During the decision-making stage, Pulmo 3D could not be deployed because the donor was hospitalised at a different clinic, and this system was not available at that location at the time. Retrospectively, we performed this analysis for donor gain $TLV_{CT}$ for the purpose of this study ($TLV_{CT}$ = 1607 ml, $TLV_{CT}$ Right Lung = 843 ml, $TLV_{CT}$ Left Lung = 764 ml). The $TLV_{CT}$ ratios between both recipients and the donor were as follows: R1 vs D1 is 0.82, and R2 vs D1 is 1.61.

**Table 6.4:** A table of $TLV_{CT}$ estimates in litres from Syngo.via Pulmo 3D, with donor-recipient ratios being presented at the bottom of the table.

| | **$TLV_{CT}$ Left Lung** | **$TLV_{CT}$ Right Lung** | **$TLV_{CT}$ Total** |
|---|---|---|---|
| R1 | 1.07 | 0.88 | 1.95 |
| R2 | 0.60 | 0.39 | 0.99 |
| D1 | 0.76 | 0.84 | 1.60 |
| **Donor vs Recipient Ratios** | | | |
| Ratio D1 vs R1 | | 0.82 | |
| Ratio D1 vs R2 | | 1.61 | |

**Size-matching in IKEM VRLab FittingRoom:**
Pre-operatively, the VRLab Fitting Room offered surgeons a volumetric comparison of the donor's lung and the thoracic cavities of both recipients. The application initially provides an estimation of the volumes for each of the lung lobes (right upper lobe (RUL), right middle lobe (RML), right lower lobe (RLL), left upper lobe (LUL), left lower lobe (LLL), as well as the total volume of both lungs.

For R1, the estimated volumes were: RUL = 418.93 ml, RML = 116.47 ml, RLL = 438.02 ml, LUL = 578.77 ml, LLL = 536.10 ml. The total volume was calculated as 973.43 ml for the right lung and 1114.88 ml, creating a total lung volume of 2088 ml. For R2, the estimated volumes were: RUL = 394.75 ml, RML = 95.12 ml, RLL = 238.30 ml, LUL = 528.91 ml, LLL = 333.16 ml. The total volume was 728.18 ml for the right lung and 862.07 ml for the left lung, creating a total lung volume of 1590 ml. Finally, for D1, the estimated volumes were RUL = 321.38 ml, RML = 160.57 ml, RLL = 355.66 ml, LUL = 361.65 ml, LLL = 391.21 ml. The total volume was 837.62 ml for the right lung and 752.86 ml for the left lung, creating a total lung volume of 1590 ml. The ratio between D1 and R1 is 0.76, and the

**Table 6.5:** TLV estimates in litres from IKEM VRLab FittingRoom with donor-recipient ratios are presented at the bottom of the table.

| | **VRLab TLV Left Lung** | **VRLab TLV Right Lung** | **VRLab TLV Total** |
|---|---|---|---|
| R1 | 1.11 | 0.97 | 2.08 |
| R2 | 0.86 | 0.72 | 1.59 |
| D1 | 0.75 | 0.83 | 1.59 |
| **Donor vs Recipient Ratios** | | | |
| Ratio D1 vs R1 | | 0.76 | |
| Ratio D1 vs R2 | | 1.00 | |

ratio between D1 and R2 is 1.00. The ratio between D1 and R1 is a perfect match. However, the right lung of R2 is significantly smaller than D1's, which disqualified R2 from receiving new organ.

During the post-operative evaluation in the immersive environment of VRLab FittingRoom, surgeons confirmed that the right side of the R2's thoracic cavity is undersized for the D1's right lung (Figure. 6.9). The R2's suffering from obstructive lung diseases caused a collapse of the chest within itself. On the other hand, the fitting of D1's left lung into the left side of the thoracic cavity shows a small amount of undersizing for R2's left side of the thoracic cavity. When mounting D1's lungs inside of the R1's thoracic cavity, the immersive VR system indicated an acceptable anatomical match (Figure. 6.8). The use of immersive environment size-matching suggests that D1's lungs were well within the acceptable size range for R1.

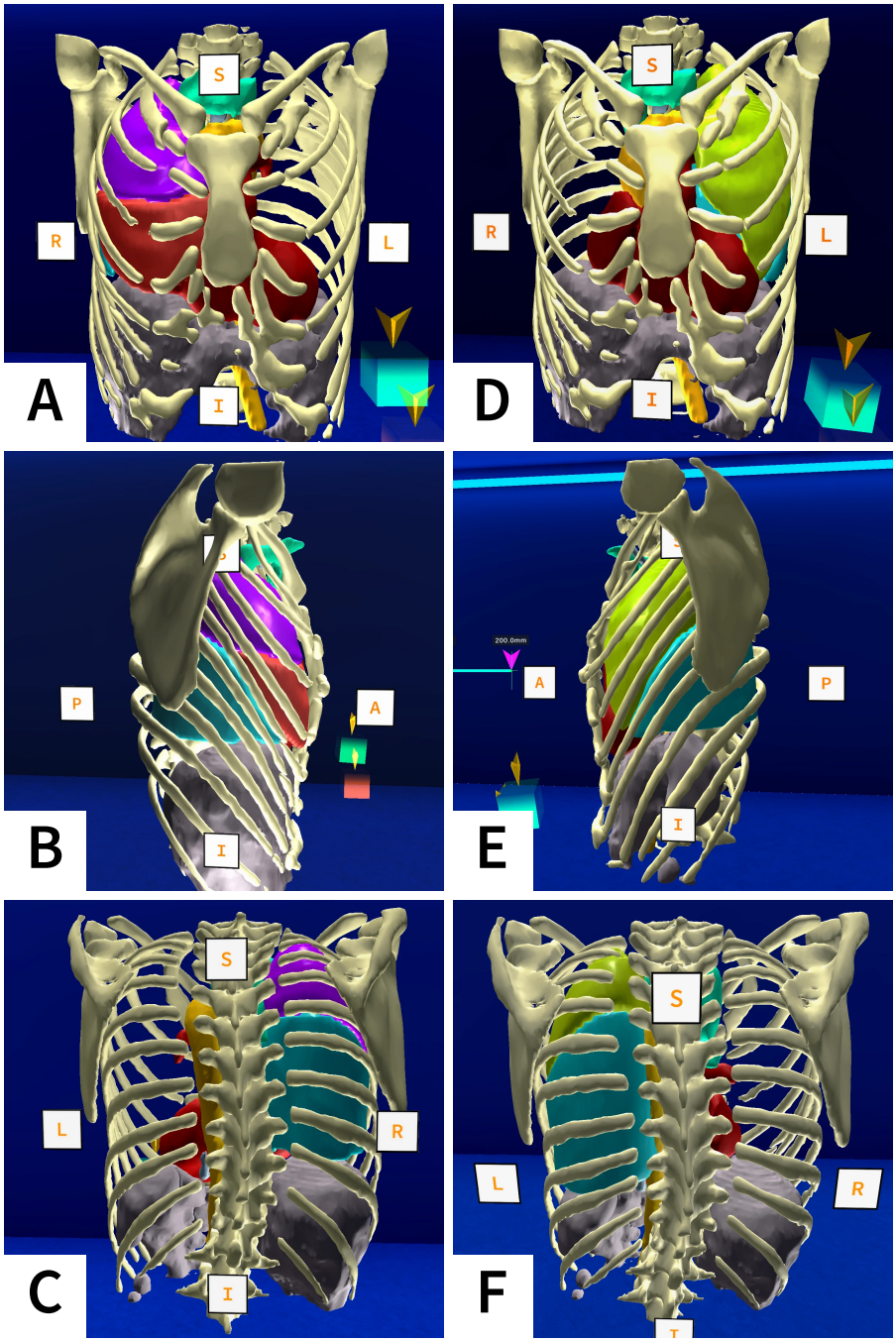


**Figure 6.8:** Screenshots taken in the FittingRoom during the immersive size-matching between D1 and R1. D1's right lung appropriately matched with the R1's right side thoracic cavity from the front (A), right side (B), and back (C). In the case of D1's left lung, R1's left side thoracic cavity from front (D), right side (E), and back (F) is also showing an appropriate match without requiring lobe reductions.

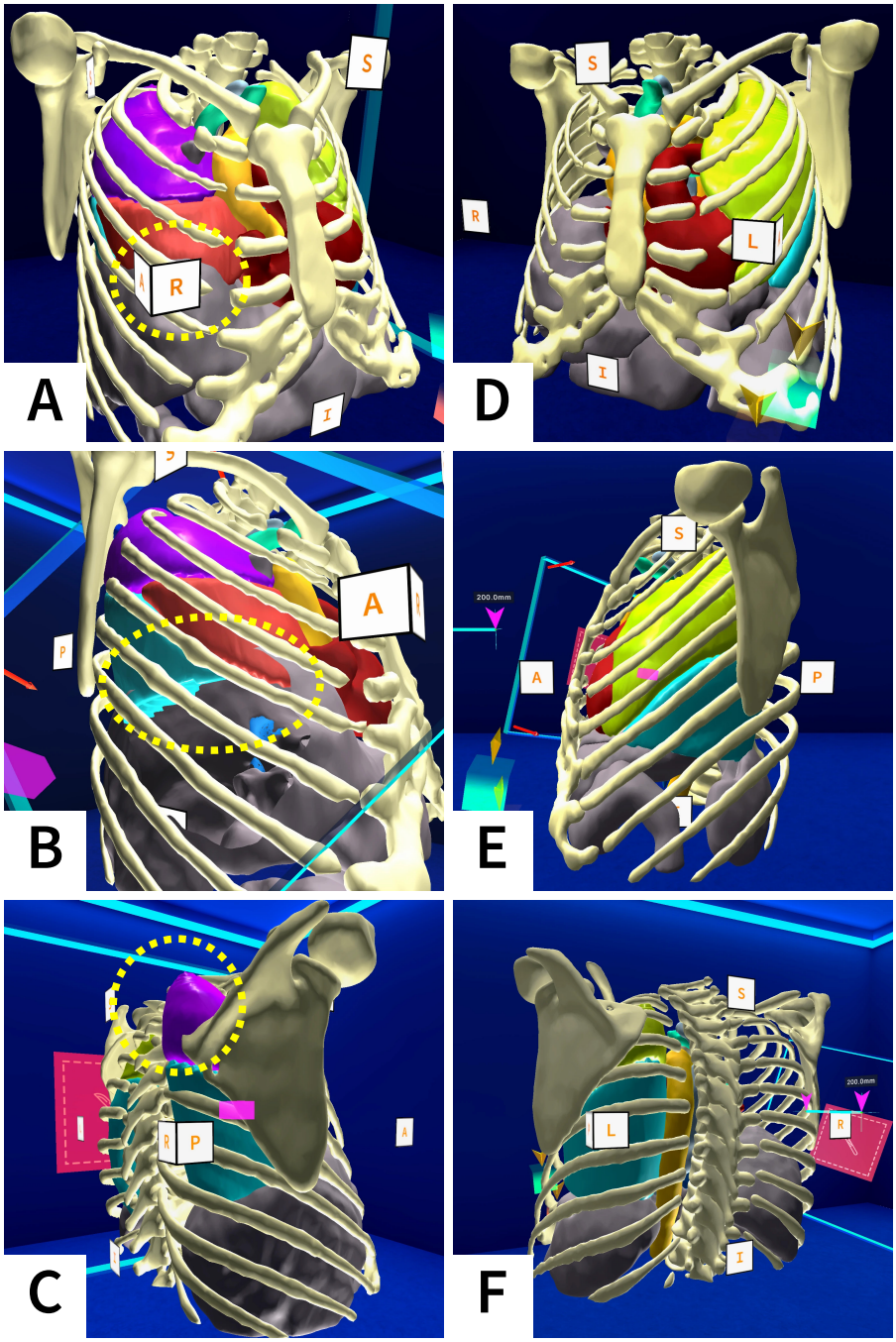


**Figure 6.9:** Screenshots taken in the FittingRoom during the immersive size-matching between D1 and R2. In the yellow dotted circles, the middle lobe of the right lung is severely oversized for the right side of the recipient's thoracic cavity and is colliding with an upper part of a liver (A, B). From the side-back view (C), it's apparent that the D1's right lung is too tall for the R2. The simulated implantation of D1's left lung into R2's cavity shows a correct match (D, E, F).

**Recipient Selection for Procedure:**
The process of selecting the most suitable recipient for donor lungs in a lung transplantation case involved an evaluation of various size-matching methods by the surgical team. This evaluation with the surgeons, having examined the compatibility between the donor and potential recipients through multiple analytical lenses, ultimately determined that the approach provided volumetric estimates by the VRLab Fitting Room was the most influential in guiding their decision. Post-operatively, the surgical team confirmed via the immersive functionality of placing the donor's lungs within R1's thoracic cavity, their informed, but heavily instinct-based decision.

Initially, the transplant team explored pTLC estimates. This method offered basic volume comparisons but lacked the depth needed to account for the unique anatomical differences and the specific impacts of lung diseases. The pTLC ratios of 0.73 for both potential recipients (R1 and R2) compared to the donor (D1) highlighted a significant undersizing of the donor's lungs. However, these assessments did not incorporate crucial factors such as the shape of the thoracic cavity or the detailed effects of pathologies. Retrospectively, we deployed GLI's TLC estimation method and compared it to pTLC estimates. According to the surgeons, GLI's TLC produced more realistic ratio estimates of volumes (R1 = 4.8, R2 = 4.89, D1 = 3.02) while still not reflecting correctly R1's and R2's medical condition. Further analysis using pTLV estimates refined the surgeons' view, yielding ratios of 0.93 for R1 and 0.92 for R2 against D1. This method represented a step forward in precision, yet it still did not capture the full complexity of anatomical fit and disease impact on thoracic structures.

Generally, the predictive total lung capacity or volume models did not very well reflect the recipients' medical conditions. Also, these predictive models don't account appropriately for child donors.

The $TVL_{CT}$ offered the surgeons with more accurate volumetric data derived directly from CT scans. This method confirmed a more *realistic* volume estimation of R1 (total lung volume of 1.95 litres) and R2 (total lung volume of 0.99 litres). Retrospectively, we performed $TVL_{CT}$ estimation on the D1's data. The calculated ratios suggested a more suitable match for R1 (ratio of 0.82) than for R2 (ratio of 1.61), indicating significant oversizing for R2, it could not alone provide a comprehensive evaluation of transplant compatibility, especially regarding dynamic anatomical considerations. Moreover, a radiologist suspected that the automatic segmentation did not encapsulate the entire lung tissue due to inconsistent contrast within the lungs in the CT image series caused by R2's medical condition, particularly in the right lung. This could potentially lead to the *unrealistic* volumetric

estimation of the right lung (390 ml).

The VRLab Fitting Room provided surgeons with insights beyond mere volumetric compatibility by simulating how the donor lungs would fit within the recipients' thoracic cavities. Despite the comparable ratios (0.76 for R1 and 1.00 for R2), the detailed visualization of anatomical fit revealed that R2 was less suitable due to anatomical and pathological constraints, a fact that volumetric data alone could not adequately convey.

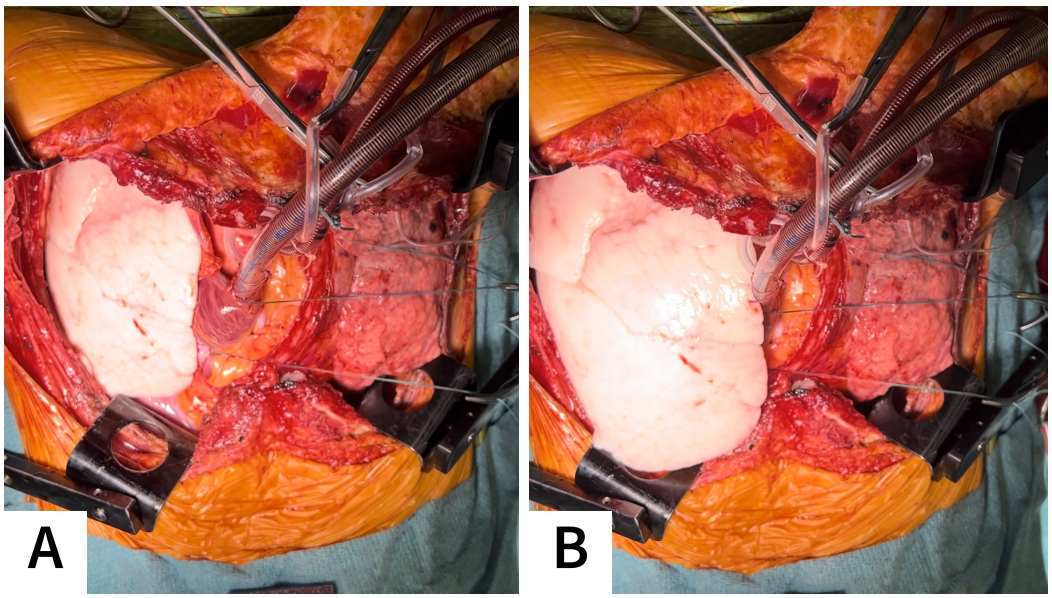


**Figure 6.10:** A photo taken after implantation of D1's right lung into R1's thoracic cavity during a simulated exhale (A), and inhale (B). This photo shows that the size match was successful. (Source: FN Motol)

### 6.3.3 Post-surgery Details:

The D1, a 9-year-old child donor weighing 35 kg and measuring 140 cm in height, was matched with an adult recipient despite being significantly smaller in stature (Figure. 6.10). VRLab FittingRoom's immersive 3D size-matching confirmed the ideal match between the donor's lungs and the recipient's thoracic cavity post-operatively. The transplantation procedure did not require any reductions in the size of the donor lungs, which is noteworthy given the recipient's relatively small physical size compared to the donor.

### 6.3.4 Transplantation Case 2:

**Donor and Recipient Details:**
The second case report describes a size-matching process for lung transplantation of a female adult donor (D2) and a male adult recipient (R3). D2 was a 52-year-old woman who weighed 80 kg and was 175 cm tall. The R3 is a 38-year-old male suffering from fibrotic exogenous allergic alveolitis. R3 weighs 101 kg and is 183 cm tall. In this case, IKEM VRLab FittingRoom was part of the decision-making process from the beginning of the size-matching procedure. There is a considerable difference in body size, weight, and age upon observing R3's and D2's body properties.

Initial data would suggest that the donor's lungs might be undersized for the recipient. Unfortunately, a standard X-ray from one meter for D2 was not acquired. Therefore, for the purposes of this study, the measurements were taken at the widest and tallest points from the CT scans. The R3's lung dimensions are 15.8 cm for the right lung and 18.3 cm for the left lung, with a horizontal width of 25.2 cm across the lungs. The D2's lung measurements are 17 cm on the right side and 18.4 cm on the left side, with a horizontal lung width of 23.8 cm. These measurements suggest similar dimensions, suggesting an acceptable size match for whole double-lung transplantation.

**Size-matching by pTLC and GLI's TLC Estimates:**
Pre-operatively, the pTLC for R3 was calculated to be 7.54 litres. The donor's pTLC (D2) was estimated at 5.76 litres. The TLC ratio of D2 to R3 is 0.76, indicating an undersizing of the donor's lung tissue for the recipient.

Post-operatively, using the GLI's TLC reference equations that incorporate sex, height, and age, R3's TLC was predicted to be 7.6 litres, and D2's TLC was 6.1 litres. This results in a TLC ratio of R3 to D2 of 0.8, which also indicates a undersizing of the donor's lung parenchyma for the recipient.

**Size-matching by pTLV Estimates:**
In evaluating the pTLV data, D2 has a pTLV of 4.55 litres, while recipient R3's pTLV is 5.5 litres. This results in a pTLV ratio of D2 to R3 of 0.82. This ratio indicates that the donor's lung volume is larger than the recipient's, which is considered undersized.

Additionally, R3's pRLV is 2.9 litres, and pLLV is 2.6 litres, while D2's pRLV is 2.41 litres and pLLV is 2.13 litres. The donor's total lung volumes are lower than the recipient's, which aligns with the overall undersizing suggested by the pTLV ratio.

**Table 6.6:** pTLC estimates in litres with donor-recipient ratio are presented at the bottom of the table.

| | **pTLC Total** |
|---|---|
| R3 | 7.54 |
| D2 | 5.76 |
| **Donor vs Recipient Ratio** | |
| Ratio D2 vs R3 | 0.76 |

**Table 6.7:** TLC estimates based on GLI's model in litres with donor-recipient ratio are presented at the bottom of the table.

| | **GLI's TLC Total** |
|---|---|
| R3 | 7.6 |
| D2 | 6.1 |
| **Donor vs Recipient Ratios** | |
| Ratio D2 vs R3 | 0.8 |

**Table 6.8:** pTLV estimates in litres with donor-recipient ratios are presented at the bottom of the table.

| | **pTLV Left Lung** | **pTLV Right Lung** | **pTLV Total** |
|---|---|---|---|
| R3 | 2.6 | 2.9 | 5.5 |
| D2 | 2.13 | 2.41 | 4.55 |
| **Donor vs Recipient Ratios** | | | |
| Ratio D2 vs R3 | | 0.82 | |

**Size-matching by $\mathbf{TLV_{CT}}$:**
Pre-operatively, Pulmo 3D estimated R3's $TLV_{CT}$ total volume at 1611 ml with the $TLV_{CT}$ of the left lung at 704 ml and the $TLV_{CT}$ of the right lung at 957 ml.

For D2, Pulmo 3D $TLV_{CT}$ was not available pre-operatively. However, for the purpose of this study, we attempted to obtain Pulmo 3D estimates post-operatively. Unfortunately, Pulmo 3D failed in the estimation of D2's volume with an unknown error message. We suspect that this might be due to the nature of the data of the post-trauma screening format.

**Size-matching by FittingRoom:**
In this case, FittingRoom's volume estimation and immersive VR size-matching capabilities were deployed during the pre-operative evaluation.

Volume estimates were calculated for individual lung lobes in both the recipient and donor. For R3, the estimated volumes were as follows: RUL = 547.79 ml, RML = 123.54 ml, RLL = 608.89 ml, LUL = 700.28 ml, LLL = 388.18 ml. The total volume was calculated as 1280.21 ml for the right lung and 1088.46 ml, creating a total lung volume of 2368.67 ml. For D2, the estimated volumes were: RUL = 700.76 ml, RML = 429.59 ml, RLL = 817.30 ml, LUL = 1038.41 ml, LLL = 556.73

ml. The total volume was 1947.65 ml for the right lung and 1595.14 ml for the left lung, creating a total lung volume of 3542.79 ml.

The ratio of 1.5 between the D2 and the recipient R3 suggested an oversizing of the donor's lung for the recipient. After analyzing the volumes, the head transplant surgeon used the immersive environment system to assess the estimated volume and ratio against the 3D reconstructions of the anatomy. The surgeon confirmed after thorough analysis that D2's right lung was too large for R3's right thoracic cavity (Figure. 6.11). D2's left lung was also slightly oversized for R3's left thoracic cavity, primarily due to the position of the diaphragm.

The surgeons then considered whether reducing D2's lung by resecting the RLL would provide an appropriate size for R3's right thoracic cavity and ensure sufficient lung capacity. The surgeon removed the RML, folded the RUL and RLL together to close the "wedge", and attempted to fit them into R3's right thoracic cavity (Figure. 6.12). The volume ratio between D2's reduced lung and R3's lung volume became 1.18, a promising borderline ratio. For the left side of D2's lung, after extensive consideration and based on the VR visualization, it was decided that D2's left lung would be reduced at the edge of the lingula by stapling, preventing "squeezing" into the diaphragm. The reduction of D2's left lung would contribute to decreasing the ratio of 1.48 between D2's and R3's left lungs.

**Table 6.9:** TLV estimates in litres from IKEM VRLab FittingRoom with donor-recipient ratios are presented at the bottom of the table.

| | **VRLab TLV Left Lung** | **VRLab TLV Right Lung** | **VRLab TLV Total** |
|---|---|---|---|
| R3 | 1.08 | 1.28 | 2.36 |
| D2 | 1.59 | 1.94 | 3.54 |
| **Donor vs Recipient Ratios** | | | |
| Ratio D1 vs R1 | | 1.5 | |

During the post-operative evaluation in the immersive environment of VRLab FittingRoom, surgeons confirmed that the right side of the R2's thoracic cavity is undersized for the D1's right lung. The R2's suffering from obstructive lung diseases caused a collapse of the chest within itself. On the other hand, the fitting of D1's left lung into the left side of the thoracic cavity shows a small amount of undersizing for R2's left side of the thoracic cavity. When mounting D1's lungs inside of the R1's thoracic cavity, the immersive VR system indicated an acceptable anatomical match. The use of immersive environment size-matching suggests that D1's lungs were well within the acceptable size range for R1.

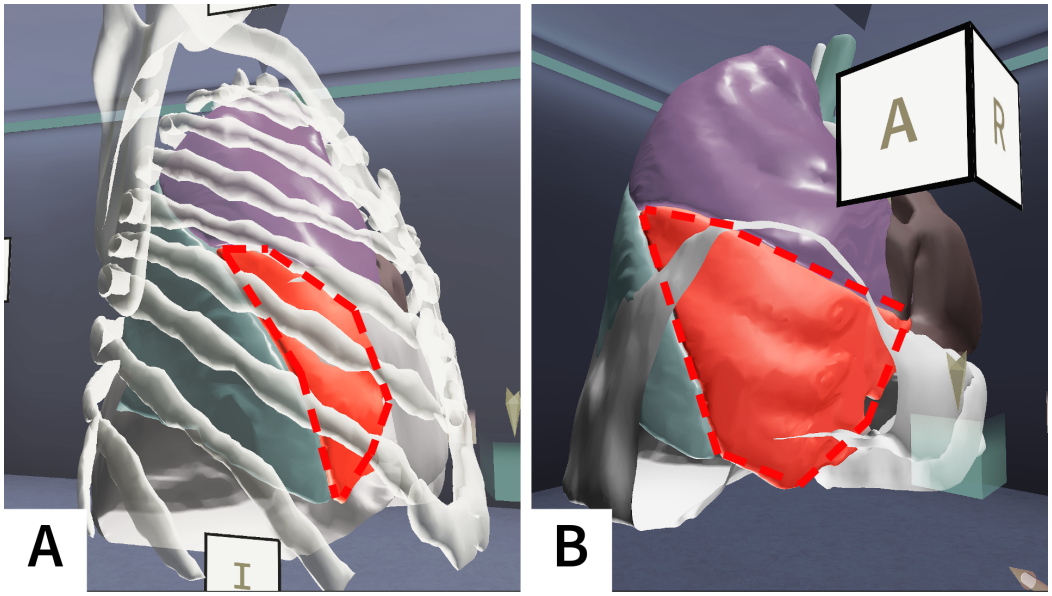


**Figure 6.11:** The D2's right middle lobe within R3's thoracic cavity highlighted in red (A). Righ middle lobe mesh crosses into the area of liver which is highlighted in red (B).

**Indication for Procedure:**

In this case the assessment and planning for lung transplantation for recipient R3 involved multiple evaluation methods, including pTLC, GLI's TLC, pTLV, TLVCT, and the FittingRoom. Each of these methods was accompanied with its own strengths and limitations.

Starting with pTLC, it estimated the donor's (D2) lung capacity at 5.76 litres and the recipient's (R3) at 7.54 litres, suggesting a donor-to-recipient ratio of 0.76. This indicated a significant undersizing of the donor's lungs. GLI's TLC provided a similar outlook, with predictions leading to a TLC ratio of 0.8, again underscoring an undersized scenario for the recipient.

The pTLV, which is an extrapolation of lung volumes from clinical data, indicated a ratio of 0.82 for D2 to R3, suggesting that the donor's lung volume would be only slightly undersized for the recipient — a discrepancy when compared to the actual surgical findings.

The $TLV_{CT}$ estimated total R3's lung volume at 1611 ml. In the case of D2 volume estimation, Pulmo 3D was not able to estimate volume from the given imaging data. However, the $TLV_{CT}$ also pointed towards a smaller volume for the recipient's needs in comparison to pTLC, GLI's TLC, and pTLV. Also, based on surgeons' feedback, the total lung volume for the recipient was underestimated in respect to the intraoperative reality. This underestimation called into question the reliability of $TLV_{CT}$ (in isolation) for surgical planning.

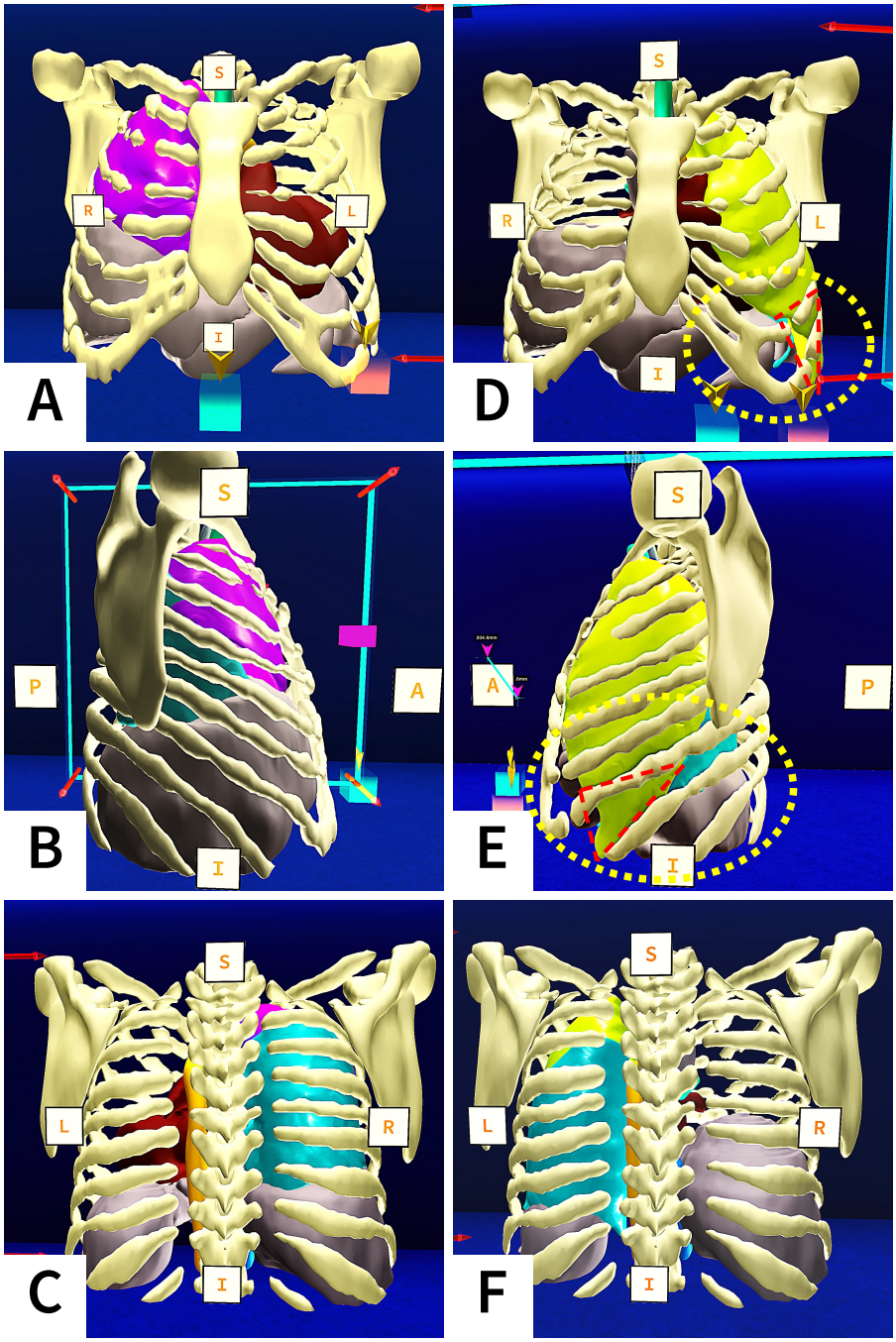


**Figure 6.12:** Screenshots taken in the FittingRoom during the immersive size-matching between D2 and R3. Removing D2's middle lobe of the right lung and closing the *wedge* in between shows a positive result when virtually implanting the reduced D2's lung inside of R3's right side of the thoracic cavity (A, B, C). Implantation of D2's left lung into the left side of R3's thoracic cavity shows an appropriate match (D, E, F). However, the visualisation shows that the resection of the lingula will be necessary (red dotted line in D, E, F).

Finally, FittingRoom's immersive VR technology provided a three-dimensional volumetric analysis that was pivotal in the decision-making process. FittingRoom's

data suggested an initial donor-to-recipient volume ratio of 1.5, indicating that the donor's lungs would be oversized for the recipient, a direct contrast to what pTLC and GLI's TLC had suggested. The FittingRoom allowed for a more dynamic and anatomical assessment, leading to the decision to resect portions of the donor's lungs (right middle lobe and lingula of the left lung) to achieve an optimal fit. This tailored approach was not apparent through the other methods.

The final decision to proceed with lung resection was guided by FittingRoom's visualization and volumetric assessment. It offered the surgical team an interactive planning tool that traditional methods did not, enabling them to anticipate and resolve size mismatch challenges more effectively. The immersive simulation of the resection within the VR environment provided confidence that the adjusted lung volumes would suit the recipient's thoracic cavity.

**Post-surgery:**
Following surgery, a transplantation procedure was performed on R3, a 38-year-old male with fibrotic exogenous allergic alveolitis, using lungs from D2, a 52-year-old female donor.

A significant part of the middle lobe was removed using an Endo GIA Stapler to fit to the recipient's thoracic cavity. The left lung was then similarly prepared and implanted. It also required resizing, with the lingula being removed to ensure an appropriate fit. The sternum was closed with an 8-hole Synthes plate secured with 7 self-tapping screws of 18 mm length.

The FittingRoom was used for pre-operative evaluation, calculating volume estimates for individual lung lobes. Despite the donor's oversized lungs, according to the initial evaluation, intraoperative adjustments and the removal of specific lung lobes resulted in a satisfactory fit within the recipient's thoracic cavities. The immersive VR system was beneficial for anatomical matching and decision-making regarding the necessary resections for a suitable match.

### 6.3.5 Discussion & Future Work

The surgical team suggested that the introduction of the IKEM VRLab FittingRoom size-matching platform into the process of lung transplant size matching is a potential game-changer in the field. Surgeons highlighted its particular effectiveness in situations where traditional methods like pTLC, pTLV, and $TLV_{CT}$ produce results that are less reliable, leading to a dependency on instinct and prior experience to make critical decisions. The VRLab FittingRoom immersive VR environment was praised for its innovative approach in addressing these challenges.

One of the standout features of the Fitting Room is its potential to democratize the decision-making process in organ harvesting and transplantation. Surgeons pointed out that it enables the sharing of responsibility to -in the field- junior surgeons harvesting organs, as it empowers them to make informed decisions about the suitability of a donor's lungs for a recipient, potentially without having to rely solely on the judgment of more experienced and often overworked senior surgeons. By providing a more data-driven approach to size matching, the platform allows for a level of precision and confidence that was previously unattainable.

Senior surgeons expressed appreciation for the FittingRoom as a validation tool that complements their extensive experience with empirical data. This blend of cutting-edge technology and seasoned expertise enriches the size-matching process, offering a more robust framework for making transplant decisions. IKEM VRLab challenges the status quo of existing size-matching methodologies, inviting a shift towards a more interactive and precise approach to determining the compatibility between donor lungs and recipient thoracic cavities.

The feedback underscores the surgical team's shared sentiment that the IKEM VRLab FittingRoom enhances size-matching accuracy and fosters a more collaborative environment. By integrating this technology into the transplant process, the team believes it can improve recipients' outcomes, streamline the decision-making process, and provide valuable learning opportunities for the next generation of transplant surgeons. Moreover, the FittingRoom has generated interest in potentially expanding the donor pool. Its ability to accommodate a broader range of size discrepancies could lead to increased utilization of available donor organs. This potential enhancement suggests a noteworthy contribution of our technology to the transplant field, not only in refining transplant matching procedures but also in possibly reducing recipient wait times and improving lung transplant success rates.

Future research should delve into the exploration of lung parenchyma elasticity properties, integrating these findings into an advanced VR simulation for size-matching. This progression will enable surgeons to assess how the transplanted organ adapts to the spatial nuances of the recipient's thoracic cavity, enhancing the precision of pre-operative planning. Furthermore, the development of a novel CT screening protocol that captures images of the recipient's thoracic cavity during both inhalation and exhalation phases would mark a significant advancement. Such a protocol could facilitate simulations of the recipient's breathing movements, offering insights into the dynamic changes of the thoracic cavity. This approach would not only predict how the chest expands and contracts during respiration but also how these movements are accommodated by both the existing and transplanted organs. Incorporating these elements into the size-matching process promises to

elevate the level of care, ensuring that transplants are not just physically compatible, but functionally harmonious with the recipient's body, thereby optimizing post-transplant recovery and long-term outcomes.

Chapter 7

# Conclusion, Limitations & Future Work

In this thesis, we presented IKEM VRLab, a modular virtual reality system for clinical use, offering advanced tools for detailed patient data visualization, and collaborative pre-operative planning for several organs. The system includes OrthopedVR, a toolkit for orthopaedic surgeons to simulate surgical interventions. It further includes toolkits specialised in oncologic liver resection planning, robotic lung segmentectomies, and donor-recipient size-matching for lung transplants. The system enhances surgical precision and patient care, demonstrating the revolutionising potential of VR technology in complex, specialized procedures.

The summary of the *four* contributions of this thesis:

1. **IKEM VRLab Development**:
    - **System Architecture**: IKEM VRLab was designed with a modular and extensible architecture, enabling seamless integration into existing medical data pipelines. The system's architecture supports detailed 3D visualization and interactive examination of patient-specific anatomical data, facilitating enhanced surgical planning and collaborative efforts among medical professionals.
    - **Validation**: We conducted rigorous validation studies to ensure the volumetric accuracy of CT-derived models within the VR environment. The results demonstrated no significant statistical difference between the ground truth organ volumes and the estimates calculated using IKEM VRLab, underscoring the system's reliability for clinical use.
2. **OrthopedVR**:

- **Toolkit**: OrthopedVR provides a specialized toolkit for the planning and visualizing of corrective surgeries for lower limb rotational abnormalities. This application allows orthopaedic surgeons to simulate derotational osteotomies in a 3D environment, enhancing their understanding of patient-specific anatomy and improving surgical precision.
- **Clinical Evaluation**: The toolkit was evaluated by experienced orthopaedic surgeons, who confirmed its superiority over traditional 2D imaging techniques. The qualitative and quantitative assessments indicated significant improvements in pre-operative planning, surgical outcomes, and clinical training.

3. **Liver Resection Planning**:
   - **Toolkit**: The liver resection toolkit within IKEM VRLab enables detailed visualization and interaction with 3D reconstructions of the liver, facilitating accurate and personalized surgical planning. The system supports real-time volumetric estimates, clipping, and measuring tools tailored for anatomical and non-anatomical resections.
   - **Clinical Impact**: The toolkit was applied in over 300 clinical cases, demonstrating its effectiveness in improving decision-making accuracy, reducing surgical complications, and enhancing procedural indications. The evaluation involving experienced liver surgeons confirmed the system's utility in achieving better surgical outcomes compared to conventional visualization methods.
4. **Robotic Lung Segmentectomies and Transplant Size-Matching**:
   - **AR Integration**: We extended IKEM VRLab to support AR applications, aiding in the precise port placement for robotic-assisted thoracic surgeries. The AR Lung toolkit enhances visualization and planning, minimizing the invasive impact of surgeries and improving the accuracy of port placements.
   - **Size-Matching for Transplants**: The FittingRoom application offers an innovative approach to donor-recipient size-matching for lung transplants, providing an immersive platform for assessing and optimizing lung transplant compatibility. This tool has the potential to improve post-operative outcomes and patient survival rates by ensuring better organ fit.

Overall, the findings from this thesis suggest that integrating advanced VR technology into clinical workflows can significantly enhance surgical planning, reduce procedural risks, and improve patient care. Future research should focus on ex-

panding the system's capabilities, validating its efficacy across larger and more diverse patient datasets, and exploring its application in other complex surgical fields.

## 7.1 Limitations

**OrthopedVR.** A limitation stemmed from the scarcity of available patient datasets, particularly those showcasing rotational abnormalities of the lower limbs in pediatric cases. The under-reporting of such cases in the NHS, often deferred in favour of knee arthroplasty, further adds to this limitation and so does the absence of post-operative CT datasets, which could provide a benchmark for pre-operative planning. The current reliance on subjective validation by surgeons, who exhibit a wide range of preferences in treating mal-tracking, further underscores the need for an objective and more comprehensive dataset.

**Surgical Planning of Liver Resections in IKEM VRLab.** When using IKEM VRLab in liver resections, the primary constraints pertained to the limited sample size of surgeons and patient cases, thus impacting the generalizability of findings. The stringent criteria for case inclusion, while ensuring the examination of complex and relevant scenarios, inadvertently narrowed the scope of potential study cases. For a more objective study, surgical complications and long-term postoperative results should be recorded to provide a deeper understanding of the impact of virtual reality on liver resection surgical planning.

**AR Navigation Tool for Correct DaVinci Xi Porting** AR's efficiency in surgical planning is contingent upon the precise calibration and registration of the AR system with the patient's actual anatomy. Misalignments could lead to inaccuracies in port placements, underscoring the need for advancements in the precision of hardware and software frameworks.

## 7.2 Future Work

**Real-time AR Tracking for Operation Rooms.** Improving the accuracy and reliability of AR hardware and software is essential for surgical applications. Future work should delve into advanced calibration techniques and algorithms that enhance the alignment between virtual models and the patient's actual anatomy. This includes real-time tracking and adjustment capabilities to accommodate intraoperative shifts and deformations, ensuring precision in surgical planning and

execution. Essentially, such a system should be simple to implement and use in order to not disturb routine medical processes.

**Interdisciplinary Collaboration, Ethical and Legal Considerations.** In future initiatives, fostering interdisciplinary collaboration among computer scientists, medical professionals, ethicists, and regulatory bodies is essential. This collective approach can expedite the development of VR and AR technologies that are not only technically advanced but are also ethically sound and well-integrated into clinical workflows. It's crucial to address ethical considerations, patient privacy, and data security from the outset to facilitate the acceptance and widespread adoption of these technologies. As these technologies become more integrated into clinical practice, the ethical and legal issues that may arise need to be addressed promptly. Future work should explore the implications of these technologies on patient consent, data privacy, and potential malpractice. To navigate these challenges, the development of clear guidelines and standards will be critical.

**Expansion to Other Surgical Specialties.** While this thesis has focused on specific applications of VR and AR in surgical planning, the potential of these technologies spans numerous surgical specialities. Future research should investigate the applicability and customization of VR and AR systems for other complex surgical procedures such as oncologic pancreatic resection or kidney resection. Further more, this is particularly pertinent in the context of organ transplants where size and anatomical compatibility between the donor and recipient are critical determinants of successful transplantation. The use of VR and AR in pre-operative planning could drastically improve the outcomes of such procedures. It could potentially reduce the incidence of post-operative complications and improve the overall quality of patient care.

**Machine Learning, Robotic Surgery and AR:** Advancements in machine learning, computer vision, and robotic systems hold great potential for the future of autonomous surgical procedures. Integrating these technologies with AR headsets for surgeon supervision offers a promising direction for enhancing surgical precision and efficiency. Future research should focus on developing AI algorithms capable of deriving comprehensive surgical plans automatically. These algorithms would analyze pre-operative imaging data, such as CT and MRI scans, to identify critical anatomical structures and plan the surgical approach, including incision sites, paths for robotic instruments, and the sequence of surgical steps.

In addition to pre-operative planning, research should explore real-time adaptive planning, where the AI system can adjust the surgical plan intraoperatively based on real-time data from sensors and imaging devices. This capability would allow

the robotic system to respond dynamically to unexpected changes in the surgical field, enhancing both safety and effectiveness.

Developing autonomous robotic systems that can execute the surgical plan with high precision is another critical area of research. These systems would utilize ML algorithms and computer vision to guide robotic arms, perform incisions, tissue manipulation, and suturing, while constantly monitoring and adjusting their actions based on sensor feedback. Incorporating advanced error detection and correction mechanisms is essential for autonomous surgical robots. Research should focus on algorithms that can detect deviations from the planned procedure and autonomously correct them or alert the supervising surgeon.

Research should also investigate the use of AR headsets for surgeons to supervise autonomous robotic surgeries. These headsets would provide surgeons with a superimposed 3D reconstruction of the patient's anatomy, including real-time visualizations of the robotic arms' movements and positions within the patient. The AR system should display all necessary information, such as the surgical plan, step-by-step procedure, vital signs, and alerts. Surgeons could interact with the AR interface using gestures or voice commands to manipulate views, access additional data, and intervene if necessary.

AR headsets can enhance situational awareness by providing real-time overlays of critical anatomical landmarks, surgical instrument trajectories, and potential hazards. This visualization helps surgeons understand the spatial relationships and anticipate the robot's actions. Future research should explore the integration of advanced imaging and computer vision systems with autonomous robots. These systems would enable the robot to perceive the surgical field with high accuracy, distinguishing between different tissue types, detecting blood vessels, and identifying anatomical structures.

**Advancing Integration and Interoperability:** Future research should focus on increasing the integration of VR and AR technologies within the existing healthcare IT ecosystems. This involves developing more robust and seamless interfaces with Electronic Health Records (EHRs), Picture Archiving and Communication Systems (PACS), and other clinical information systems. Enhancing interoperability will lead to a more streamlined workflow, allowing clinicians to access and utilize VR and AR applications more efficiently in their practice.

# Bibliography


[1] N. Sakakura and T. Eguchi, "Port Placement Variations for Robotic Lung Resection: Focusing on Their History, Conventional Look-Up-View and Horizontal Open-Thoracotomy-View Techniques, and More," *Journal of Personalized Medicine*, vol. 13, no. 2, p. 230, 1 2023.

[2] A. D. Calvert and T. R. Hazelton, "Role of imaging in lung transplantation evaluation," *Journal of Thoracic Disease*, vol. 12, no. 9, pp. 5147–5158, 9 2020.

[3] J. Brooke, "SUS: A quick and dirty usability scale," *Usability Eval. Ind.*, vol. 189, 3 1995. [Online]. Available: https://www.researchgate.net/publication/228593520_SUS_A_quick_and_dirty_usability_scale

[4] Usability.gov, "System Usability Scale (SUS)." [Online]. Available: https://www.usability.gov/how-to-and-tools/methods/system-usability-scale.html

[5] C. Hansen, J. Wieferich, F. Ritter, C. Rieder, and H.-O. Peitgen, "Illustrative visualization of 3D planning models for augmented reality in liver surgery," *International Journal of Computer Assisted Radiology and Surgery*, vol. 5, no. 2, pp. 133–141, 3 2010. [Online]. Available: http://link.springer.com/10.1007/s11548-009-0365-3

[6] C. Lin, J. Gao, H. Zheng, J. Zhao, H. Yang, G. Lin, H. Li, H. Pan, Q. Liao, and Y. Zhao, "Three-Dimensional Visualization Technology Used in Pancreatic Surgery: a Valuable Tool for Surgical Trainees," *Journal of Gastrointestinal Surgery*, vol. 24, no. 4, pp. 866–873, 4 2020. [Online]. Available: https://linkinghub.elsevier.com/retrieve/pii/S1091255X23014282

[7] M. McDonald and J. D. Shirk, "Application of Three-Dimensional Virtual Reality Models to Improve the Pre-Surgical Plan for Robotic Partial Neph-

rectomy," *JSLS : Journal of the Society of Laparoscopic & Robotic Surgeons*, vol. 25, no. 3, p. e2021.00011, 2021.

[8] D. v. Seggern, "PDF/X and the other PDF standards," 1 2017. [Online]. Available: https://www.pdfa.org/pdfx-and-the-other-pdf-standards/http://files/541/pdfx-and-the-other-pdf-standards.html

[9] B. Wilcox, R. J. Mobbs, A.-M. Wu, and K. Phan, "Systematic review of 3D printing in spinal surgery: the current state of play," *Journal of Spine Surgery*, vol. 3, no. 3, pp. 433–443, 9 2017.

[10] R. A. Moore, K. W. Riggs, S. Kourtidou, K. Schneider, N. Szugye, W. Troja, G. D'Souza, M. Rattan, R. Bryant, M. D. Taylor, and D. L. Morales, "Three-dimensional printing and virtual surgery for congenital heart procedural planning," *Birth Defects Research*, vol. 110, no. 13, pp. 1082–1090, 8 2018.

[11] H. Chim, N. Wetjen, and S. Mardini, "Virtual Surgical Planning in Craniofacial Surgery," *Seminars in Plastic Surgery*, vol. 28, no. 03, pp. 150–158, 9 2014.

[12] S. M. D. Sørensen, M. M. Savran, L. Konge, and F. Bjerrum, "Three-dimensional versus two-dimensional vision in laparoscopy: a systematic review," *Surgical Endoscopy*, vol. 30, no. 1, pp. 11–23, 1 2016.

[13] F. Huettl, P. Saalfeld, C. Hansen, B. Preim, A. Poplawski, W. Kneist, H. Lang, and T. Huber, "Virtual reality and 3D printing improve preoperative visualization of 3D liver reconstructions—results from a preclinical comparison of presentation modalities and user's preference," *Annals of Translational Medicine*, vol. 9, no. 13, pp. 1074–1074, 7 2021.

[14] B. P. Müller-Stich, N. Löb, D. Wald, T. Bruckner, H. P. Meinzer, M. Kadmon, M. W. Büchler, and L. Fischer, "Regular three-dimensional presentations improve in the identification of surgical liver anatomy - A randomized study," *BMC Medical Education*, vol. 13, no. 1, pp. 1–8, 9 2013. [Online]. Available: http://www.biomedcentral.com/1472-6920/13/131

[15] C. Boedecker, F. Huettl, P. Saalfeld, M. Paschold, W. Kneist, J. Baumgart, B. Preim, C. Hansen, H. Lang, and T. Huber, "Using virtual 3D-models in surgical planning: workflow of an immersive virtual reality application in liver surgery," *Langenbeck's Archives of Surgery*, vol. 406, no. 3, pp. 911–915, 3 2021. [Online]. Available: https://doi.org/10.1007/s00423-021-02127-7

[16] S. Zawy Alsofy, I. Sakellaropoulou, and R. Stroop, "Evaluation of Surgical Approaches for Tumor Resection in the Deep Infratentorial Region and

Impact of Virtual Reality Technique for the Surgical Planning and Strategy," *The Journal of craniofacial surgery*, vol. 31, no. 7, pp. 1865–1869, 10 2020. [Online]. Available: https://journals.lww.com/jcraniofacialsurgery/Fulltext/2020/10000/Evaluation_of_Surgical_Approaches_for_Tumor.5.aspx

[17] A. T. Stadie, R. A. Kockro, R. Reisch, A. Tropine, S. Boor, P. Stoeter, and A. Perneczky, "Virtual reality system for planning minimally invasive neurosurgery: Technical note," *Journal of Neurosurgery*, vol. 108, no. 2, pp. 382–394, 2008.

[18] M. Pfeiffer, H. Kenngott, A. Preukschas, M. Huber, L. Bettscheider, B. Müller-Stich, and S. Speidel, "IMHOTEP: virtual reality framework for surgical applications," *International Journal of Computer Assisted Radiology and Surgery*, vol. 13, no. 5, pp. 741–748, 5 2018. [Online]. Available: https://doi.org/10.1007/s11548-018-1730-x

[19] S. González Izard, J. A. Juanes Méndez, P. Ruisoto Palomera, and F. J. García-Peñalvo, "Applications of Virtual and Augmented Reality in Biomedical Imaging," *Journal of Medical Systems*, vol. 43, no. 4, 2019. [Online]. Available: http://files/254/display.html

[20] L. W. Goldman, "Principles of CT and CT technology," pp. 115–128, 9 2007. [Online]. Available: http://www.snm.org/ce_online

[21] S. B. Tomlinson, B. K. Hendricks, and A. Cohen-Gadol, "Immersive Three-Dimensional Modeling and Virtual Reality for Enhanced Visualization of Operative Neurosurgical Anatomy," *World Neurosurgery*, vol. 131, pp. 313–320, 11 2019. [Online]. Available: http://www.sciencedirect.com/science/article/pii/S1878875019316237http://files/280/Tomlinsonetal.-2019-ImmersiveThree-DimensionalModelingandVirtualR.pdfhttp://files/281/S1878875019316237.html

[22] R. A. Kockro, T. Killeen, A. Ayyad, M. Glaser, A. Stadie, R. Reisch, A. Giese, and E. Schwandt, "Aneurysm Surgery with Preoperative Three-Dimensional Planning in a Virtual Reality Environment: Technique and Outcome Analysis," *World Neurosurgery*, vol. 96, pp. 489–499, 2016. [Online]. Available: http://www.sciencedirect.com/science/article/pii/S1878875016308087

[23] G. Quero, A. Lapergola, L. Soler, M. Shabaz, A. Hostettler, T. Collins, J. Marescaux, D. Mutter, M. Diana, and P. Pessaux, "Virtual and Augmented Reality in Oncologic Liver Surgery," *Surgical Oncology Clinics*

*of North America*, vol. 28, no. 1, pp. 31–44, 1 2019. [Online]. Available: https://linkinghub.elsevier.com/retrieve/pii/S1055320718306835

[24] T. Timonen, M. Iso-Mustajärvi, P. Linder, A. Lehtimäki, H. Löppönen, A. P. Elomaa, and A. Dietz, "Virtual reality improves the accuracy of simulated preoperative planning in temporal bones: a feasibility and validation study," *European Archives of Oto-Rhino-Laryngology*, vol. 278, no. 8, pp. 2795–2806, 8 2021.

[25] S. B. Murphy, "Tibial osteotomy for genu varum: Indications preoperative planning, and technique," *Orthopedic Clinics of North America*, vol. 25, no. 3, pp. 477–482, 1994. [Online]. Available: https://pubmed.ncbi.nlm.nih.gov/8028888/

[26] W. Baur, W. Hönle, and A. Schuh, "Tibiakopfosteotomie bei Varusgonarthrose," *Operative Orthopädie und Traumatologie*, vol. 17, no. 3, pp. 326–344, 8 2005. [Online]. Available: http://link.springer.com/10.1007/s00064-005-1136-0

[27] T. Y. Kuo, J. G. Skedros, and R. D. Bloebaum, "Measurement of femoral anteversion by biplane radiography and computed tomography imaging: Comparison with an anatomic reference," *Investigative Radiology*, vol. 38, no. 4, pp. 221–229, 2003.

[28] P. A. Ruwe, J. R. Gage, M. B. Ozonoff, and P. A. DeLuca, "Clinical determination of femoral anteversion. A comparison with established techniques." *The Journal of bone and joint surgery. American volume*, vol. 74, no. 6, pp. 820–30, 7 1992. [Online]. Available: http://www.ncbi.nlm.nih.gov/pubmed/1634572

[29] J. A. Gruskay, A. T. Fragomen, and S. R. Rozbruch, "Idiopathic Rotational Abnormalities of the Lower Extremities in Children and Adults," *JBJS Reviews*, vol. 7, no. 1, pp. e3–e3, 1 2019. [Online]. Available: https://journals.lww.com/01874474-201901000-00005

[30] M. Yamamoto, T. Kobayashi, S. Kuroda, M. Hamaoka, N. Honmyo, M. Yamaguchi, D. Takei, and H. Ohdan, "Impact of postoperative bile leakage on long-term outcome in patients following liver resection for hepatocellular carcinoma," *Journal of Hepato-Biliary-Pancreatic Sciences*, vol. 27, no. 12, pp. 931–941, 12 2020.

[31] S. Dinant, W. de Graaf, B. J. Verwer, R. J. Bennink, K. P. van Lienden, D. J. Gouma, A. K. van Vliet, and T. M. van Gulik, "Risk Assessment

of Posthepatectomy Liver Failure Using Hepatobiliary Scintigraphy and CT Volumetry," *Journal of Nuclear Medicine*, vol. 48, no. 5, pp. 685–692, 5 2007.

[32] R. Bauernschmitt, M. Feuerstein, J. Traub, E. U. Schirmbeck, G. Klinker, and R. Lange, "Optimal port placement and enhanced guidance in robotically assisted cardiac surgery," *Surgical Endoscopy*, vol. 21, no. 4, pp. 684–687, 4 2007. [Online]. Available: https://link.springer.com/10.1007/s00464-006-9057-z

[33] J. H. Park, S. Park, C. H. Kang, B. S. Na, S. Y. Bae, K. J. Na, H. J. Lee, I. K. Park, and Y. T. Kim, "Early Outcomes of Robotic Versus Video-Assisted Thoracoscopic Anatomical Resection for Lung Cancer," *Journal of Chest Surgery*, vol. 55, no. 1, pp. 49–54, 2 2022. [Online]. Available: http://www.jchestsurg.org/journal/view.html?doi=10.5090/jcs.21.128

[34] J. Usuda, T. Inoue, T. Sonokawa, M. Matsumoto, Y. Enomoto, K. Suzuki, and Y. Tomioka, "New Technique for Introducing a Surgical Stapler during Robot-Assisted Lobectomy for Lung Cancer," *Journal of Nippon Medical School*, vol. 89, no. 2, pp. 89–211, 4 2022. [Online]. Available: https://www.jstage.jst.go.jp/article/jnms/89/2/89_JNMS.2022_89-211/_article

[35] D. Pereda and E. Sandoval, "Minimally-Invasive Surgery of Mitral Valve. State of the Art," in *Advances in Minimally Invasive Surgery*. IntechOpen, 1 2022. [Online]. Available: https://www.intechopen.com/chapters/77457

[36] M. Eberlein, R. M. Reed, M. Maidaa, S. Bolukbas, G. J. Arnaoutakis, J. B. Orens, R. G. Brower, C. A. Merlo, and L. G. Hunsicker, "Donor–Recipient Size Matching and Survival after Lung Transplantation. A Cohort Study," *Annals of the American Thoracic Society*, vol. 10, no. 5, pp. 418–425, 10 2013. [Online]. Available: https://www.atsjournals.org/doi/10.1513/AnnalsATS.201301-008OC

[37] J. B. Barnard, O. Davies, P. Curry, P. Catarino, J. Dunning, D. Jenkins, C. Sudarshan, S. Nair, S. Tsui, and J. Parmar, "Size matching in lung transplantation: An evidence-based review," *The Journal of Heart and Lung Transplantation*, vol. 32, no. 9, pp. 849–860, 9 2013. [Online]. Available: https://linkinghub.elsevier.com/retrieve/pii/S1053249813013429

[38] S. H. Hwang, J. G. Lee, T. H. Kim, H. C. Paik, C. H. Park, and S. Haam, "Comparison of Predicted Total Lung Capacity and Total Lung Capacity by Computed Tomography in Lung Transplantation Candidates," *Yonsei Medical Journal*, vol. 57, no. 4, p. 963, 2016. [Online]. Available: https://eymj.org/DOIx.php?id=10.3349/ymj.2016.57.4.963

[39] D. Hayes, W. S. Cherikh, D. C. Chambers, M. O. Harhay, K. K. Khush, R. R. Lehman, B. Meiser, J. W. Rossano, E. Hsich, L. Potena, A. Sadavarte, T. P. Singh, A. Zuckermann, and J. Stehlik, "The International Thoracic Organ Transplant Registry of the International Society for Heart and Lung Transplantation: Twenty-second pediatric lung and heart-lung transplantation report—2019; Focus theme: Donor and recipient size match," *The Journal of Heart and Lung Transplantation*, vol. 38, no. 10, pp. 1015–1027, 10 2019. [Online]. Available: https://linkinghub.elsevier.com/retrieve/pii/S1053249819316213

[40] V. Chheang, P. Saalfeld, F. Joeres, C. Boedecker, T. Huber, F. Huettl, H. Lang, B. Preim, and C. Hansen, "A collaborative virtual reality environment for liver surgery planning," *Computers and Graphics (Pergamon)*, vol. 99, pp. 234–246, 10 2021.

[41] C. Fang, J. An, A. Bruno, X. Cai, J. Fan, J. Fujimoto, R. Golfieri, X. Hao, H. Jiang, L. R. Jiao, A. V. Kulkarni, H. Lang, C. R. A. Lesmana, Q. Li, L. Liu, Y. Liu, W. Lau, Q. Lu, K. Man, H. Maruyama, C. Mosconi, N. Örmeci, M. Pavlides, G. Rezende, J. H. Sohn, S. Treeprasertsuk, V. Vilgrain, H. Wen, S. Wen, X. Quan, R. Ximenes, Y. Yang, B. Zhang, W. Zhang, P. Zhang, S. Zhang, and X. Qi, "Consensus recommendations of three-dimensional visualization for diagnosis and management of liver diseases," *Hepatology International*, vol. 14, no. 4, pp. 437–453, 7 2020.

[42] N. Wake, A. B. Rosenkrantz, R. Huang, K. U. Park, J. S. Wysock, S. S. Taneja, W. C. Huang, D. K. Sodickson, and H. Chandarana, "Patient-specific 3D printed and augmented reality kidney and prostate cancer models: impact on patient education," *3D Printing in Medicine*, vol. 5, no. 1, p. 4, 12 2019. [Online]. Available: https://threedmedprint.biomedcentral.com/articles/10.1186/s41205-019-0041-3

[43] M. Galvez, T. Asahi, A. Baar, G. Carcuro, N. Cuchacovich, J. A. Fuentes, R. Mardones, C. E. Montoya, R. Negrin, F. Otayza, G. M. Rojas, and A. Chahin, "Use of Three-dimensional Printing in Orthopaedic Surgical Planning," *JAAOS: Global Research and Reviews*, vol. 2, no. 5, p. e071, 5 2018. [Online]. Available: https://journals.lww.com/01979360-201805000-00004

[44] E. George, M. Barile, A. Tang, O. Wiesel, A. Coppolino, A. Giannopoulos, S. Mentzer, M. Jaklitsch, A. Hunsaker, and D. Mitsouras, "Utility and reproducibility of 3-dimensional printed models in pre-operative planning of complex thoracic tumors," *Journal of Surgical Oncology*,

vol. 116, no. 3, pp. 407–415, 9 2017. [Online]. Available: https://onlinelibrary.wiley.com/doi/10.1002/jso.24684

[45] I. M. El-Sayed, T. G. Shoukr, T. M. ElBanoby, and W. A. Moustafa, "3D visualization and simulation in surgical planning of orbital hypertelorism," *International journal of health sciences*, pp. 3887–3905, 7 2022. [Online]. Available: https://sciencescholar.us/journal/index.php/ijhs/article/view/10147

[46] P. Meister, J. Miller, K. Wang, M. C. Dorneich, E. Winer, L. Brown, and G. Whitehurst, "Using Three-Dimensional Augmented Reality to Enhance General Aviation Weather Training," *Proceedings of the Human Factors and Ergonomics Society Annual Meeting*, vol. 65, no. 1, pp. 272–276, 9 2021. [Online]. Available: http://journals.sagepub.com/doi/10.1177/1071181321651163

[47] P. C. van de Woestijne, W. Bakhuis, A. H. Sadeghi, J. J. Peek, Y. J. Taverne, and A. J. Bogers, "3D Virtual Reality Imaging of Major Aortopulmonary Collateral Arteries: A Novel Diagnostic Modality," *World Journal for Pediatric and Congenital Heart Surgery*, vol. 12, no. 6, pp. 765–772, 11 2021. [Online]. Available: http://journals.sagepub.com/doi/10.1177/21501351211045064

[48] T. Žele, B. Matos, J. Knific, F. F. Bajrović, and B. Prestor, "Use of 3D visualisation of medical images for planning and intraoperative localisation of superficial brain tumours: our experience," *British Journal of Neurosurgery*, vol. 24, no. 5, pp. 555–560, 10 2010. [Online]. Available: http://www.tandfonline.com/doi/full/10.3109/02688697.2010.496876

[49] G. L. Presti, M. Carbone, D. Ciriaci, D. Aramini, M. Ferrari, and V. Ferrari, "Assessment of DICOM Viewers Capable of Loading Patient-specific 3D Models Obtained by Different Segmentation Platforms in the Operating Room," *Journal of Digital Imaging*, vol. 28, no. 5, pp. 518–527, 10 2015. [Online]. Available: http://link.springer.com/10.1007/s10278-015-9786-4

[50] Y. Oshiro and N. Ohkohchi, "Three-Dimensional Liver Surgery Simulation: Computer-Assisted Surgical Planning with Three-Dimensional Simulation Software and Three-Dimensional Printing <sup/>," *Tissue Engineering Part A*, vol. 23, no. 11-12, pp. 474–480, 6 2017.

[51] D. Zhao, K.-J. Zhang, T.-S. Fang, X. Yan, X. Jin, Z.-M. Liang, J.-X. Tang, and L.-J. Xie, "Topological approach of liver segmentation based on 3D

visualization technology in surgical planning for split liver transplantation," *World Journal of Gastrointestinal Surgery*, vol. 14, no. 10, pp. 1141–1149, 10 2022.

[52] N. N. Zein, I. A. Hanouneh, P. D. Bishop, M. Samaan, B. Eghtesad, C. Quintini, C. Miller, L. Yerian, and R. Klatte, "Three-dimensional print of a liver for preoperative planning in living donor liver transplantation," *Liver Transplantation: Official Publication of the American Association for the Study of Liver Diseases and the International Liver Transplantation Society*, vol. 19, no. 12, pp. 1304–1310, 2013. [Online]. Available: http://www.ncbi.nlm.nih.gov/pubmed/23959637

[53] E. Pelanis, R. P. Kumar, D. L. Aghayan, R. Palomar, A. Fretland, H. Brun, O. J. Elle, and B. Edwin, "Use of mixed reality for improved spatial understanding of liver anatomy," *Minimally Invasive Therapy & Allied Technologies*, vol. 29, no. 3, pp. 154–160, 6 2020.

[54] P. Bangeas, V. Tsioukas, V. N. Papadopoulos, and G. Tsoulfas, "Role of innovative 3D printing models in the management of hepatobiliary malignancies," *World Journal of Hepatology*, vol. 11, no. 7, pp. 574–585, 2019.

[55] P. M. Maloca, B. Faludi, M. Zelechowski, C. Jud, T. Vollmar, S. Hug, P. L. Müller, E. R. de Carvalho, J. Zarranz-Ventura, M. Reich, C. Lange, C. Egan, A. Tufail, P. W. Hasler, H. P. N. Scholl, and P. C. Cattin, "Validation of virtual reality orbitometry bridges digital and physical worlds," *Scientific Reports*, vol. 10, no. 1, p. 11815, 7 2020.

[56] C. Guérinot, V. Marcon, C. Godard, T. Blanc, H. Verdier, G. Planchon, F. Raimondi, N. Boddaert, M. Alonso, K. Sailor, P.-M. Lledo, B. Hajj, M. El Beheiry, and J.-B. Masson, "New Approach to Accelerated Image Annotation by Leveraging Virtual Reality and Cloud Computing," *Frontiers in Bioinformatics*, vol. 1, 1 2022.

[57] S. Napa, M. Moore, and T. Bardyn, "Advancing Cardiac Surgery Case Planning and Case Review Conferences Using Virtual Reality in Medical Libraries: Evaluation of the Usability of Two Virtual Reality Apps," *JMIR Human Factors*, vol. 6, no. 1, p. e12008, 2019.

[58] S. Wicky, P. F. Blaser, C. H. Blanc, P. F. Leyvraz, P. Schnyder, and R. A. Meuli, "Comparison between standard radiography and spiral CT with 3D reconstruction in the evaluation, classification and management of tibial plateau fractures," *European Radiology*, vol. 10, no. 8, pp. 1227–1232, 7 2000. [Online]. Available: http://link.springer.com/10.1007/s003300000326

[59] P. K. Haribabu, M. Verma, and A. Vij, "Model-assisted marsupialization of a large odontogenic keratocyst in the maxillofacial region using a multicolored 3D-printed model: A novel approach in surgical planning and teaching," *Clinical Case Reports*, vol. 11, no. 5, 5 2023. [Online]. Available: https://onlinelibrary.wiley.com/doi/10.1002/ccr3.7286

[60] C. Boedecker, F. Huettl, P. Saalfeld, M. Paschold, W. Kneist, J. Baumgart, B. Preim, C. Hansen, H. Lang, and T. Huber, "Using virtual 3D-models in surgical planning: workflow of an immersive virtual reality application in liver surgery," *Langenbeck's Archives of Surgery*, vol. 406, no. 3, pp. 911–915, 2021. [Online]. Available: https://doi.org/10.1007/s00423-021-02127-7

[61] H. W. Goo, S. J. Park, and S.-J. Yoo, "Advanced Medical Use of Three-Dimensional Imaging in Congenital Heart Disease: Augmented Reality, Mixed Reality, Virtual Reality, and Three-Dimensional Printing," *Korean Journal of Radiology*, vol. 21, no. 2, p. 133, 2020.

[62] D. Wang, N. Li, M. Luo, and Y.-k. Chen, "One visualization simulation operation system for distal femoral fracture," *Medicine*, vol. 96, no. 32, p. e7770, 8 2017. [Online]. Available: https://journals.lww.com/00005792-201708110-00045

[63] H.-J. Kim, Y.-J. Jo, J.-S. Choi, H.-J. Kim, I.-S. Park, J.-S. You, J.-S. Oh, and S.-Y. Moon, "Virtual Reality Simulation and Augmented Reality-Guided Surgery for Total Maxillectomy: A Case Report," *Applied Sciences*, vol. 10, no. 18, 2020.

[64] A. Gustafsson, P. Pedersen, T. B. Rømer, B. Viberg, H. Palm, and L. Konge, "Hip-fracture osteosynthesis training: exploring learning curves and setting proficiency standards," *Acta Orthopaedica*, vol. 90, no. 4, pp. 348–353, 7 2019. [Online]. Available: https://actaorthop.org/actao/article/view/600

[65] G. S. Goh, R. Lohre, J. Parvizi, and D. P. Goel, "Virtual and augmented reality for surgical training and simulation in knee arthroplasty," *Archives of Orthopaedic and Trauma Surgery*, vol. 141, no. 12, pp. 2303–2312, 12 2021. [Online]. Available: https://link.springer.com/article/10.1007/s00402-021-04037-1

[66] D. Bian, "The Application of Extended Reality Technology-Assisted Intraoperative Navigation in Orthopedic Surgery," *Frontiers in Surgery*, 2024.

[67] T. Morimoto, T. Kobayashi, H. Hirata, K. Otani, M. Sugimoto, M. Tsukamoto, T. Yoshihara, M. Ueno, and M. Mawatari, "XR (Extended

Reality: Virtual Reality, Augmented Reality, Mixed Reality) Technology in Spine Medicine: Status Quo and Quo Vadis," *Journal of Clinical Medicine*, 2022.

[68] S. Nanchahal, A. A. Rad, V. Naruka, C. Jacob, G. Liu, J. Afoke, G. Miller, J. Malawana, and P. P. Punjabi, "Mitral Valve Surgery Assisted by Virtual and Augmented Reality: Cardiac Surgery at the Front of Innovation," *Perfusion*, 2022.

[69] A. H. Sadeghi, Y. J. Taverne, A. J. Bogers, and E. A. Mahtab, "Immersive virtual reality surgical planning of minimally invasive coronary artery bypass for kawasaki disease," p. 3279, 9 2020. [Online]. Available: https://academic.oup.com/eurheartj/article/41/34/3279/5868577

[70] D. Schott, P. Saalfeld, G. Schmidt, F. Joeres, C. Boedecker, F. Huettl, H. Lang, T. Huber, B. Preim, and C. Hansen, "A VR/AR environment for multi-user liver anatomy education," in *Proceedings - 2021 IEEE Conference on Virtual Reality and 3D User Interfaces, VR 2021*. Piscataway: Institute of Electrical and Electronics Engineers Inc., 3 2021, pp. 296–305.

[71] J. Gugenheimer, W.-J. Tseng, A. H. Mhaidli, J. O. Rixen, M. McGill, M. Nebeling, M. Khamis, F. Schaub, and S. Das, "Novel Challenges of Safety, Security and Privacy in Extended Reality," 2022.

[72] W. J. Woodall, "Does Extended Reality Simulation Improve Surgical/Procedural Learning and Patient Outcomes When Compared With Standard Training Methods?" *Simulation in Healthcare the Journal of the Society for Simulation in Healthcare*, 2024.

[73] R. R. Thakrar, O. Al-Obaedi, K. Theivendran, and M. Snow, "Assessment of lower limb rotational profile and its correlation with the tibial tuberosity-trochlea groove distance: A radiological study," *Journal of Orthopaedic Surgery*, vol. 27, no. 3, pp. 1–6, 2019.

[74] Z. Jibri, P. Jamieson, K. S. Rakhra, M. L. Sampaio, and G. Dervin, "Patellar maltracking: an update on the diagnosis and treatment strategies," *Insights into Imaging*, vol. 10, no. 1, pp. 1–11, 12 2019. [Online]. Available: https://link.springer.com/articles/10.1186/s13244-019-0755-1https://link.springer.com/article/10.1186/s13244-019-0755-1

[75] A. M. Dobbe and P. J. Gibbons, "Common paediatric conditions of the lower limb," *Journal of Paediatrics and Child*

*Health*, vol. 53, no. 11, pp. 1077–1085, 11 2017. [Online]. Available: https://onlinelibrary.wiley.com/doi/full/10.1111/jpc.13756https://onlinelibrary.wiley.com/doi/abs/10.1111/jpc.13756https://onlinelibrary.wiley.com/doi/10.1111/jpc.13756

[76] Hospital for Special Surgery, "Hip/Femoral Anteversion: Causes, Symptoms, Treatment," 2021. [Online]. Available: https://www.hss.edu/condition-list_hip-femoral-anteversion.asp#diagnosis

[77] Y. Chaibi, T. Cresson, B. Aubert, J. Hausselle, P. Neyret, O. Hauger, J. A. de Guise, and W. Skalli, "Fast 3D reconstruction of the lower limb using a parametric model and statistical inferences and clinical measurements calculation from biplanar X-rays," *Computer Methods in Biomechanics and Biomedical Engineering*, vol. 15, no. 5, pp. 457–466, 2012.

[78] R. Guggenberger, C. W. A. Pfirrmann, P. P. Koch, and F. M. Buck, "Assessment of Lower Limb Length and Alignment by Biplanar Linear Radiography: Comparison With Supine CT and Upright Full-Length Radiography," *American Journal of Roentgenology*, vol. 202, no. 2, pp. W161–W167, 2014.

[79] P. Kaiser, R. Attal, M. Kammerer, M. Thauerer, L. Hamberger, R. Mayr, and W. Schmoelz, "Significant differences in femoral torsion values depending on the CT measurement technique," *Archives of Orthopaedic and Trauma Surgery*, vol. 136, no. 9, pp. 1259–1264, 9 2016. [Online]. Available: https://www.ncbi.nlm.nih.gov/pmc/articles/PMC4990621/

[80] S.K. Chauhan, G.W. Clark, R.G. Scott, S. Lloyd, and J.M. Sikorski, "THE PERTH CT PROTOCOL FOR TOTAL KNEE ARTHROPLASTY | Orthopaedic Proceedings," *Orthopaedic Proceedings*, vol. 90, no. B, 2 2008. [Online]. Available: https://online.boneandjoint.org.uk/doi/abs/10.1302/0301-620X.90BSUPP_I.0880007c

[81] C. L. Holland, A. Kamil, A. Puttanna, and C. Applications-general, "CT assessment of children with in-toeing gait," *ECR 2011*, pp. 1–13, 2011. [Online]. Available: https://epos.myesr.org/poster/esr/ecr2011/C-0234

[82] J. Farr, B. J. Cole, J. Kercher, L. Batty, and S. Bajaj, "Anteromedial Tibial Tubercle Osteotomy (Fulkerson Osteotomy)," *Anterior Knee Pain and Patellar Instability*, pp. 455–462, 2011. [Online]. Available: https://link.springer.com/chapter/10.1007/978-0-85729-507-1_40

[83] F. Rosso and F. Margheritini, "Distal femoral osteotomy," *Current Reviews in Musculoskeletal Medicine*, vol. 7, no. 4, pp. 302–311, 12 2014. [Online]. Available: https://link.springer.com/article/10.1007/s12178-014-9233-z

[84] P. Hosseinzadeh, D. R. Ross, J. L. Walker, V. R. Talwalkar, H. J. Iwinski, and T. A. Milbrandt, "Three Methods Of Guided Growth For Pediatric Lower Extremity Angular Deformity Correction," *The Iowa Orthopaedic Journal*, vol. 36, p. 123, 2016. [Online]. Available: https://www.ncbi.nlm.nih.gov/pmc/articles/PMC4910790/

[85] R. Murray, P. W. Winkler, H. S. Shaikh, and V. Musahl, "High Tibial Osteotomy for Varus Deformity of the Knee," *Journal of the American Academy of Orthopaedic Surgeons Global Research and Reviews*, vol. 5, no. 7, 7 2021.

[86] P. Bertuccio, G. Alicandro, M. Malvezzi, G. Carioli, P. Boffetta, F. Levi, C. La Vecchia, and E. Negri, "Cancer mortality in Europe in 2015 and an overview of trends since 1990," *Annals of Oncology*, vol. 30, no. 8, pp. 1356–1369, 8 2019. [Online]. Available: https://linkinghub.elsevier.com/retrieve/pii/S0923753419312931

[87] European Union, "ECIS - European Cancer Information System," 12 2023. [Online]. Available: https://ecis.jrc.ec.europa.eu/

[88] U.S. Department of Health and Human Services, Centers for Disease Control and Prevention, and National Cancer Institute, "U.S. Cancer Statistics Working Group. U.S. Cancer Statistics Data Visualizations Tool," 11 2023. [Online]. Available: https://gis.cdc.gov/Cancer/USCS/

[89] J. Park, M. Chen, M. Colombo, L. R. Roberts, M. Schwartz, P. Chen, M. Kudo, P. Johnson, S. Wagner, L. S. Orsini, and M. Sherman, "Global Patterns of Hepatocellular Carcinoma Management From Diagnosis to Death: The BRIDGE Study," *Liver International*, vol. 35, no. 9, pp. 2155–2166, 9 2015. [Online]. Available: https://onlinelibrary.wiley.com/doi/10.1111/liv.12818

[90] Y. Miyake, Y. Iwasaki, and K. Yamamoto, "Meta-analysis: Reduced incidence of hepatocellular carcinoma in patients not responding to interferon therapy of chronic hepatitis C," *International Journal of Cancer*, vol. 127, no. 4, pp. 989–996, 8 2010. [Online]. Available: https://onlinelibrary.wiley.com/doi/10.1002/ijc.25090

[91] J. Lin, J. Shi, H. Guo, X. Yang, Y. Jiang, J. Long, Y. Bai, D. Wang, X. Yang, X. Wan, L. Zhang, J. Pan, K. Hu, M. Guan, L. Huo, X. Sang, K. Wang, and H. Zhao, "Alterations in DNA Damage Repair Genes in Primary Liver Cancer," *Clinical Cancer Research*, vol. 25, no. 15, pp. 4701–4711, 8 2019. [Online]. Available: https://aacrjournals.org/clincancerres/article/25/15/4701/81659/Alterations-in-DNA-Damage-Repair-Genes-in-Primary

[92] E. Woodall, V. Taylor, C. Teh, L. Li, E. Acorda, S.-P. Tu, Y. Yasui, and T. G. Hislop, "Sources of Health Information Among Chinese Immigrants to the Pacific Northwest," *Journal of Cancer Education*, vol. 24, no. 4, pp. 334–340, 10 2009. [Online]. Available: http://link.springer.com/10.1080/08858190902854533

[93] Y. Tsujita, K. Sofue, E. Ueshima, Y. Ueno, M. Hori, M. Tsurusaki, and T. Murakami, "Evaluation and Prediction of Treatment Response for Hepatocellular Carcinoma," *Magnetic Resonance in Medical Sciences*, vol. 22, no. 2, pp. 2022–0118, 2023. [Online]. Available: https://www.jstage.jst.go.jp/article/mrms/22/2/22_rev.2022-0118/_article

[94] Z.-G. Wang, Z.-Y. He, Y.-Y. Chen, H. Gao, and X.-L. Du, "Incidence and survival outcomes of secondary liver cancer: a Surveillance Epidemiology and End Results database analysis," *Translational Cancer Research*, vol. 10, no. 3, pp. 1273–1283, 3 2021. [Online]. Available: https://tcr.amegroups.com/article/view/50241/html

[95] J. Wang, H. Xu, Y. Wang, L. Feng, and F. Yi, "Efficacy and Safety of Drug-Eluting Bead TACE in the Treatment of Primary or Secondary Liver Cancer," *Canadian Journal of Gastroenterology and Hepatology*, vol. 2023, pp. 1–8, 4 2023. [Online]. Available: https://www.hindawi.com/journals/cjgh/2023/5492931/

[96] P.-D. Line and S. Dueland, "Liver transplantation for secondary liver tumours: The difficult balance between survival and recurrence," *Journal of Hepatology*, vol. 73, no. 6, pp. 1557–1562, 12 2020. [Online]. Available: https://linkinghub.elsevier.com/retrieve/pii/S0168827820305390

[97] S. Yu, H. Wang, T. Hu, C. Yu, H. Liu, X. Chen, J. Jiang, and M. Deng, "Disease burden of liver cancer attributable to specific etiologies in China from 1990 to 2019: An age-period-cohort analysis," *Science Progress*, vol. 104, no. 2, p. 003685042110180, 4 2021. [Online]. Available: http://journals.sagepub.com/doi/10.1177/00368504211018081

[98] B. Aryal, T. Komokata, H. Yasumura, D. Kamiimabeppu, M. Inoue, K. Yoshikawa, M. Kaieda, and Y. Imoto, "Evaluation of THUNDERBEAT® in open liver resection- a single-center experience," *BMC Surgery*, vol. 18, no. 1, p. 86, 12 2018.

[99] S. Strasberg, J. Belghiti, P.-A. Clavien, E. Gadzijev, J. Garden, W.-Y. Lau, M. Makuuchi, and R. Strong, "The Brisbane 2000 Terminology of Liver Anatomy and Resections," *HPB*, vol. 2, no. 3, pp. 333–339, 2000.

[100] M. A. C. MACHADO, M. M. LOBO-FILHO, B. H. MATTOS, A. O. ARDENGH, and F. F. MAKDISSI, "Robotic Liver Resection. Report Of the First 50 Cases," *Arquivos de Gastroenterologia*, vol. 58, no. 4, pp. 514–519, 10 2021. [Online]. Available: http://www.scielo.br/scielo.php?script=sci_arttext&pid=S0004-28032021000400514&tlng=en

[101] D. W. Hwang, H. Han, Y. Yoon, J. Y. Cho, Y. Kwon, J. H. Kim, J. S. Park, D. S. Yoon, I. S. Choi, K. S. Ahn, Y. H. Kim, K. J. Kang, Y. H. Kim, Y. H. Roh, C. W. Chu, H. C. Kim, C. M. Kang, G. H. Choi, J. S. Choi, K. S. Kim, W. J. Lee, S. S. Yun, H. J. Kim, S. K. Min, H. K. Lee, I. Song, K. Chun, E. Cho, S. Han, and S. Park, "Laparoscopic major liver resection in Korea: a multicenter study," *Journal of Hepato-Biliary-Pancreatic Sciences*, vol. 20, no. 2, pp. 125–130, 2 2013.

[102] A. Younos, M. Touadi, S. Ross, and I. Sucandy, "Open Parenchymal Sparing Posterosuperior Liver Tumor Resection for Colorectal Liver Metastasis With Proximity to Hepatic Veins," *The American Surgeon™*, vol. 89, no. 8, pp. 3609–3611, 8 2023.

[103] T. Pakala, M. Molina, and G. Y. Wu, "Hepatic Echinococcal Cysts: A Review," *Journal of Clinical and Translational Hepatology*, vol. 4, no. 1, pp. 39–46, 3 2016. [Online]. Available: http://www.xiahepublishing.com/ArticleFullText.aspx?sid=2&jid=1&id=10.14218%2fJCTH.2015.00036

[104] A. Ribeiro, L. J. Burgart, D. M. Nagorney, and G. J. Gores, "Management of liver adenomatosis: Results with a conservative surgical approach," *Liver Transplantation and Surgery*, vol. 4, no. 5, pp. 388–398, 9 1998.

[105] J. Jin, J. Jin, S. Woodfield, R. Patel, N. Jin, Y. Shi, B. Liu, W. Sun, X. Chen, Y. Yu, and S. Vasudevan, "Targeting LRH-1 in hepatoblastoma cell lines causes decreased proliferation," *Oncology Reports*, 10 2018. [Online]. Available: http://www.spandidos-publications.com/10.3892/or.2018.6793

[106] M. Momiyama, T. Kumamoto, A. Suetsugu, H. Kishimoto, T. Chishima, K. Tanaka, H. Akiyama, Y. Ichikawa, M. Bouvet, I. Endo, and R. M. Hoffman, "Major liver resection stimulates stromal recruitment and metastasis compared with repeated minor resection," *Journal of Surgical Research*, vol. 178, no. 1, pp. 280–287, 11 2012.

[107] A. R. V. Rao, V. N. S, and S. C. Gudimani, "Hydatid Cyst Liver Excision: The Twin Problems Of Anaphylaxis And Hypernatremia," *Journal of Evolution of Medical and Dental Sciences*, vol. 4, no. 38, pp. 6675–6678,

5 2015. [Online]. Available: http://www.jemds.com/data_pdf/Anand%20Rampure%20Vittal%20Rao--vijaya--Mah.pdf

[108] S. T. Fan, C. Mau Lo, R. T. P. Poon, C. Yeung, C. Leung Liu, W. K. Yuen, C. Ming Lam, K. K. C. Ng, and S. Ching Chan, "Continuous Improvement of Survival Outcomes of Resection of Hepatocellular Carcinoma," *Annals of Surgery*, vol. 253, no. 4, pp. 745–758, 4 2011.

[109] Y. S. Patel, W. C. Hanna, C. Fahim, Y. Shargall, T. K. Waddell, K. Yasufuku, T. N. Machuca, M. Pipkin, J.-M. Baste, F. Xie, A. Shiwcharan, G. Foster, and L. Thabane, "RAVAL trial: Protocol of an international, multi-centered, blinded, randomized controlled trial comparing robotic-assisted versus video-assisted lobectomy for early-stage lung cancer," *PLOS ONE*, vol. 17, no. 2, p. e0261767, 2 2022. [Online]. Available: https://dx.plos.org/10.1371/journal.pone.0261767

[110] C. Chao, V. Vanguri, and K. Uy, "Robot-Assisted Thoracoscopic Resection of a Posterior Mediastinal Mullerian Cyst," *Case Reports in Pulmonology*, vol. 2018, pp. 1–4, 2018. [Online]. Available: https://www.hindawi.com/journals/cripu/2018/1424275/

[111] P. C. Obasi, A. Hebra, and J. C. Varela, "Excision of Esophageal Duplication Cysts with Robotic-Assisted Thoracoscopic Surgery," *JSLS : Journal of the Society of Laparoendoscopic Surgeons*, vol. 15, no. 2, pp. 244–247, 2011. [Online]. Available: http://www.ncbi.nlm.nih.gov/pmc/articles/PMC3148881/

[112] R. E. Ross, G. S. Schwartz, C. Thomas, and S. K. Balaram, "Robotic-assisted resection of an intrapericardial bronchogenic cyst," *Journal of Robotic Surgery*, vol. 5, no. 2, pp. 141–143, 6 2011. [Online]. Available: http://link.springer.com/10.1007/s11701-010-0228-5

[113] E. S. Singer, P. J. Kneuertz, J. Nishimura, D. M. D'Souza, E. Diefenderfer, S. D. Moffatt-Bruce, and R. E. Merritt, "Effect of operative approach on quality of life following anatomic lung cancer resection," *Journal of Thoracic Disease*, vol. 12, no. 11, pp. 6913–6919, 11 2020. [Online]. Available: http://jtd.amegroups.com/article/view/35047/html

[114] R. Nakamura, K. Okuda, K. Chiba, T. Matsui, R. Oda, T. Tatematsu, K. Yokota, and R. Nakanishi, "A large intrathoracic goiter with tracheal stenosis: Complete resection using a robot-assisted thoracoscopic approach," *Thoracic Cancer*, vol. 13, no. 12, pp. 1874–1877, 6 2022. [Online]. Available: https://onlinelibrary.wiley.com/doi/10.1111/1759-7714.14470

[115] J. Konecna, W. Karenovics, G. Veronesi, and F. Triponez, "Robot-assisted segmental resection for intralobar pulmonary sequestration," *International Journal of Surgery Case Reports*, vol. 22, pp. 83–85, 2016. [Online]. Available: https://linkinghub.elsevier.com/retrieve/pii/S221026121630013X

[116] Y. Yang, L. Song, J. Huang, X. Cheng, and Q. Luo, "A uniportal right upper lobectomy by three-arm robotic-assisted thoracoscopic surgery using the da Vinci (Xi) Surgical System in the treatment of early-stage lung cancer," *Translational Lung Cancer Research*, vol. 10, no. 3, pp. 1571–1575, 3 2021. [Online]. Available: https://tlcr.amegroups.com/article/view/50582/html

[117] P. L. Linsky and B. Wei, "Training in robotic thoracic surgery," *Journal of Visualized Surgery*, vol. 4, pp. 1–1, 1 2018. [Online]. Available: http://jovs.amegroups.com/article/view/17903/18236

[118] M. Eberlein, R. Reed, S. Bolukbas, J. Orens, R. Brower, C. Merlo, L. Ware, K. Wille, A. Weinacker, R. Shah, J. Diamond, S. Kawut, and J. Christie, "Lung Size Mismatch and Primary Graft Dysfunction after Bilateral Lung Transplantation," *The Journal of Heart and Lung Transplantation*, vol. 32, no. 4, p. S41, 4 2013. [Online]. Available: https://linkinghub.elsevier.com/retrieve/pii/S1053249813009194

[119] G. K. Casswell, D. V. Pilcher, R. S. Martin, V. A. Pellegrino, S. F. Marasco, C. Robertson, W. Butt, M. Buckland, J. Gooi, G. I. Snell, and G. P. Westall, "Buying time: The use of extracorporeal membrane oxygenation as a bridge to lung transplantation in pediatric patients," *Pediatric Transplantation*, vol. 17, no. 8, 12 2013. [Online]. Available: https://onlinelibrary.wiley.com/doi/10.1111/petr.12152

[120] C. D. Fraser, X. Zhou, J. C. Grimm, A. Suarez-Pierre, T. C. Crawford, C. Lui, E. L. Bush, N. Hibino, M. L. Jacobs, L. A. Vricella, and C. Merlo, "Size Mismatching Increases Mortality After Lung Transplantation in Preadolescent Patients," *The Annals of Thoracic Surgery*, vol. 108, no. 1, pp. 130–137, 7 2019. [Online]. Available: https://linkinghub.elsevier.com/retrieve/pii/S0003497519301924

[121] M. Baldwin, E. Peterson, I. Easthausen, I. Quintanilla, E. Colago, J. Sonett, F. D'Ovidio, J. Costa, J. Diamond, J. Christie, S. Arcasoy, and D. Lederer, "Donor Age and Early Graft Failure After Lung Transplantation: A Cohort Study," *American Journal of Transplantation*, vol. 13, no. 10, pp. 2685–2695, 10 2013. [Online]. Available: https://linkinghub.elsevier.com/retrieve/pii/S160061352226153X

[122] A. Slama, B. Ghanim, T. Klikovits, A. Scheed, M. A. Hoda, K. Hoetzenecker, P. Jaksch, J. Matilla, S. Taghavi, W. Klepetko, and C. Aigner, "Lobar lung transplantation-Is it comparable with standard lung transplantation?" *Transplant International*, vol. 27, no. 9, pp. 909–916, 9 2014. [Online]. Available: https://onlinelibrary.wiley.com/doi/10.1111/tri.12348

[123] A. Sabashnikov, M. Zeriouh, P. N. Mohite, N. P. Patil, D. García-Sáez, B. Schmack, S. Soresi, P. M. Dohmen, A.-F. Popov, A. Weymann, A. R. Simon, and F. De Robertis, "Moving Back to the Future: Use of Organ Care System Lung for Lobectomy Before Lobar Lung Transplantation," *Medical Science Monitor Basic Research*, vol. 22, pp. 70–74, 7 2016. [Online]. Available: https://basic.medscimonit.com/abstract/index/idArt/900200

[124] C. Benden, I. Inci, W. Weder, and A. Boehler, "Size-reduced lung transplantation in children - an option worth to consider!" *Pediatric Transplantation*, vol. 14, no. 4, pp. 529–533, 6 2010. [Online]. Available: https://onlinelibrary.wiley.com/doi/10.1111/j.1399-3046.2009.01267.x

[125] W. S. Jung, S. Haam, J. M. Shin, K. Han, C. H. Park, M. K. Byun, Y. S. Chang, H. J. Kim, and T. H. Kim, "The feasibility of CT lung volume as a surrogate marker of donor–recipient size matching in lung transplantation," *Medicine*, vol. 95, no. 27, p. e3957, 7 2016. [Online]. Available: https://journals.lww.com/00005792-201607050-00013

[126] J. A. Konheim, Z. N. Kon, C. Pasrija, Q. Luo, P. G. Sanchez, J. P. Garcia, B. P. Griffith, and J. Jeudy, "Predictive equations for lung volumes from computed tomography for size matching in pulmonary transplantation," *The Journal of Thoracic and Cardiovascular Surgery*, vol. 151, no. 4, pp. 1163–1169, 4 2016. [Online]. Available: https://linkinghub.elsevier.com/retrieve/pii/S0022522315021145

[127] J. Stocks and P. Quanjer, "Reference values for residual volume, functional residual capacity and total lung capacity. ATS Workshop on Lung Volume Measurements. Official Statement of The European Respiratory Society," *European Respiratory Journal*, vol. 8, no. 3, pp. 492–506, 3 1995. [Online]. Available: http://erj.ersjournals.com/lookup/doi/10.1183/09031936.95.08030492

[128] P. H. Quanjer, G. J. Tammeling, J. E. Cotes, O. F. Pedersen, R. Peslin, and J.-C. Yernault, "Lung volumes and forced ventilatory flows," *European Respiratory Journal*, vol. 6, no. Suppl 16, pp. 5–40, 3 1993.

[129] D. Li, J. Weinkauf, A. Hirji, J. Nagendran, A. Kapasi, D. Lien, and K. Halloran, "Chest X-ray Sizing for Lung Transplants Reflects Pulmonary Diagnosis and Body Composition and Is Associated With Primary Graft Dysfunction Risk," *Transplantation*, vol. 105, no. 2, pp. 382–389, 2 2021.

[130] H. M. Shepherd, K. Farahnak, M. S. Harrison, C. C. Frye, G. F. Marklin, A. J. Bierhals, R. R. Hachem, C. A. Witt, R. V. Guillamet, D. E. Byers, B. D. Kozower, B. F. Meyers, R. G. Nava, G. A. Patterson, D. Kreisel, and V. Puri, "Utilizing computed tomography volumetry for size matching prior to lung transplantation: a case series," *Journal of Thoracic Disease*, vol. 15, no. 4, pp. 2233–2239, 4 2023.

[131] R. Vazquez Guillamet, M. C. Vazquez Guillamet, A. Rjob, A. Bierhals, I. Bello, A. J. Abularach, L. Tague, M. Wallendorf, G. F. Marklin, C. Witt, D. E. Byers, D. Kreisel, R. Nava, V. Puri, R. Hachem, and E. P. Trulock, "Uncertainty analysis of chest X-ray lung height measurements and size matching for lung transplantation," *Journal of Thoracic Disease*, vol. 14, no. 4, pp. 1042–1051, 4 2022. [Online]. Available: https://jtd.amegroups.com/article/view/62458/html

[132] R. Fujimoto, D. Nakajima, S. Tanaka, Y. Yamada, Y. Yutaka, A. Ohsumi, M. Hamaji, T. Menju, and H. Date, "Efficacy of Three-Dimensional Computed Tomography Volumetry for Recipients in Downsizing Oversized Grafts in Brain-Dead Donor Lung Transplantation," *General Thoracic and Cardiovascular Surgery*, 2021.

[133] D. Sibrina, S. Bethapudi, and G. A. Koulieris, "OrthopedVR: clinical assessment and pre-operative planning of paediatric patients with lower limb rotational abnormalities in virtual reality," *The Visual Computer*, vol. 39, no. 8, pp. 3621–3633, 8 2023.

[134] Unity Technologies, "Unity Technologies," 2021. [Online]. Available: https://docs.unity3d.com/Manual/LightMode-MixedShadowmask.html

[135] Exit Games GmbH, "Multi-User Solutions Tailored for Professional Use Cases." 2 2024. [Online]. Available: https://www.photonengine.com/industries

[136] Wavefront Technologies, "Wavefront OBJ File Format," 1 2023. [Online]. Available: https://www.loc.gov/preservation/digital/formats/fdd/fdd000507.shtml#useful

[137] Dawson-Haggerty et al., "Trimesh." [Online]. Available: https://trimesh.org/

[138] Schroeder, Ken, and Bill, *The Visualization Toolkit*, 4th ed. New York: Kitware, 7 2018.

[139] Unity Technologies, "Unity - Manual: The Progressive Lightmapper," 2021. [Online]. Available: https://docs.unity3d.com/Manual/progressive-lightmapper.html

[140] Oculus, "Configure Unity Settings | Oculus Developers." [Online]. Available: https://developer.oculus.com/documentation/unity/unity-conf-settings/

[141] Unity Technologies, "Unity - Manual: Lighting Mode: Shadowmask." [Online]. Available: https://docs.unity3d.com/Manual/LightMode-Mixed-Shadowmask.html

[142] Django Software Foundation, "Django," 2 2024. [Online]. Available: https://djangoproject.com

[143] D. Sibrina, S. Bethapudi, and G. A. Koulieris, "A Virtual Reality System for the Assessment of Patients with Lower Limb Rotational Abnormalities," in *2023 IEEE Conference on Virtual Reality and 3D User Interfaces Abstracts and Workshops (VRW)*. IEEE, 3 2023, pp. 783–784.

[144] M. Sereno, X. Wang, L. Besancon, M. J. Mcguffin, and T. Isenberg, "Collaborative Work in Augmented Reality: A Survey," *IEEE Transactions on Visualization and Computer Graphics*, pp. 1–1, 10 2020.

[145] J. J. LaViola, E. Kruijff, R. P. McMahan, D. Bowman, and I. P. Poupyrev, *3D User Interfaces: Theory and Practice*, 2nd ed., ser. Addison-Wesley usability and HCI series. Boston: Addison-Wesley, 2017.

[146] J. C. Yen, F. J. Chang, and S. Chang, "A New Criterion for Automatic Multilevel Thresholding," *IEEE Transactions on Image Processing*, vol. 4, no. 3, pp. 370–378, 1995.

[147] Slicer, "Slicer Wiki." [Online]. Available: https://www.slicer.org/wiki/Documentation/4.2/Modules/RobustStatisticsSegmenterhttps://www.slicer.org/wiki/Documentation/Nightly/Developers/FAQ/Extensions#How_to_build_an_extension_.3F

[148] M. Garland and P. S. Heckbert, "Surface Simplification Using Quadric Error Metrics." [Online]. Available: http://www.cs.cmu.edu/

[149] H. Palmer, D. Elson, T. Baddeley, and A. Porthouse, "The United Kingdom Knee Osteotomy Registry: the first annual report 2018," 2019. [Online]. Available: www.ukkor.co.uk

[150] American Cancer Society Atlanta, "Cancer facts & figures 2017," 2013.

[151] R. L. Siegel, K. D. Miller, and A. Jemal, "Cancer statistics, 2016," *CA: A Cancer Journal for Clinicians*, vol. 66, no. 1, pp. 7–30, 1 2016.

[152] J.-N. Vauthey, A. Chaoui, K.-A. Do, M. M. Bilimoria, M. J. Fenstermacher, C. Charnsangavej, M. Hicks, G. Alsfasser, G. Lauwers, I. F. Hawkins, and J. Caridi, "Standardized measurement of the future liver remnant prior to extended liver resection: Methodology and clinical associations," *Surgery*, vol. 127, no. 5, pp. 512–519, 5 2000.

[153] H. Lang, "Impact of Virtual Tumor Resection and Computer-Assisted Risk Analysis on Operation Planning and Intraoperative Strategy in Major Hepatic Resection," *Archives of Surgery*, vol. 140, no. 7, p. 629, 7 2005.

[154] Y. Mise, K. Tani, T. Aoki, Y. Sakamoto, K. Hasegawa, Y. Sugawara, and N. Kokudo, "Virtual liver resection: computer-assisted operation planning using a three-dimensional liver representation," *Journal of Hepato-Biliary-Pancreatic Sciences*, vol. 20, no. 2, pp. 157–164, 2 2013.

[155] P. Leon, R. Rivellini, F. Giudici, A. Sciuto, F. Pirozzi, and F. Corcione, "3D Vision Provides Shorter Operative Time and More Accurate Intraoperative Surgical Performance in Laparoscopic Hiatal Hernia Repair Compared With 2D Vision," *Surgical Innovation*, vol. 24, no. 2, pp. 155–161, 4 2017.

[156] L. Cai, B. P. Nguyen, C. Chui, and S. Ong, "Rule-Enhanced Transfer Function Generation for Medical Volume Visualization," *Computer Graphics Forum*, vol. 34, no. 3, pp. 121–130, 6 2015.

[157] S. Gül, D. Podborski, J. Son, G. S. Bhullar, T. Buchholz, T. Schierl, and C. Hellge, "Cloud rendering-based volumetric video streaming system for mixed reality services," in *Proceedings of the 11th ACM Multimedia Systems Conference*. New York, NY, USA: ACM, 5 2020, pp. 357–360. [Online]. Available: https://dl.acm.org/doi/10.1145/3339825.3393583

[158] D. Ribero, M. Amisano, F. Bertuzzo, S. Langella, R. Lo Tesoriere, A. Ferrero, D. Regge, and L. Capussotti, "Measured versus Estimated Total Liver Volume to Preoperatively Assess the Adequacy of the Future Liver Remnant," *Annals of Surgery*, vol. 258, no. 5, pp. 801–807, 11 2013.

[159] C. Pulitano, M. Crawford, D. Joseph, L. Aldrighetti, and C. Sandroussi, "Preoperative assessment of postoperative liver function: The importance of residual liver volume," *Journal of Surgical Oncology*, vol. 110, no. 4, pp. 445–450, 9 2014.

[160] T. Schubert and H. Regenbrecht, "Wer hat Angst vor virtueller Realität? Angst, Therapie und Präsenz in virtuellen Welten," 3 2002. [Online]. Available: https://www.researchgate.net/publication/242714882_Wer_hat_Angst_vor_virtueller_Realitat_Angst_Therapie_und_Prasenz_in_virtuellen_Welten/citations

[161] T. Schubert, "The sense of presence in virtual environments: A three-component scale measuring spatial presence, involvement, and realness," *Zeitschrift für Medienpsychologie*, vol. 15, pp. 69–71, 3 2003.

[162] P. Whitney and D. Budd, "Think-aloud protocols and the study of comprehension," *Discourse Processes*, vol. 21, no. 3, pp. 341–351, 5 1996.

[163] Kolařík J, Tavandžis J, Novysedlák R, Vachtenheim J, Sibřina D, Švorcová M, Pozniak J, Šimonek J, Schützner J, and Lischke R, "Robotic pulmonary segmentectomy, initial experience in the Czech Republic," *Perspectives in Surgery*, vol. 102, no. 5, 5 2023.

[164] D. Sibrina, R. Novysedlak, J. Kolarik, R. Lischke, and G. A. Koulieris, "Fitting Room: Lung Transplantation Donor-Recipient Size-matching in Virtual Reality," *Special Interest Group on Computer Graphics and Interactive Techniques Conference Posters (SIGGRAPH Posters '24), July 27 - August 01, 2024, Denver, CO, USA*, vol. 1, 2024. [Online]. Available: https://doi.org/10.1145/3641234.3671048

[165] A. A. Alsheikhy, Y. Said, T. Shawly, A. K. Alzahrani, and H. Lahza, "A CAD System for Lung Cancer Detection Using Hybrid Deep Learning Techniques," *Diagnostics*, vol. 13, no. 6, p. 1174, 3 2023. [Online]. Available: https://www.mdpi.com/2075-4418/13/6/1174

[166] F. Acheampong, T. Ostlund, M. Mahnashi, and F. Halaweish, "Estrone analogs as potential inhibitors targeting EGFR-MAPK pathway in non-small-cell lung cancer," *Chemical Biology & Drug Design*, vol. 101, no. 6, pp. 1356–1366, 6 2023. [Online]. Available: https://onlinelibrary.wiley.com/doi/10.1111/cbdd.14218

[167] R. M. Karmacharya, A. K. Singh, S. Vaidya, S. M. Tuladhar, M. Devbhandari, B. Lama, B. B. Kharel, and S. Basnet, "Analysis of Lung Cancer Cases Presenting in Outpatient Department of University Hospital of Nepal," *Kathmandu University Medical Journal*, vol. 20, no. 4, pp. 452–455, 12 2022. [Online]. Available: https://www.nepjol.info/index.php/KUMJ/article/view/54084

[168] K. A. Papavassiliou and A. G. Papavassiliou, "The Biology and Therapeutic Potential of the Src-YAP Axis in Non-Small Cell Lung Cancer (NSCLC)," *Cancers*, vol. 14, no. 24, p. 6178, 12 2022. [Online]. Available: https://www.mdpi.com/2072-6694/14/24/6178

[169] M. A. Baz, M. D. Pitts, and S. Keshavamurthy, "Indications, pre-operative evaluation, and timing for lung transplantation listing," *Current Challenges in Thoracic Surgery*, vol. 5, pp. 13–13, 4 2023. [Online]. Available: https://ccts.amegroups.com/article/view/49189/html

[170] L. K. Tague, W. Adams, K. A. Young, O. J. Kwon, E. Mahoney, and E. M. Lowery, "Association between diverticular disease requiring surgical intervention and mortality in the postlung transplant population - a retrospective cohort study," *Transplant International*, vol. 32, no. 7, pp. 739–750, 7 2019. [Online]. Available: https://onlinelibrary.wiley.com/doi/10.1111/tri.13417

[171] R. Goetz, N. Kumar Jain, H. Anjum, and T. S. Kaleekal, "Lung Transplantation in Idiopathic Pulmonary Fibrosis," in *Idiopathic Pulmonary Fibrosis*. IntechOpen, 10 2022. [Online]. Available: https://www.intechopen.com/chapters/83181

[172] D. Weill, "Lung transplantation: indications and contraindications," *Journal of Thoracic Disease*, vol. 10, no. 7, pp. 4574–4587, 7 2018. [Online]. Available: http://jtd.amegroups.com/article/view/22975/17488

[173] M. R. Morrell, S. C. Kiel, and J. M. Pilewski, "Organ Transplantation for Cystic Fibrosis," *Seminars in Respiratory and Critical Care Medicine*, vol. 40, no. 06, pp. 842–856, 12 2019. [Online]. Available: http://www.thieme-connect.de/DOI/DOI?10.1055/s-0039-3399554

[174] J. Morton and A. Glanville, "Lung Transplantation in Patients with Cystic Fibrosis," *Seminars in Respiratory and Critical Care Medicine*, vol. 30, no. 05, pp. 559–568, 10 2009. [Online]. Available: http://www.thieme-connect.de/DOI/DOI?10.1055/s-0029-1238914

[175] E. Melicoff, D. Hayes, and C. Benden, "Lung transplantation as an intervention for pediatric pulmonary hypertension," *Pediatric Pulmonology*, vol. 56, no. 3, pp. 587–592, 3 2021. [Online]. Available: https://onlinelibrary.wiley.com/doi/10.1002/ppul.25154

[176] C. Benden, "Pediatric lung transplantation," *Journal of Thoracic Disease*, vol. 9, no. 8, pp. 2675–2683, 8 2017. [Online]. Available: http://jtd.amegroups.com/article/view/14757/12298

[177] T. M. Benoit and C. Benden, "Pediatric lung transplantation: supply and demand," *Current Opinion in Organ Transplantation*, vol. 24, no. 3, pp. 324–328, 6 2019. [Online]. Available: https://journals.lww.com/00075200-201906000-00019

[178] J. C. Yeung and S. Keshavjee, "Overview of Clinical Lung Transplantation," *Cold Spring Harbor Perspectives in Medicine*, vol. 4, no. 1, pp. a015 628–a015 628, 1 2014. [Online]. Available: http://perspectivesinmedicine.cshlp.org/lookup/doi/10.1101/cshperspect.a015628

[179] S. S. F. Yip, C. Parmar, D. Blezek, R. S. J. Estepar, S. Pieper, J. Kim, and H. J. W. L. Aerts, "Application of the 3D slicer chest imaging platform segmentation algorithm for large lung nodule delineation," *PLOS ONE*, vol. 12, no. 6, p. e0178944, 6 2017. [Online]. Available: https://dx.plos.org/10.1371/journal.pone.0178944

[180] Slicer, "Slicer Wiki," 2021. [Online]. Available: https://www.slicer.org/wiki

[181] J. Wasserthal, H.-C. Breit, M. T. Meyer, M. Pradella, D. Hinck, A. W. Sauter, T. Heye, D. T. Boll, J. Cyriac, S. Yang, M. Bach, and M. Segeroth, "TotalSegmentator: Robust Segmentation of 104 Anatomic Structures in CT Images," *Radiology: Artificial Intelligence*, vol. 5, no. 5, p. e230024, 9 2023. [Online]. Available: http://pubs.rsna.org/doi/10.1148/ryai.230024

[182] Y. Baashar, G. Alkawsi, W. N. Wan Ahmad, M. A. Alomari, H. Alhussian, and S. K. Tiong, "Towards Wearable Augmented Reality in Healthcare: A Comparative Survey and Analysis of Head-Mounted Displays," *International Journal of Environmental Research and Public Health*, 2023.

[183] A. Palumbo, "Microsoft HoloLens 2 in Medical and Healthcare Context: State of the Art and Future Prospects," *Sensors*, 2022.

[184] G. Rus, I. Andraș, C. Vaida, N. Crişan, B. Gherman, C. Radu, P. Tucan, S. Iakab, N. A. Hajjar, and D. Pîslă, "Artificial Intelligence-Based Hazard Detection in Robotic-Assisted Single-Incision Oncologic Surgery," *Cancers*, 2023.

[185] M. Connolly, "Delivering Clinical Tutorials to Medical Students Using the Microsoft HoloLens 2: A Mixed-Methods Evaluation," *BMC Medical Education*, 2024.

[186] A. Acar, "Intraoperative Gaze Guidance With Mixed Reality," 2023.

[187] K. Hari, R. C. Thompson, L. B. Chambless, and M. I. Miga, "Development of a Mixed Reality Application to Simulate Neurosurgical Procedures," 2023.

[188] S. Teruggi and F. Fassi, "Mixed Reality Content Alignment in Monumental Environments," *The International Archives of the Photogrammetry Remote Sensing and Spatial Information Sciences*, 2022.

[189] M. Eberlein, R. M. Reed, S. Bolukbas, J. M. Diamond, K. M. Wille, J. B. Orens, R. G. Brower, and J. D. Christie, "Lung size mismatch and primary graft dysfunction after bilateral lung transplantation," *The Journal of Heart and Lung Transplantation*, vol. 34, no. 2, pp. 233–240, 2 2015.

[190] B. Li, W. Zhang, T. Tan, W. Liu, X. Luo, J. Zhang, Y. Yang, R. Li, and Z. Ge, "Chinese Herbal Formulas Miao-Yi-Ai-Tang Inhibits the Proliferation and Migration of Lung Cancer Cells Through Targeting<i>$\beta$</I>-Catenin/Axin and Presents Synergistic Effect With Cisplatin Suppressing Lung Cancer," *Biomed Research International*, 2020.

[191] G. L. Hall, N. Filipow, G. Ruppel, T. Okitika, B. Thompson, J. Kirkby, I. Steenbruggen, B. G. Cooper, and S. Stanojevic, "Official ERS technical standard: Global Lung Function Initiative reference values for static lung volumes in individuals of European ancestry," *European Respiratory Journal*, vol. 57, no. 3, p. 2000289, 3 2021.

# Appendices

## A Qualitative Questionnaire for OrthopedVR

**Question 1:** Were you generally satisfied with visual performance of the virtual reality application for the osteotomy planning? (1 = Not satisfied at all, 10 = Extremely satisfied)

**Question 2:** Was the virtual reality application stable during the testing session? (1 = Very unstable, 10 = Very stable)

**Question 3:** Do you find the multi-user interaction capability in the virtual reality environment for collaborative, education, and training purposes useful? (1 = Not useful at all, 10 = Extremely useful)

**Question 4:** Did you find the multi-user tutorial more helpful than watching a pre-recorded educative video? (1 = Not helpful at all, 10 = Extremely helpful)

**Question 5:** Did you find the user interface intuitive and easy to navigate? (1 = Not intuitive at all, 10 = Extremely intuitive)

**Question 6:** Did you find the virtual reality environment visually appealing? (1 = Not appealing at all, 10 = Extremely appealing)

**Question 7:** Do you have any suggestions which would improve the virtual reality application in terms of design, ease of use, or other user interface sug-

gestions?

**Question 8:** Do you think VR has a role in pre-operative orthopaedic assessment? (1 = No role at all, 10 = Very significant role)

**Question 9:** Do you think that VR will be used in pre-operative orthopaedic planning in future? (1 = Not at all, 10 = Definitely)

**Question 10:** With relevance to current research, do you feel VR can offer better input and understanding of lower limb alignment and rotational profile in comparison to isolated 2D CT evaluation? (1 = Not at all, 10 = Significantly)

**Question 11:** Do you think that use of VR software could reduce your reliance on conventional Radiologists' manual measurement of angles on CT? (1 = Not at all, 10 = Significantly)

**Question 12:** Do you think use of VR can increase reproducibility of lower limb rotational profile angles as part of pre-operative planning and reduce variation in angles related to human factors? (1 = Not at all, 10 = Significantly)

**Question 13:** Do you think use of VR software in conjunction with Radiology reports could improve pre-operative planning, surgical precision and post-operative outcomes for patients? (1 = Not at all, 10 = Significantly)

**Question 14:** Would you be happy to incorporate use of VR in future clinical practice? (1 = Not at all, 10 = Very happy)

**Question 15:** Would you be happy to recommend VR rotational profile alignment software for pre-operative planning to orthopaedic colleagues and trainees? (1 = Not at all, 10 = Very happy)

# B Igroup Presence Questionnaire for XR Medical Software Evaluation (IPQ-XRMSE)

### Immersion

**Spatial Understanding:** Has the VR application improved your spatial understanding of the organ and its anatomical structures? (0 = Greatly improved, 7 = No improvement at all)

**Anatomical Relationship Understanding:** To what extent has the VR application allowed you to comprehend the relationship between the organ and surrounding anatomical structures? (0 = Fully allowed, 7 = Did not allow at all)

**3D Movement Control:** How well did the VR application enable control over your movements in a 3D environment? (0 = Poorly, 7 = Very well)

**Immersive Engagement:** To what extent did the VR application provide an immersive experience that facilitated your decision-making process? (0 = Not at all, 7 = Significantly)

### Realism

**Accuracy of Representation:** How accurately does the VR application represent the organ and its anatomical structures? (0 = Very inaccurately, 7 = Very accurately)

**Clarity of 3D Data:** How clear was the 3D data presented in the VR application? (0 = Very vague, 7 = Very clear)

**Differentiation of Organ Tissues:** How difficult was it to differentiate between different organ tissues in the VR application? (0 = Very simple, 7 = Very complicated)

**Detailed Visualization:** To what extent has the VR application enabled detailed visualization of the organ and surrounding tissues? (0 = To a very

small extent, 7 = To a very great extent)

**Involvement**

**Involvement in Decision-Making:** How involved were you in determining the appropriate course of action for each patient case? (0 = Not involved at all, 7 = Very involved)

**Planning and Strategy:** To what extent has the VR application allowed you to effectively plan and strategize for potential surgical interventions? (0 = Insufficiently, 7 = Extensively)

**Confidence in Decision-Making:** How confident were you in making decisions using the VR application? (0 = Not confident at all, 7 = Extremely confident)

**Intuitive Interaction:** To what extent did the VR application allow intuitive and natural manipulation of and interaction with the organ object and surrounding tissues? (0 = Not at all, 7 = To a great extent)

**Focus and Concentration:** To what degree has the VR application helped you maintain focus and concentration during medical virtual reality visualization? (0 = Insufficiently, 7 = Extensively)

# C System Usability Scale (SUS)

**Question 1:** I think that I would like to use this system frequently. (1 = Disagree vehemently, 5 = Agree completely)

**Question 2:** I found the system unnecessarily complex. (1 = Disagree vehemently, 5 = Agree completely)

**Question 3:** I thought the system was easy to use. (1 = Disagree vehemently, 5 = Agree completely)

**Question 4:** I think that I would need the support of a technical person to be able to use this system. (1 = Disagree vehemently, 5 = Agree completely)

**Question 5:** I found the various functions in this system were well integrated. (1 = Disagree vehemently, 5 = Agree completely)

**Question 6:** I thought there was too much inconsistency in this system. (1 = Disagree vehemently, 5 = Agree completely)

**Question 7:** I would imagine that most people would learn to use this system very quickly. (1 = Disagree vehemently, 5 = Agree completely)

**Question 8:** I found the system very cumbersome to use. (1 = Disagree vehemently, 5 = Agree completely)

**Question 9:** I felt very confident using the system. (1 = Disagree vehemently, 5 = Agree completely)

**Question 10:** I needed to learn a lot of things before I could get going with this system. (1 = Disagree vehemently, 5 = Agree completely)

# D System Evaluation Questionnaire for Evaluating AR System in RATS

**Question 1:** How clear do you find the 3D patient reconstructions provided by the system? (0 = Lowest, 10 = Highest)

**Question 2:** How can the system enhance the educational understanding of surgical procedures for supporting medical staff (nurses and anesthesiologists) or novice surgeons? (0 = Lowest, 10 = Highest, and provide a brief explanation if possible)

**Question 3:** How accurately do the 3D reconstructions mirror real-life conditions? (0 = Lowest, 10 = Highest)

**Question 4:** How has the system affected the overall quality of surgical procedures? (0 = Lowest, 10 = Highest)

**Question 5:** Has the system improved your comfort in port placement? (0 = Lowest, 10 = Highest)

**Question 6:** How effectively has the system aided in the precise localization of tumours? (0 = Lowest, 10 = Highest)

**Question 7:** How has the system enhanced your understanding of the patient's vascular and bronchial structures? (0 = Lowest, 10 = Highest)